Physiology of Multiple Sulfur Isotope Fractionation during Microbial Sulfate Reduction

by

Min Sub Sim

B.S. Earth System Sciences
Seoul National University, 2002

M.S. Earth and Environmental Sciences
Seoul National University, 2004

SUBMITTED TO THE DEPARTMENT OF EARTH, ATMOSPHERIC AND PLANETARY SCIENCES IN PARTIAL FULFILLMENT OF THE REQUIREMENTS FOR THE DEGREE OF

DOCTOR OF PHILOSOPHY IN GEOBIOLOGY
AT THE
MASSACHUSETTS INSTITUTE OF TECHNOLOGY

JUNE 2012

Signature of Author .....

Department of Earth, Atmospheric, and Planetary Sciences
May 16, 2012

Certified by .....

Tanja Bosak
Professor of Geobiology
Thesis Supervisor

Certified by .....

Shuhei Ono
Professor of Geochemistry
Thesis Supervisor

Accepted by .....

Robert D. van der Hilst
Schlumberger Professor of Geosciences
Head of the Department of Earth, Atmospheric and Planetary Sciences

Physiology of Multiple Sulfur Isotope Fractionation during Microbial Sulfate Reduction

by

Min Sub Sim

Submitted to the Department of Earth, Atmospheric, and Planetary Sciences
on May 16, 2012 in Partial Fulfillment of the Requirements for the Degree of Doctor of Philosophy in Geobiology

Abstract

Microbial sulfate reduction (MSR) utilizes sulfate as an electron acceptor and produces sulfide that is depleted in heavy isotopes of sulfur relative to starting sulfate. The fractionation of S-isotopes is commonly used to trace the biogeochemical cycling of sulfur in nature, but a mechanistic understanding of factors that control the range of isotope fractionation is still lacking. This thesis investigates links between the physiology of sulfate reducing bacteria in pure cultures and multiple sulfur isotope (^{32}S, ^{33}S, ^{34}S, and ^{36}S) fractionation during MSR in batch and continuous culture experiments. Experiments address the influence of nutrient and electron donor conditions, including organic carbon, nitrogen, and iron, in cultures of a newly isolated marine sulfate reducing bacterium (DMSS-1). An actively growing culture of DMSS-1 produced sulfide depleted in ^{34}S by 6 to 66‰, depending on the availability and chemistry of organic electron donors. The magnitude of isotope effect correlated well with the cell specific sulfate reduction rate (csSRR), and the largest isotope effects occurred when cultures grew slowly on glucose, a recalcitrant organic substrate. These findings bridge the long-standing discrepancy between the upper limit for S-isotope effect in laboratory cultures and the corresponding observations in nature and indicate that the large (>46 ‰) fractionation of S-isotopes does not unambiguously record the oxidative sulfur-recycling. When the availability of iron was limited, the increase in S-isotope fractionation was accompanied by a decrease in the cytochrome *c* content as well as csSRR. In contrast, growth in nitrogen-limited cultures increased both csSRR and S-isotope fractionation. The influence of individual enzymes and electron carriers involved in sulfate respiration on the fractionation of S-isotopes was also investigated in cultures of mutant strains of *Desulfovibrio vulgaris* Hildenborough. The mutant lacking Type I tetraheme cytochrome c_3 fractionated $^{34}S/^{32}S$ ratio 50% greater relative to the wild type. The increasing S-isotope fractionation accompanied the evolution of H_2 in the headspace and the decreasing csSRR. These results further demonstrate that the flow of electrons to terminal reductases imparts the primary control on the magnitude of the fractionation of S-isotopes, suggested by culture experiments using DMSS-1.

Acknowledgements

My first gratitude must go to my two wonderful advisors, Tanja Bosak and Shuhei Ono. Tanja is the very first person who guided me into the world of microbes, and Shuhei convinced me to get involved in sulfur isotope geochemistry. Since all of us started working at MIT in 2007, they have patiently encouraged me, always had an open ear for my small and big problems, and served as a role model to me as a junior member of academia. It is with their mentorship that I made a smooth transition from classical carbonate sedimentology to geomicrobiology and eventually complete this thesis.

Special thanks to the members of my thesis committee, Roger Summons and Jeffrey Seewald. Roger served as a chair of my thesis committee and provided insightful suggestions on my research. I am grateful to Jeff not only for his helpful comments but also for teaching me aquatic chemistry in my first semester at MIT. What I learned in his class has been a basic asset through the course of my study. My appreciation extends to Sam Bowring and Janelle Thompson. Both ware on my general exam committee, and their comments were invaluable help to develop this thesis. I also want to thank Judy Wall and Gerrit Voordouw for providing their mutant strains.

I would like to express my deep gratitude to everyone in Tanja's Geomicrobiology Laboratory and Shuhei's Stable Isotope Laboratory. In particular, Bill Olszewski has been very helpful with isotope analysis, and Stefanie Templer helped me with her expertise in molecular biology. My first field trip to Yellowstone National Park with Alex, Biqing, and Kate was one of the most memorable moments in my graduate career. Two undergraduate researchers, Katie and Eileen, helped me in everyday laboratory work. Thank you all.

I wish to thank my Korean friends, Gill-Ran Jeong, Byeongju Jung, Kang Hyeun Ji, Dong-Chul Kim, and Eunjee Lee. I was fortunate to spend the last five years with my great cousin, Jong-Mi Lee, in the same department at MIT and even on the same floor.

Last but not the least, my family deserves my sincerest thanks. My parents always trust me, encourage me to follow my dreams, and support me. My sister took cared well for the household matters in Korea so that I could focus on my work in the US. I deeply thank my grandmother for her unconditional love. I would also like to dedicate this thesis to my wife, Young Ji Joo. Since we met as lab mates 10 years ago, we have been encouraging each other as friends, family, and colleagues. Without her help, this dissertation would not have been finished.

Table of contents

List of Figures

List of Tables

1. Introduction

Microbial sulfate reduction (MSR) is the principal anaerobic metabolism in marine environments that remineralizes organic compounds, using sulfate as an electron donor, and producing sulfide. This process produces significant isotope effects, where the product sulfide is depleted in heavy isotopes, ^{33}S, ^{34}S, and ^{36}S with respect to the starting sulfate. Consequently, the isotopic composition of various sulfur species is used to qualitatively probe microbial sulfur metabolism in nature (Canfield and Teske, 1996; Lyons, 1997; Wortmann *et al.*, 2001; Zerkle *et al.*, 2010). While sulfate reducing microbes (SRM) utilize light S-isotopes faster, the magnitude of fractionation varies spatially and temporally from 0 to 77‰ in nature (Fry *et al.*, 1995; Canfield and Teske, 1996; Rudnicki *et al.*, 2001). On the other hand, laboratory culture studies of MSR have not reported sulfur isotope effects larger than 47‰ under chemically and biologically defined reproducible conditions (Canfield and Teske, 1996). Although laboratory studies over the past five decades have provided essential insights into biological sulfur isotope effects (Kaplan and Rittenberg, 1964; Chambers *et al.*, 1975; Canfield, 2001; Detmers *et al.*, 2001; Johnston *et al.*, 2005; Hoek *et al.*, 2006), mechanisms behind the wide range of fractionation and the discrepancy between those observed in laboratory cultures and nature are not fully understood.

So far, because terminal electron donors and acceptors are two major players in any respiration process, most studies have focused on their impacts on S-isotope fractionation. Habicht *et al.* (2002 and 2005) demonstrated the influence of sulfate concentration on the magnitude of S-isotope fractionation during MSR, which decreases as sulfate concentrations fall below 200 μM. On the other hand, when limited by the low concentration of electron donors, MSR produced greater fractionations (Chambers *et al.*, 1975; Hoek et al., 2006). Since SRM are metabolically versatile and capable of utilizing a wide range of electron donors (Rabus *et al.*, 2006), not only the availability of electron donors but also their chemistry likely affects the magnitude of S-isotope fractionation during MSR in nature. Yet, few previous iotopic studies cultured a single strain with different electrons donors, and could not draw clear conclusions with respect to the effect of different electron donors on S-isotope fractionation (Kaplan and Rittenberg, 1964; Kemp and Thode, 1968; Kleikemper *et al.*, 2004).

SRM do not translocate electrons from the organic substrate directly to the terminal electron acceptor, sulfate. Instead, the rates of electron transfer depend on many enzymes and electron carriers, containing various metal cofactors in their active sites (Rabus *et al.*, 2006; Keller and Wall, 2011; Pereira *et al.*, 2011). Moreover, the cellular energy and redox budgets change if some of the reducing equivalents generated by the oxidation of organic substrates can be diverted toward metabolic processes such as

carbon and nitrogen fixation. Hence, a wide range of nutrient limitations, such as iron and nitrogen, can alter the coupling between the electron donor and sulfate, ultimately influencing the magnitude of S-isotope fractionation. To the best of our knowledge, none of the previous studies investigated the effect of nutrients other than electron donors and acceptors on S-isotope fractionation during MSR.

In terms of experimental strategy, cultivation of specific SRM under different growth conditions helps resolve the effects of individual environmental factors on the magnitude of isotope fractionation, but it provides little information about intracellular processes. Only a few studies have attempted to address intracellular mechanisms and enzymatic activities dictating the measured fractionation of S-isotopes. Specifically, Mangalo *et al.* (2008) used excess nitrite to impair the activity of dissimilatory sulfite reductase and measured the overall isotope effect during MSR. Fortunately, recent advances in molecular biology have enabled investigations of intracellular processes by mutant analyses (Dolla *et al.*, 2000; Pohorelic *et al.*, 2002; Caffrey *et al.*, 2007; Keller *et al.*, 2009; Walker *et al.*, 2009; Zane *et al.*, 2010). These analyses probe the contribution of individual enzymes to MSR and the resulting S-isotope effects, providing complementary information to classical culture studies that often treat the cell as a black box.

This thesis presents the results of series of batch and flow-trough culture experiments with a newly-isolated marine sulfate reducing bacterium, DMSS-1, and the genetically modified strains of *Desulfovibrio vulgaris* Hildenborough, and proposes the links between the physiology of sulfate reducing microbes and multiple S-isotope (^{32}S, ^{33}S, ^{34}S, and ^{36}S) fractionations. In Chapter 2, I describe the relationship between the growth of a newly isolated marine sulfate reducing bacterium, DMSS-1 and the fractionation of sulfur isotopes as a function of seven different organic electron donors in batch cultures, and as a function of the dilution rate in lactate-limited continuous cultures. Depending on the availability and chemistry of organic electron donors, an actively growing culture of DMSS-1 produced sulfide depleted in ^{34}S by up to 66‰, which is much larger than 46‰ that has served as a boundary discriminating oxidative recycling of sulfur from sulfate reduction (Canfield and Teske, 1996). The geological and environmental significance of those extreme fractionations is discussed in Chapter 3. Other than organic substrates, the influence of iron and nitrogen on S-isotope fractionation was also examined using DMSS-1. Chapter 4 asks how the availability of iron and reduced nitrogen influences multiple-S isotope fractionation during MSR and finds that the availability of iron controls S-isotope fractionation in a manner similar to that of the organic electron donor, but nitrogen limitation produces smaller, but distinct isotopic signatures. Chapter 5 explores intracellular processes relevant to the fractionation of sulfur isotopes by using mutant strains of *Desulfovibrio vulgaris* Hildenborough, lacking cytochromes and hydrogenases, and confirms a link between the flow of electrons and the fractionation of

S-isotopes at the enzymatic level. Finally, Chapter 6 describes two future experiments: one that would address the relative significance of organic electron donors and other nutrients to S-isotope fractionation in nature, and the other, which would focus on the fate of intermediate sulfur species and the associated isotope effect.

References

Caffrey SM, Park H-S, Voordouw JK, He Z, Zhou J, Voordouw G. 2007. Function of periplasmic hydrogenases in the sulfate-reducing bacterium Desulfovibrio vulgaris Hildenborough. J. Bacteriol. 189: 6159-6167.

Canfield DE. 2001. Isotope fractionation by natural populations of sulfate-reducing bacteria. Geochim. Cosmochim. Acta 65: 1117-1124.

Canfield DE, Teske A. 1996. Late Proterozoic rise in atmospheric oxygen concentration inferred from phylogenetic and sulphur-isotope studies. Nature 382: 127-132.

Chambers LA, Trudinger PA, Smith JW, Burns MS. 1975. Fractionation of sulfur isotopes by continuous cultures of Desulfovibrio desulfuricans. Can. J. Microbiol. 21: 1602-1607.

Detmers J, Bruchert V, Habicht K, Kuever J. 2001. Diversity of sulfur isotope fractionations by sulfate reducing prokaryotes. Appl. Environ. Microbiol. 67: 888-894.

Dolla A, Pohorelic KJ, Voordouw KJ, Voordouw G. 2000. Deletion of the hmc-operon of Desulfovibrio vulgaris subsp. vulgaris Hildenborough hampers hydrogen metabolism and low-redox potential niche establishment. Arch. Microbiol. 174: 143-151.

Fry B, Giblin A, Dornblaser M, Peterson B. 1995. Stable sulfur isotopic compositions of chromium-reducible sulfur in lake sediments. In Geochemical Transformation of Sedimentary Sulfur (eds. Vairavamurthy MA, Schoonen MAA), ACS Symposium Series 612. American Chemical Society, Washington, DC, pp. 397-410.

Habicht KS, Gabe M, Thamdrup B, Berg P, Canfield DE. 2002. Calibration of sulfate levels in the Archean ocean. Science 298: 2372-2374.

Habicht KS, Salling L, Thamdrup B, Canfield DE. 2005. Effect of low sulfate concentrations on lactate oxidation and isotope fractionation during sulfate reduction by Archaeoglobus fulgidus Strain Z. Appl. Environ. Microbiol. 71: 3770-3777.

Hoek J, Reysenbach A, Habicht KS, Canfield DE. 2006. Effect of hydrogen limitation and temperature on the fractionation of sulfur isotopes by a deep-sea hydrothermal vent sulfate-reducing bacterium. Geochim. Cosmochim. Acta 70: 5831-5841.

Johnston DT, Farquhar J, Wing BA, Kaufman AJ, Canfield DE, Habicht KS. 2005. Multiple sulfur isotope fractionations in biological systems: A case study with sulfate reducers and sulfur disproportionators. Am. J. Sci. 305: 645-660.

Kaplan IR, Rittenberg SC. 1964. Microbiological fractionation of sulphur isotopes. J. Gen Microbiol. 34: 195-212.

Keller KL, Bender KS, Wall JD. 2009. Development of a markerless genetic exchange system for Desulfovibrio vulgaris Hildenborough and its use in generating a strain with increased transformation efficiency. Appl. Environ. Microbiol. 75: 7682-7691.

Keller KL, Wall JD. 2011. Genetics and molecular biology of the electron flow for sulfate respiration in Desulfovibrio. Front. Microbio. 2:135.

Kemp ALW, Thode HG. 1968. The mechanism of bacterial reduction of sulphate and of sulphite from isotope fractionation studies. Geochim. Cosmochim. Acta 32: 71-91.

Kleikemper J, Schroth MH, Bernasconi SM, Brunner B, Zeyer J. 2004. Sulfur isotope fractionation during growth of sulfate reducing bacteria on various carbon sources. Geochim. Cosmochim. Acta 68: 4891-4904.

Lyons TW. 1997. Sulfur isotopic trends and pathways of iron sulfide formation in upper Holocene sediments of the anoxic Black Sea. Geochim. Cosmochim. Acta 61: 3367-3382.

Mangalo M, Einsiedl F, Meckenstock RU, Stichler W. 2008. Influence of the enzyme dissimilatory sulfite reductase on stable isotope fractionation during sulfate reduction. Geochim. Cosmochim. Acta 71: 4161-4171.

Pereira IAC, Ramos AR, Grein F, Marques MC, Marques da Silva S, Venceslau SS. 2011. A comparative genomic analysis of energy metabolism in sulfate reducing bacteria and archaea. Front. Microbio. 2: 69.

Pohorelic BK, Voordouw JK, Lojou E, Dolla A, Harder J, Voordouw G. 2002. Effect of deletion of genes encoding Fe-only hydrogenase of Desulfovibrio vulgaris Hildenborough on hydrogen and lactate metabolism. J. Bacteriol. 184: 679-686.

Rabus R, Hansen TA, Widdel F. 2006. Dissimilatory sulfate- and sulfur- reducing prokaryotes. In The Prokaryotes (eds. Dworkin M, Falkow S, Rosenberg E, Schleifer KH, Stackbrandt E). Springer-Verlag, New York.

Rudnicki MD, Elderfield H, Spiro B. 2001. Fractionation of sulfur isotopes during bacterial sulfate reduction in deep ocean sediments at elevated temperatures. Geochim. Cosmochim. Acta 65: 777-789.

Walker CB, He Z, Yang ZK, Ringbauer JA, He Q, Zhou J, Voordouw G, Wall JD, Arkin AP, Hazen TC, Stolyar S, Stahl DA. 2009. The electron transfer system of syntrophically grown Desulfovibrio vulgaris. J. Bacterol. 191: 5793-5801.

Wortmann UG, Bernasconi SM, Bottcher ME. 2001. Hypersulfidic deep biosphere indicates extreme sulfur isotope fractionation during single-step microbial sulfate reduction. Geology 29: 647-650.

Zane GM, Bill Yen H, Wall JD. 2010. Effect of the deletion of qmoABC and the promoter-distal gene encoding a hypothetical protein on sulfate reduction in *Desulfovibrio vulgaris* Hildenborough. Appl. Environ. Microbiol. 76: 5500-5509.

Zerkle AL, Kamyshny A, Kump LR, Farquhar J, Oduro H, Arthur MA. 2010. Sulfur cycling in a stratified euxinic lake with moderately high sulfate: Constraints from quadruple S isotopes. Geochim. Cosmochim. Acta 74: 4953-4970.

2. Effect of Electron Donors on the Fractionation of Sulfur Isotopes by a Marine *Desulfovibrio* sp.

2.1. Abstract

Sulfur isotope effects produced by microbial dissimilatory sulfate reduction are used to reconstruct the coupled cycling of carbon and sulfur through geologic time, to constrain the evolution of sulfur-based metabolisms, and to track the oxygenation of Earth's surface. In this study, we investigate how the coupling of carbon and sulfur metabolisms in batch and continuous cultures of a recently isolated marine sulfate reducing bacterium DMSS-1, a *Desulfovibrio* sp., influences the fractionation of sulfur isotopes.

DMSS-1 grown in batch culture on seven different electron donors (ethanol, glycerol, fructose, glucose, lactate, malate and pyruvate) fractionates $^{34}S/^{32}S$ ratio from 6 to 44‰, demonstrating that the fractionations by an actively growing culture of a single incomplete oxidizing sulfate reducing microbe can span almost the entire range of previously reported values in defined cultures. The magnitude of isotope effect correlates well with cell specific sulfate reduction rates (from 0.7 to 26.1 fmol/cell/day). DMSS-1 grown on lactate in continuous culture produces a larger isotope effect (21-37‰) than the lactate-grown batch culture (6 ‰), indicating that the isotope effect also depends on the supply rate of the electron donor and microbial growth rate. The largest isotope effect in continuous culture is accompanied by measurable changes in cell length and cellular yield that suggest starvation. The use of multiple sulfur isotopes in the model of metabolic fluxes of sulfur shows that the loss of sulfate from the cell and the intracellular reoxidation of reduced sulfur species contribute to the increase in isotope effects in a correlated manner. Isotope fractionations produced during sulfate reduction in the pure culture of DMSS-1 expand the previously reported range of triple sulfur isotope effects (^{32}S, ^{33}S, and ^{34}S) by marine sulfate reducing bacteria, implying that microbial sulfur disproportionation may have a smaller ^{33}S isotopic fingerprint than previously thought.

2.2. Introduction

Microbial sulfate reduction (MSR) remineralizes organic compounds in anaerobic environments, controlling biogeochemical budgets of organic carbon and sulfur (e.g., Garrels and Lerman, 1981; Berner, 1989; Canfield, 2004; Wortmann and Chernyavsky, 2007). This process produces significant sulfur isotope effects, where the product sulfide (H_2S) is depleted in heavy isotopes, ^{33}S, ^{34}S, and ^{36}S with respect to the starting sulfate. The isotopic signatures of MSR can be recognized in dissolved sulfur species and sedimentary sulfides in nature (Fry, 1991; Canfield and Teske, 1996; Strauss, 1997;

Wortmann et al., 2001; Canfield and Farquhar, 2009). Over the past five decades, laboratory studies of pure and enrichment cultures of sulfate reducing microbes (SRM) have provided essential insights into biological sulfur isotope effects (e.g., Harrison and Thode, 1958; Kemp and Thode, 1968; Chambers et al., 1975; Canfield and Teske, 1996; Habicht and Canfield 1997; Bolliger et al., 2001; Canfield, 2001; Detmers et al., 2001; Kleikemper et al., 2004; Hoek et al., 2006; Davidson et al., 2009). In spite of this, a mechanistic understanding of factors that control the range of isotope fractionation in pure cultures and in nature is still lacking.

To date, a number of studies of the S-isotope effect in pure cultures have used *Desulfovibrio desulfuricans*. This bacterium generally produces the larger isotope effects at the lower cell specific sulfate reduction rates (csSRR, mole SO_4^{2-} reduced/cell/time, Kaplan and Rittenberg, 1964; Chambers et al., 1975). The csSRR is thus widely used as a parameter against which to compare isotope enrichment factors ($^{34}\varepsilon$, defined in section 2.4) produced by various sulfate reducing microbes (Harrison and Thode, 1958; Kemp and Thode, 1968; Chambers et al., 1975; Chambers and Trudinger, 1979; Habicht and Canfield, 1997; Bottcher et al., 1999; Hoek et al., 2006; Mangalo et al., 2007). Rees (1973) and Brunner and Bernasconi (2005) proposed metabolic flux models of sulfur, relating the overall isotope effect produced during sulfate reduction ($^{34}\varepsilon$) to the ratios of backward to forward flows (or reversibilities) between various sulfur reservoirs. Together, experimental observations and Rees's model suggested the existence of functional relationships among csSRR, reversibility and the magnitude of $^{34}\varepsilon$ values. Recent studies using oxygen (^{17}O and ^{18}O) and/or sulfur isotopes (^{33}S, ^{34}S, and ^{36}S) explored this relationship in pure cultures (Johnston et al., 2007; Mangalo et al., 2007, 2008) and in natural population (Wortmann et al., 2007; Farquhar et al., 2008), but the basis for the correlation between microbial growth conditions, csSRR and $^{34}\varepsilon$ remains unclear. Multiple studies thus questioned the adequacy of csSRR as a predictor for the magnitude of $^{34}\varepsilon$ both in culture and in nature (Bolliger et al., 2001; Bruchert et al., 2001; Detmers et al., 2001; Kleikemper et al., 2004; Mangalo et al., 2007).

The magnitude of $^{34}\varepsilon$ in nature and culture may depend on the availability and nature of organic matter (e.g., Bolliger et al., 2001; Bruchert et al., 2001; Canfield 2001; Kleikemper, 2004; Zerkle et al., 2010), but only a few studies of pure cultures systematically explored this relationship. Kaplan and Rittenberg (1964) found that *D. desulfuricans* produced a larger S-isotope effect when it used ethanol or lactate as an electron donor, than when it used molecular hydrogen (~15‰). In contrast, *Thermodesulfatator indicus* can deplete $^{34}S/^{32}S$ by an appreciable 37‰ in hydrogen-limited fed-batch cultures (Hoek et al., 2006). The dependence of the sulfur isotope effect on the substrate is also pronounced in the cultures of PRTOL1, a sulfate reducer that fractionates $^{34}S/^{32}S$ by 47‰ when it oxidizes toluene (Bolliger et al., 2001), but

produces a relatively small range of S-isotope effects (~ 33‰) when it uses acetate, pyruvate, benzoate or 3-phenylpropionate (Kleikemper et al., 2004). Generally, MSR limited by the low concentration of the electron donor yields higher fractionations than MSR that occurs in the presence of abundant electron donor (Canfield, 2001), but relationships between the type of electron donor and the fractionation of sulfur isotopes are poorly understood.

The magnitude of $^{34}\varepsilon$ in nature is also hypothesized to reflect biochemical differences among species (the "species effect", e.g., Bruchert et al., 2001). $^{34}\varepsilon$ values smaller than 18‰ are thus tentatively attributed to MSR by sulfate reducing microbes that cannot oxidize acetate to CO_2 and those larger than 18‰ as produced by microbes that oxidize acetate to CO_2 (Detmers et al., 2001). However, *D. desulfuricans*, an incompletely oxidizing organism, fractionates $^{34}S/^{32}S$ by anywhere from < 10‰ to as much as 46‰ when its dense resting suspensions are limited by the electron donor (Kaplan and Rittenberg, 1964). Even though it is questionable whether the upper end of this range (46‰) was produced under physiologically relevant conditions (Bruchert et al., 2001), the wide range of fractionations produced by *D. desulfuricans* underscores the importance of growth conditions to the magnitude of sulfur isotope effect even in incompletely oxidizing sulfate reducers.

Here, we investigate the relationship between the growth of a newly isolated marine sulfate reducing bacterium (*Desulfovibrio* sp., DMSS-1) on seven different electron donors and the resulting fractionation of sulfur isotopes. Focusing both on the nature of the electron donor, as well as on the rate at which this donor is supplied to the organism, we examine the S-isotope (^{32}S, ^{33}S, and ^{34}S) effect produced in batch cultures and in lactate-limited continuous cultures. Metabolic flux modeling with multiple sulfur isotopes allows us to examine the effect of electron donors on the magnitude of isotope fractionation in terms of the ratio of forward and backward fluxes in MSR pathway. Finally, we compare and contrast the S-isotope signatures produced by DMSS-1 to the previous studies of sulfur isotope systematics from modern and ancient environments.

2.3. Methods

2.3.1. Sampling and Isolation

Marine sulfate reducing microbes were enriched and isolated from upper 20 cm of surface sediment from a salt marsh in Cape Cod, Massachusetts, USA. A previous study reported the fractionation between sulfate and sulfide of 50.4‰ at this site (Peterson et al., 1986). Enrichment cultures were initially established in Postgate C medium (Postgate, 1984) as follows. Sediment was prepared as slurry in the

seawater from the same location. 5 ml of the slurry were inoculated into glass bottles containing 100 ml of medium with N_2 in the headspace, incubated at room temperature in the dark and transferred into a chemically-defined medium consisting of (per liter): $NaHCO_3$, 9g; Na_2SO_4, 3g; KH_2PO_4, 0.2g; NH_4Cl, 0.3g; NaCl, 21g; $MgCl_2 \cdot 6H_2O$, 3g; KCl, 0.5g; $CaCl_2 \cdot 2H_2O$, 0.15g; resazurin, 1 mg, as well as 1 ml of trace element solution SL-10 (Widdel et al., 1983), 10 ml of vitamin solution described as a part of DSMZ medium 141 (DSMZ, Braunschweig, Germany: Catalogue of strains 1993), and 1 ml of selenium stock solution (0.4mg of Na_2SeO_3 per 200 ml of 0.01N NaOH). Sodium ascorbate (1.5 g per liter) was added as a reducing agent. Lactate (20 mM) was used both as an electron donor and as a carbon source. The medium was titrated to pH 7.5 and prepared anaerobically under 80% N_2/20% CO_2.

Liquid SRM cultures established in the defined medium were used to inoculate deep agar shake tubes and obtain single colonies of SRM (Widdel and Bak, 1992). Defined medium with 2% agar was prepared as described above and dispensed into sterile Hungate tubes. Liquid enrichment culture was serially diluted into a series of Hungate tubes (deep agar shake tubes), the agar was allowed to solidify, and the tubes were incubated at room temperature in the dark for a week. A single sulfide-producing colony was picked from the agar by a sterile Pasteur pipette and inoculated into the liquid medium. This liquid culture was used as the inoculum for another set of serial dilutions in deep agar shake tubes to ensure the purification and the isolation of a single colony. The subsequent growth of this colony in the liquid medium yielded a culture of vibrio-shaped cells that do not form spores under our experimental conditions.

The purity of the isolate was confirmed by the amplification of the 16s rRNA gene with general bacterial primers 27F-1492R (Lane, 1991) using genomic DNA extracted from the liquid culture as a template. The amplification conditions were as previously described (Newberry et al., 2004; Webster et al., 2006) and yielded a 1450 base pair long product (Accession number JF968436) that was sequenced and found to be 90% similar to *Desulfovibrio* sp. To confirm that the amplification of the 16s rRNA gene yielded a single product, the product of the initial amplification was re-amplified by nested PCR with primers 357-518R by adding a GC-clamp to the 5′ end of the forward primers (Muyzer et al., 1993) as previously described (Webster et al., 2006) and analyzed by denaturing gradient gel electrophoresis (DGGE) using previously described conditions (Webster et al., 2006) (data not shown). To test whether any Archaea were present, the 16s rRNA gene from the genomic DNA isolated from the liquid culture was amplified separately with general archeal primers 109F-958R. This amplification did not yield any products, confirming that the culture did not contain any Archaea. Dissimilatory sulfite reductase gene (*dsrAB*) of the isolate was amplified using the genomic DNA as the template and primers Dsr1F (ACS

CAC TGG AAG CAC G) and Dsr4R (GTG TAG CAG TTA CCG CA) (Wagner et al., 1998) to determine its similarity to the *dsrAB* genes of other sulfate reducing microbes. The resulting sequence (Accession number JF968437) was 767 bp long and 97% similar (with a query coverage of 100%) to a *Desulfovibrio desulfuricans* subsp. *desulfuricans* (Accession number AF334592). We proceed to call this isolate DMSS-1 (*see Electronic annex*).

2.3.2. Culture Experiments

Batch Cultures

DMSS-1 was incubated in batch cultures to test the effect of seven different electron donors on the fractionation of sulfur isotope ratios. Each of these cultures contained basal medium buffered by bicarbonate and one of the following: lactate (20 mM), malate (17 mM), ethanol (20 mM), glycerol (10 mM), pyruvate (30 mM), fructose (8.5 mM), and glucose (8.5 mM). These organic compounds served both as electron donors and as carbon sources. A set of 10-ml vials containing each electron donor was inoculated with 5% v/v of mid- to late-exponential phase cells of DMSS-1 from a culture that had been grown on the same electron donor. All vials were incubated at room temperature (20 °C). Growth (optical density and cell counts) and hydrogen sulfide concentration were monitored by sacrificing a vial. Sulfide concentration was measured in 200 µL culture samples by fixing H_2S by 1 ml of 0.05 M Zn-acetate solution and using a modified methylene blue assay (Cline, 1969). Growth was monitored by measuring the optical density at 630 nm (using the Synergy2 Biotek microplate reader, BioTek, VT, USA) and by microscopic counts of cells stained by SYTOX-Green nucleic acid stain (Invitrogen S7020, Paisley, UK) using a Zeiss Axio Imager M1 epifluorescence microscope (Carl Zeiss, Thornwood, NY, USA). The onset of the exponential phase during growth on each electron donor was determined from growth curves (Fig. 2.1, Table 2.A1). The onset was the first time point after which cell densities increased exponentially (day 1). Growth rates on each substrate were determined before isotope sampling experiments to ensure the appropriate frequency of sampling. Because cellular yield (i.e., the synthesis of cellular biomass) varies with varying cell sizes, the length of vibrio-shaped cells was determined from the same images by approximating a curve with several straight lines. The size of cells varied demonstrably only during growth at the lowest dilution rate in the continuous culture (Table 2.1). After the subsampling, 2 ml of 1 M Zn-acetate were added to terminate microbial activity in each 10 ml vial and to precipitate dissolved sulfide as zinc sulfide (Detmers et al., 2001). These samples were stored at 4°C until the extraction of sulfur and the subsequent isotope analysis.

Continuous Cultures

A flow-through culture was established to examine the effect of limitation by the electron donor on isotope fractionation. The reactor was continuously flushed by 80% N_2/20% CO_2 to buffer the pH and to strip the sulfide. Sulfide was sampled by bubbling through a 0.18 M zinc acetate solution. Basal defined medium containing 3.5 mM lactate and 21 mM sulfate was prepared as described above and pumped into and out of a 500 ml reactor by a peristaltic pump. The 500 ml reactor was inoculated by the addition of 200 ml of early stationary phase cells (~ 10^8 cells/ml) from a culture grown on lactate. The flow was started after the cell density increased by more than 20%. Cell density was monitored daily until it stopped changing for at least three successive days, indicating a steady state.

2.3.3. Isotope Analysis

Sulfide from batch cultures was extracted by acidifying the culture medium with 6N HCl at 80°C under nitrogen gas for two hours. H_2S(g) produced during this distillation was precipitated as ZnS in a Zn-acetate solution (0.18 M). After the extraction of sulfide, the samples were purged by nitrogen gas for an additional hour to ensure the removal of sulfide. Sulfate in the remaining medium was reduced to sulfide by reacting with 30 ml of the reducing agent (mixture of HI, H_3PO_2 and HCl, Thode et al., 1961). The samples were boiled and purged by N_2 gas. After the volatile products were passed through a condenser and a trap containing distilled water, the H_2S(g) was collected in the Zn-acetate trap. H_2S(g) from continuous cultures was collected directly by passing the effluent gas through a sulfide trap containing a 0.18 M Zn-acetate solution. Sulfate was extracted from a 2-3 ml sample of the effluent as described above.

ZnS produced in the trap was converted to Ag_2S by the addition of $AgNO_3$ and the incubation at 70 °C for one day. Ag_2S was centrifuged, washed with distilled water three times and dried at 70 °C. For isotope measurements, Ag_2S samples were reacted with an excess of fluorine gas for more than 5 hours at 300°C, and the produced SF_6 was purified by gas chromatography. The purified SF_6 was transferred into an isotope-ratio mass spectrometer for multiple sulfur isotope measurements in dual inlet mode (Ono et al., 2006). The analytical reproducibility of measurements using the fluorination method, as determined by repeated analyses of international reference material, is ±0.1‰, ±0.2‰, and ±0.01‰ (2σ) for $\delta^{33}S$, $\delta^{34}S$, and $\delta^{33}S$-0.515·$\delta^{34}S$, respectively.

2.3.4. Data Processing

Specific growth rates (day^{-1}) of exponentially growing cells in batch cultures were calculated as:

$$k = \frac{\ln(c_x) - \ln(c_1)}{t_x - t_1} \quad (1)$$

where t_1 and t_x are the start of exponential growth and the time of sampling (in days), respectively, and C_1 and C_x are cell densities (number of cells/ml) at time t_1 and t_x, respectively. The exponential growth of DMSS-1 started within 24 hours after the inoculation (Fig. 2.1), so the first day after the inoculation (day 1) was set as t_1 (Table 2.1). Growth yield (number of cells/mol of reduced SO_4^{2-}) during the same interval was calculated as the ratio of the increase in the number of cells and of the sulfate consumed (sulfide produced, in moles) (Table 2.1):

$$Y = \frac{C_x - C_1}{[H_2S]_x - [H_2S]_1} \quad (2)$$

The average cell-specific sulfate reduction rates (csSRR) were calculated from the specific growth rate and the growth yield:

$$csSRR = \frac{k}{Y} = \frac{\ln(c_x) - \ln(c_1)}{t_x - t_1} \cdot \frac{[H_2S]_x - [H_2S]_1}{c_x - c_1} \quad (3)$$

In previous studies, csSRR was calculated by assuming a linear increase in cell density with time (e.g., Detmers et al., 2001). Equations 1 and 3 assume a more realistic exponential increase of cell numbers during the exponential growth phase. The two equations yield similar values of csSRR when t_x-t_1 is small, but the linear approximation yields lower values when applied to the entire exponential growth phase.

Sulfur isotopic compositions are reported using conventional delta notation

$$\delta^x S = 1000 \cdot \left(\frac{{}^x R_{sample}}{{}^x R_{reference}} - 1\right) \quad (4)$$

where ${}^xR$ are the isotopic ratios (${}^xS/{}^{32}S$, where x = 33, 34) of sample and reference materials. In this study, the isotopic ratios are reported with respect to the laboratory working reference SF_6.

The isotope fractionation factor (α) in the batch culture experiment was calculated based on the Rayleigh distillation equation, assuming the isotope mass balance between sulfate and sulfide during MSR (Hoek et al., 2006; Johnston et al., 2007).

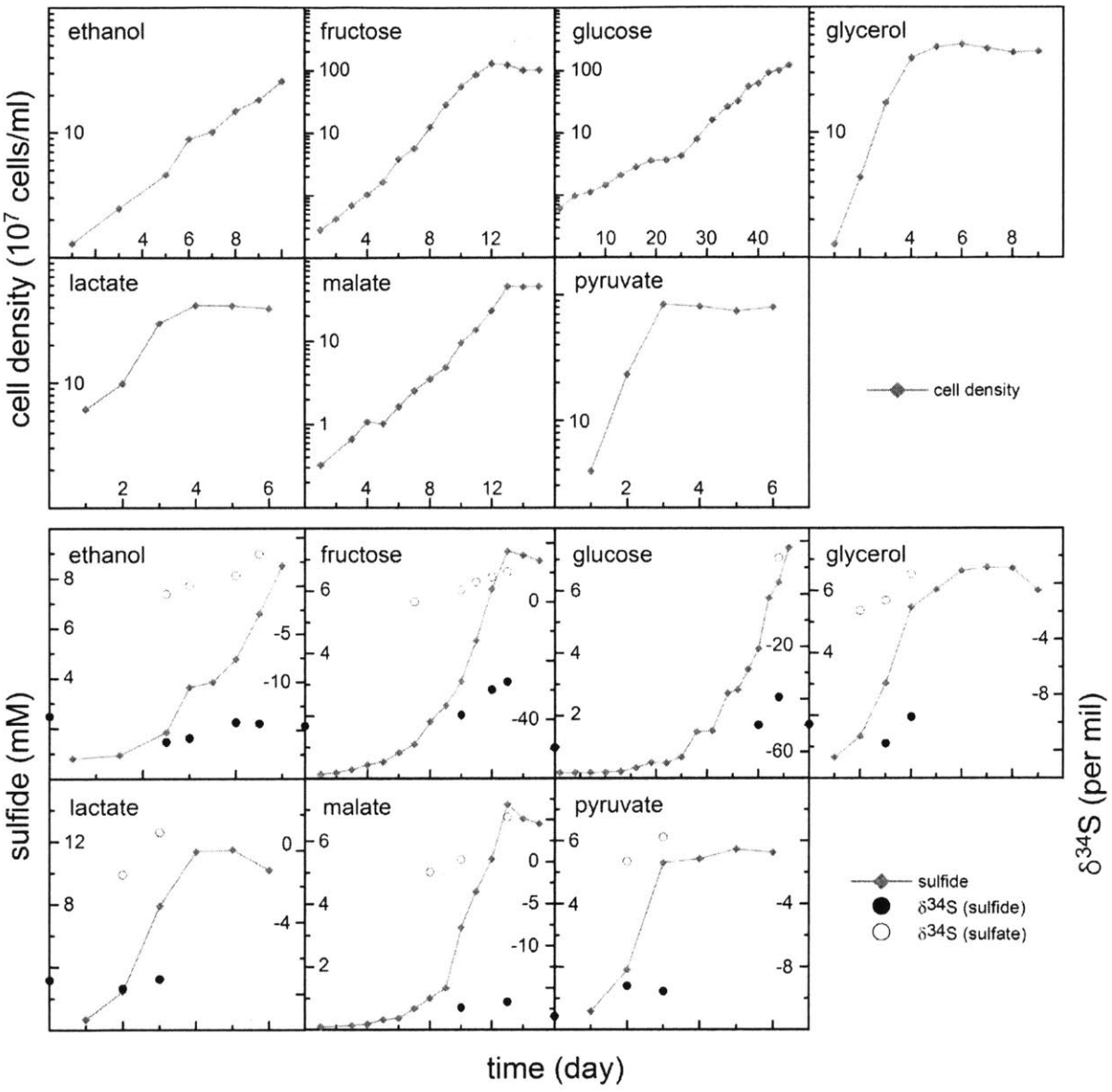

Figure 2.1. Growth of DMSS-1 on various electron donors in batch cultures. Upper panels show the cell density. Lower panels show the concentration of sulfide and isotope compositions of the sulfur species. The time scale of growth and sulfide production differs among individual electron donors. The time scales are identical for the upper and the lower panels corresponding to the same electron donor. Cell density is subject to a ±15% error, and the analytical uncertainty of the measurement of sulfide concentrations is ±5%.

electron donor		time (day)	cell density (10^7 cells/ml)	sulfide (mM)	f	growth rate (day^{-1})	growth yield (10^6cells/μmole SO_4)	csSRR (fmol/cell/day)	cell length (μm)	sulfide $\delta^{33}S$	sulfide $\delta^{34}S$	sulfate $\delta^{33}S$	sulfate $\delta^{34}S$	$^{34}\varepsilon$	^{33}E	$^{33}\lambda$
batch culture	ethanol	0		0.4	1.00					-6.98	-13.52					
		1	1.3	0.8	0.98											
		5	4.6	1.9	0.93	0.32 ± 0.05	31 ± 13	10.1 ± 4.6		-8.35	-16.20	-0.44	-0.79	15.5 ± 0.4	-0.055 ± 0.019	0.5114 ± 0.0012
		6	8.9	3.6	0.84	0.39 ± 0.04	27 ± 6	14.4 ± 3.4		-8.13	-15.78	0.02	0.09	14.8 ± 0.3	-0.061 ± 0.016	0.5109 ± 0.0010
		8	15.0	4.8	0.79	0.35 ± 0.03	34 ± 6	10.1 ± 2.0		-7.28	-14.15	0.55	1.13	13.7 ± 0.3	-0.065 ± 0.013	0.5102 ± 0.0010
		9	18.4	6.6	0.70	0.33 ± 0.03	30 ± 5	11.2 ± 2.0		-7.35	-14.27	1.69	3.33	14.7 ± 0.3	-0.050 ± 0.012	0.5116 ± 0.0008
	fructose	0		0.1	1.00					-21.76	-42.12					
		1	0.3	0.1	1.00											
		7	5.7	1.1	0.95	0.50 ± 0.04	56 ± 9	9.0 ± 1.6				0.01	0.07			
		10	55.3	3.1	0.86	0.59 ± 0.02	186 ± 30	3.2 ± 0.5		-19.87	-38.41	2.11	4.12	39.3 ± 0.3	-0.108 ± 0.016	0.5122 ± 0.0004
		11	85.8	4.4	0.79	0.57 ± 0.02	200 ± 32	2.9 ± 0.5				3.52	6.84			
		12	129.6	6.1	0.71	0.56 ± 0.02	219 ± 35	2.6 ± 0.4		-15.36	-29.80	4.35	8.50	32.2 ± 0.3	-0.114 ± 0.012	0.5115 ± 0.0004
		13	124.6	7.3	0.66	0.51 ± 0.02	174 ± 28	2.9 ± 0.5		-13.98	-27.12	5.31	10.35	30.4 ± 0.5	-0.094 ± 0.012	0.5119 ± 0.0004
	glucose	0		0.1	1.00					-30.37	-58.26					
		1	0.6	0.2	1.00											
		40	60.8	4.1	0.81	0.12 ± 0.01	153 ± 23	0.8 ± 0.1		-25.90	-49.81					
		44	97.6	6.3	0.70	0.12 ± 0.00	160 ± 25	0.7 ± 0.1		-20.32	-39.25	7.10	13.76	44.1 ± 0.4	-0.089 ± 0.012	0.5130 ± 0.0003
	glycerol	0		0.3	1.00					-5.21	-10.12					
		1	1.3	0.7	0.98											
		2	4.4	1.3	0.95	1.24 ± 0.21	47 ± 9	26.1 ± 6.5				-1.01	-1.95			
		3	17.3	3.0	0.87	1.30 ± 0.11	68 ± 11	19.3 ± 3.5		-5.98	-11.51	-0.67	-1.21	9.8 ± 0.3	-0.009 ± 0.016	0.5141 ± 0.0016
		4	39.3	5.5	0.75	1.14 ± 0.07	79 ± 13	14.4 ± 2.5		-4.95	-9.60	0.34	0.70	8.9 ± 0.3	-0.023 ± 0.012	0.5124 ± 0.0014
	lactate	0		0.4	1.00					-3.74	-7.23					
		1	6.1	0.7	0.98											
		2	9.9	2.4	0.90	0.48 ± 0.21	21 ± 13	22.4 ± 16.6		-3.95	-7.67	-0.71	-1.34	6.1 ± 0.3	-0.037 ± 0.015	0.5090 ± 0.0024
		3	30.0	7.9	0.63	0.79 ± 0.11	33 ± 6	24.1 ± 5.4	2.34 ±0.47	-3.69	-7.15	0.49	1.02	6.5 ± 0.3	-0.032 ± 0.012	0.5101 ± 0.0017
	malate	0		0.0	1.00											
		1	0.3	0.1	1.00											
		8	3.5	1.0	0.95	0.34 ± 0.04	34 ± 5	10.0 ± 1.8				-0.64	-1.19			
		10	9.5	3.2	0.85	0.38 ± 0.02	29 ± 5	13.0 ± 2.6		-8.94	-17.32	0.10	0.26	16.2 ± 0.3	-0.050 ± 0.013	0.5119 ± 0.0008
		13	44.8	7.2	0.66	0.41 ± 0.02	83 ± 10	6.6 ± 1.1		-8.56	-16.64	2.71	5.36	18.0 ± 0.3	-0.082 ± 0.012	0.5104 ± 0.0006
	pyruvate	0		0.3	1.00					-5.74	-11.13					
		1	3.9	0.6	0.98											
		2	23.3	1.9	0.92	1.78 ± 0.21	147 ± 95	12.1 ± 7.9		-4.73	-9.19	-0.71	-1.32	7.3 ± 0.3	-0.046 ± 0.017	0.5086 ± 0.0023
		3	84.2	5.3	0.76	1.53 ± 0.11	170 ± 34	9.0 ± 1.9		-4.91	-9.54	0.08	0.22	8.5 ± 0.3	-0.042 ± 0.013	0.5101 ± 0.0015
lactate continuous culture ($0.07\ day^{-1}$)						0.07	39 ± 6	1.7 ± 0.3	1.77 ±0.22	-18.77	-36.19	0.63	1.28	37.4 ± 0.3	-0.063 ± 0.015	0.5133 ± 0.0004
lactate continuous culture ($0.12\ day^{-1}$)						0.12	63 ± 12	1.9 ± 0.3	1.94 ±0.32	-18.19	-35.22	0.28	0.60	35.8 ± 0.3	-0.123 ± 0.015	0.5116 ± 0.0004
lactate continuous culture ($0.48\ day^{-1}$)						0.48	65 ± 19	7.4 ± 2.1	2.35 ±0.42	-11.06	-21.48	-0.28	-0.48	21.0 ± 0.3	-0.093 ± 0.014	0.5106 ± 0.0007

Table 2.1. Growth parameters and isotopic data from batch and continuous cultures. Errors (excluding the measurements of cell length) were propagated from analytic uncertainties of cell density, sulfide, and isotope measurements. Errors of cell length are reported as standard deviation (n>70). Growth rate, yield, csSRR, 34ε, 33E, and 33λ, are accumulative (i.e., calculated up to the day of sampling). Isotope composition of the initial sulfide (day=0) was measured in the inoculum, and 5 % of the inoculum was added to inoculate the fresh medium (v/v).

$$\alpha = -\frac{1}{\ln f_r} \ln\left(1 + \frac{(1-f_r)}{f_r} \frac{\delta_{\Delta p} + 1000}{\delta_r + 1000}\right) \quad (5)$$

where f_r is the fraction of the remaining sulfate, and δ_r and $\delta_{\Delta p}$ are sulfur isotope compositions (^{33}S or ^{34}S) of the sulfate remaining at the time of sampling (t_x) and the sulfide produced between the day of inoculation (day 0) and the day of sampling (t_x), respectively (Table 2.1). The value of $\delta_{\Delta p}$ was derived using isotope mass-balance using the concentration and $\delta^x S$ of sulfide in the inoculum (5% v/v inoculum/fresh medium) and the corresponding measurements from the culture medium at the time of sampling (Table 2.1). When the value of f_r is larger than 0.5, this equation more accurately calculates fractionation than that using only sulfate isotope compositions. Because of the initial lag phase in growth (day 0 - day 1), growth parameters were estimated from day 1 to t_x. The values of α, however, were calculated using the isotope measurements from day 0 because sulfide concentrations on day 1 were usually too low to allow precise isotopic measurements (Table 2.1). In a strict sense, Eq. 5 assumes a constant α value between two time points. Therefore, when α changes over the course of experiment (e.g., fructose), this equation estimates the α value averaged over time, resulting in the observed net fractionation.

Isotope fractionation factors in continuous cultures at the steady state were calculated according to:

$$^x\alpha = \frac{\delta^x S_{HS} + 1000}{\delta^x S_{SO_4} + 1000} \quad (6)$$

where, x is 33 or 34.

The isotope enrichment factor is defined as:

$$^x\varepsilon = 1000 \cdot (1 - {}^x\alpha) \quad (7)$$

In this definition, positive values represent the depletion of heavy isotopes in the product.

To characterize the mass-dependent fractionation for sulfate reduction, $^{33}\lambda$ values are defined as:

$$^{33}\lambda = \frac{\ln(^{33}\alpha)}{\ln(^{34}\alpha)} \quad (8)$$

and ^{33}E values are calculated as:

$$^{33}E = 1000 \cdot (^{33}\alpha - ^{34}\alpha^{0.515}) \quad (9)$$

According to the above definition, ^{33}E values are negative when the product is enriched in ^{33}S with respect to the canonical mass-dependence. This convention was previously used by Johnston et al. (2007)

To estimate errors for batch cultures, $^{34}\varepsilon$, $^{33}\lambda$, and ^{33}E values, errors from isotope analysis (0.1‰ for $\delta^{33}S$, 0.2‰ for $\delta^{34}S$, and 0.01‰ for $\delta^{33}S - 0.515 \cdot \delta^{34}S$) and sulfide concentration measurement (±5%) were propagated according to the methods described by Bevington and Robinson (2002).

2.4. Results

2.4.1 Growth Kinetics and Yields

The isolated strain, DMSS-1, reduced sulfate to sulfide using various organic compounds or hydrogen as electron donors (Table 2.2). Its growth rates varied by an order of magnitude, with a maximum during the growth on pyruvate (1.78 day^{-1}) and a minimum during the growth on glucose (0.12 day^{-1}) (Fig. 2.1 and Table 2.1). After the inoculation, the exponential growth started within 24 hours and continued until DMSS-1 depleted the electron donor, as predicted by the stoichiometry of the reactions for cultures limited by various electron donors (Fig. 2.1 and Table 2.3). The cell yield varied from 21 to 219 x 10^6 cells/μmole SO_4 depending on the electron donor (Table 2.1). The csSRRs ranged from 0.7 fmol/cell/day to 26.1 fmol/cell/day with the lowest csSRRs observed during the growth on hexose sugars (fructose and glucose) (Table 2.1).

The concentration of lactate in the continuous culture was always lower than 300 μM (the detection limit is less than 5μM). Due to the vigorous bubbling with 80% N_2/20% CO_2, the concentration of sulfide in the reactor was lower than 60 μM throughout the incubation (the detection limit is 50 μM). Lactate-limited chemostat experiments yielded a steady-state csSRR that increased with the increasing dilution rate (flow rate divided by the volume of reactor) and ranged from 1.7 to 7.4 fmol/cell/day (Table 2.1). The growth yields in continuous cultures were between 39 and 65 x 10^6 cells/mole SO_4 (Table 2.1). At higher dilution rates (0.48 and 0.12 day^{-1}), the growth yields in the continuous culture exceeded the yield in batch cultures grown on lactate (31 x 10^6 cells/mole). The average length of DMSS-1 cells at the highest dilution rate (2.35 ± 0.42 μm, N=109) was comparable to that in batch culture (2.34 ± 0.47 μm, N=111), but the cells were shorter at the lowest dilution rate (1.8 ± 0.22 μm, N=85) ($p < 0.05$, t-test) (Table 2.2). Thus, less biomass (dry weight) was synthesized at the lowest dilution rate than in batch culture even though the two cultures contained the same number of cells per ml.

substrate	growth
acetate	-
ascorbate	-
ethanol	+
fructose	+
glucose	+
glycerol	++
hydrogen/acetate	+
lactate	++
malate	+
pyruvate	++
succinate	-
sucrose	-

Table 2.2. Growth of DMSS-1 on various organic and inorganic substrates. ++, cell density more than doubled in one week; +, cell density doubled at least in two weeks; -, no growth [cell density either decreased or remained unchanged within the limit of experimental error (15%) over the course of one month.

electron donor	reaction	ΔGo' (KJ/reaction)	ΔG (KJ/reaction)
ethanol	$2ethanol + SO_4^{2-} \rightarrow 2acetate^- + HS^- + H^+ + 2H_2O$	-131.6	-136.4
fructose	$fructose + SO_4^{2-} \rightarrow 2acetate^- + 2HCO_3^- + HS^- + 3H^+$	-360.1	-393.5
glucose	$glucose + SO_4^{2-} \rightarrow 2acetate^- + 2HCO_3^- + HS^- + 3H^+$	-358.3	-391.6
glycerol	$4/3glycerol + SO_4^{2-} + \rightarrow 4/3acetate^- + 4/3HCO_3^- + HS^- + 5/3H^+ + 4/3H_2O$	-264.9	-280.9
lactate	$2lactate^- + SO_4^{2-} \rightarrow 2acetate^- + 2HCO_3^- + HS^- + H^+$	-160.1	-176.3
malate	$2malate^{2-} + SO_4^{2-} + 2H_2O \rightarrow 2acetate^- + 4HCO_3^- + HS^- + H^+$	-204.9	-233.2
pyruvate	$4pyruvate^- + SO_4^{2-} + 4H_2O \rightarrow 4acetate^- + 4HCO_3^- + HS^- + 3H^+$	-340.7	-375.8

Table 2.3. Free energy released by the incomplete oxidation of electron donors used in this study coupled with the reduction of sulfate. The calculations assume standard conditions [ΔGo'; pH = 7, T = 298.15 K, aqueous concentration of reactants and products (except for H+) = 1 M] or actual conditions (ΔG). The stoichiometry of individual reactions is based on previous studies of incompletely oxidizing strains (Cord-Ruwisch et al., 1986; Kremer and Hansen, 1987; Kremer et al., 1989; Fareleira et al., 1997; Detmers et al., 2001). Standard free energy values from Thauer et al. (1977).

2.4.2 Fractionation of Sulfur Isotopes

The calculated enrichment factors ($^{34}\varepsilon$) varied from 6.1‰ in lactate-grown cultures to 44.1‰ in glucose-grown cultures (Fig. 2.2). $^{34}\varepsilon$ values calculated at various time points during the exponential growth phase varied by less than 1.8‰ for all electron donors other than fructose (Table 2.1). In contrast, the $^{34}\varepsilon$ value for fructose batch culture decreased by ~10‰ over the course of experiment (Table 2.1). Currently, the reasons behind this decrease in $^{34}\varepsilon$ values are unknown, but this trend was reproduced in two subsequent experiments. The isotope enrichment factor ($^{34}\varepsilon$) in lactate-limited continuous cultures increased from 21.0‰ at dilution rate 0.48/day to a maximum of 37.4‰ at dilution rate 0.07/day (Fig. 2.2). In both batch and continuous cultures, the magnitude of isotope fractionation ($^{34}\varepsilon$) produced by DMSS-1 was inversely related to csSRR (Fig. 2.3).

DMSS-1 mass-dependently fractionated $^{32}S/^{33}S/^{34}S$ triple isotope ratios, here presented as ^{33}E from -0.009‰ to -0.123‰ (Fig. 2.2). In general, the values of ^{33}E linearly decreased with an increasing $^{34}\varepsilon$ and attained a plateau at $^{34}\varepsilon$ larger than 20‰.

2.5. Discussion

2.5.1. Effect of Electron Donors on the Magnitude of Isotope Fractionation

The isotope enrichment factor ($^{34}\varepsilon$) produced by DMSS-1 in this study ranges from 6.1 to 44.1‰ and spans nearly the entire range of fractionation factors reported by previous laboratory studies of defined cultures under controlled conditions (Kaplan and Rittenberg, 1964; Chambers et al., 1975; Bolliger et al., 2001; Detmers et al., 2001; Hoek et al., 2006; Johnston et al., 2007; Mangalo et al., 2007; Davidson et al., 2009). Therefore, our study demonstrates that the variations in isotope fractionation produced by a single SRM grown on different organic substrates can be as large as the interspecies variations. The highest previously reported fractionations were observed in the pure cultures of completely oxidizing strains that grew on aromatic substrates such as toluene (Bolliger et al., 2001; Detmers et al., 2001), or in very dense resting suspensions of an incompletely oxidizing strain, *D. desulfuricans* that coupled very low sulfate reduction rates with the oxidation of ethanol (Kaplan and Rittenberg, 1964). Bruchert et al. (2001) questioned whether the latter experiments by Kaplan and Rittenberg (1964) reflected physiologically relevant and unstressed conditions. Our results demonstrate that an incompletely oxidizing strain can deplete ^{34}S by ~ 44‰ during active growth. DMSS-1 produces the highest

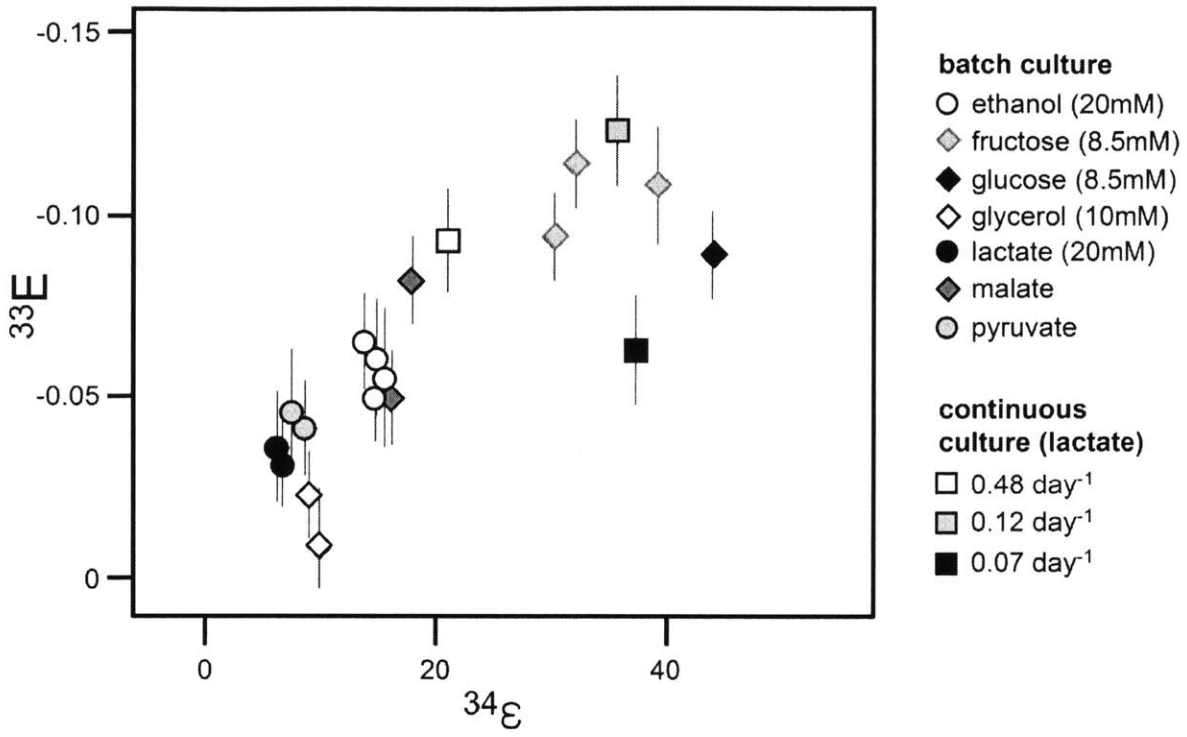

Figure 2.2. $^{34}\varepsilon$ vs. ^{33}E produced by DMSS-1 growing on different electron donors in batch cultures or growing at different rates in the lactate-limited continuous culture. In batch cultures, multiple data points for one electron donor indicate different stages of exponential growth phase.

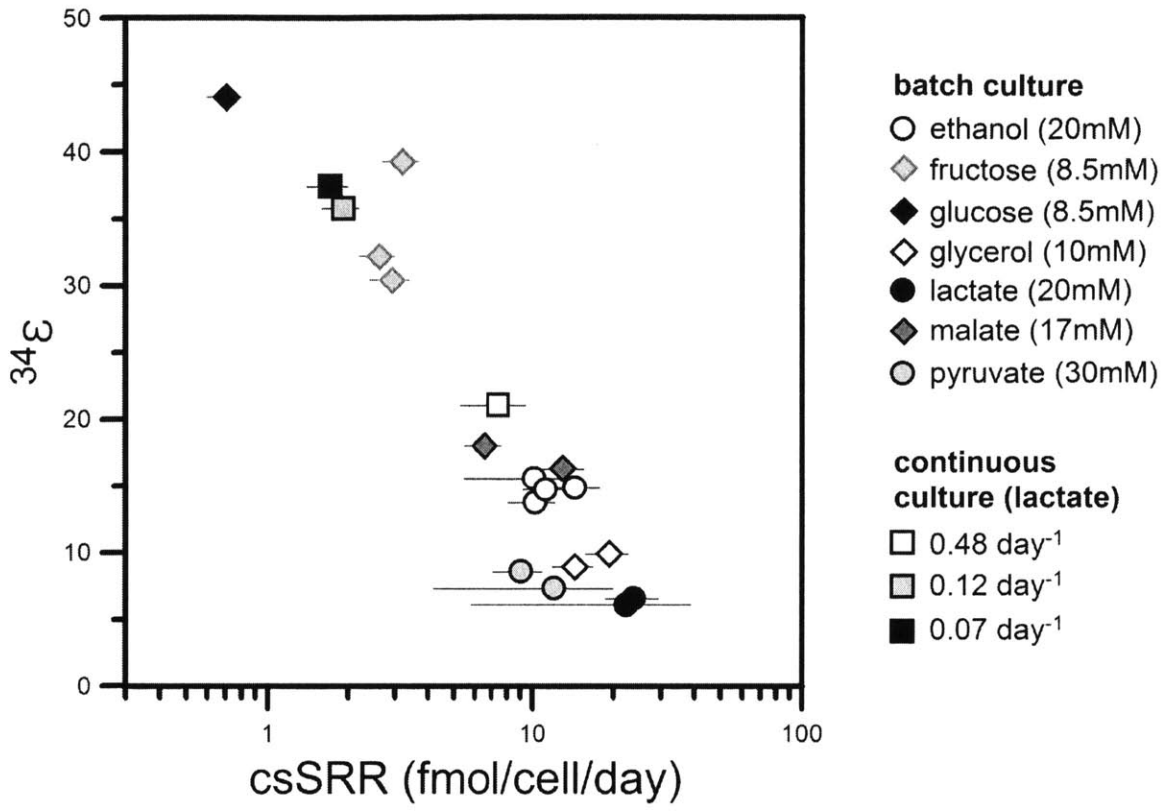

Figure 2.3. Correlation between isotope fractionation ($^{34}\varepsilon$) produced by DMSS-1 and cell-specific sulfate reduction rate (csSRR).

$^{34}\varepsilon$ values in cultures grown on hexose sugars, suggesting that some of the high values of $^{34}\varepsilon$ in nature may be due to the degradation of similar substrates, including sugary matrices of natural biofilms (Jeanloz, 1967; Vu et al., 2009) by SRM. To the best of our knowledge, this is the first report of fractionations during MSR coupled with the oxidation of glucose and fructose.

Our experiments highlight the difference between S-isotope effects produced in batch and continuous cultures. This difference was also observed in some previous studies (Chambers et al., 1975; Canfield, 2001; Hoek et al., 2006; Davidson et al., 2009). When SRMs grow in batch cultures, the concentrations of the electron donor and sulfate decrease and those of sulfide and excreted organics increase. Consequently, isotope effects in batch cultures are averaged over an array of changing culture conditions that include very large and environmentally unrealistic concentrations of organic substrates. In contrast, growth in continuous culture is a better representation of open natural systems and allows one to examine the fractionation by the same microbe as a function of very low growth rates and high growth rates, respectively. Growth of DMSS-1 in lactate-limited continuous culture thus results in > 15‰ larger fractionations relative to those produced in lactate-limited batch cultures (Fig. 2.2 and Table 2.1). The increasing fractionation in continuous lactate-limited cultures at decreasing dilution rates shows that SRM produce a larger S-isotope effect when their growth rates and csSRR are limited by the supply rates of electron donor (Tables 2.2). These observations are consistent with previous culture measurements (Chambers et al., 1975) and with the predictions of model studies for the relationship between the magnitude of S-isotope effect and the limitation of organic substrates (Rees, 1973; Brunner and Bernasconi, 2005). The relatively large S-isotope effects produced in the lactate-limited chemostat are also associated with observable changes in growth physiology: a 40% decrease in the cellular yield and a 25% decrease in the cell length at the lowest dilution rate (Table 2.1). The reduced cell length and cellular yield indicate that less cellular biomass is synthesized per mole of reduced sulfate, possibly as a result of starvation (Okabe et al., 1992; Matz and Jurgens, 2005). These starvation-related physiological changes may be responsible for the upper range of sulfur isotope effects in natural settings, because the largest isotope effects (Rudnicki et al., 2001) are reported in areas that receive very little organic matter (Barber, 1968; Goldhaber and Kaplan, 1975). This relationship between cell physiology at low dilution rates and large isotope effects merits further exploration.

Although the concentration of the electron donor can greatly influence the fractionation, the concentrations of different electron donors in batch cultures does not limit growth until the very end of the exponential phase (Fig. 2.1). Yet, when oxidizing sugars (glucose and fructose), DMSS-1 fractionates $^{34}S/^{32}S$ by > 12‰ more than when oxidizing alcohols (glycerol and ethanol) or organic acids (lactate, pyruvate, and malate). These differences in the magnitude of S-isotope effect among batch cultures show that the exact nature of electron donors can be as important as their concentrations in determining the magnitude of fractionation. The increase in isotope fractionation correlates well with the decrease in csSRR (Fig. 2.3), suggesting that the type of electron donor affects the isotope fractionation by controlling the metabolic fluxes in MSR pathway (as discussed later in Section 2.4.2). This may occur because the rate of carbon catabolism (uptake, activation, and oxidation of electron donor) dictates the rate at which electrons are supplied to the sulfate reducing pathway (Fig. 2.4). Therefore, refractory organic substrates ("slow food") would yield lower csSSR and results in larger isotope fractionations. Larger fractionations associated with "slow food" may explain why laboratory culture studies using simple organic acids or hydrogen have not approached large isotope fractionations observed in natural habitats where sulfate reducers are known to degrade more complex organic substances including long-chain saturated fatty acids and hydrocarbons, aromatic compounds, and sugars (Jørgensen, 1982; Reichenbecher and Schink, 1997; Widdel and Rabus, 2001; Rabus et al., 2006).

2.5.2. Analysis of Metabolic Sulfur Fluxes by Multiple Sulfur Isotopes

Initially developed by Rees (1973) and modified by Brunner and Bernasconi (2005), the model predicts $^{34}\varepsilon$ as a function of the ratio of forward and backward fluxes (reversibility) at several biochemical steps and confirmed intermediate species (e.g., Rabus et al. 2006) (Fig. 2.4). Recent studies using labeled oxygen isotopes (^{17}O and ^{18}O) provided independent tests for the Rees's model by demonstrating the relationship between the degrees of oxidative backward flux and the magnitude of $^{34}\varepsilon$ (Mangalo et al., 2007, 2008; Farquhar et al., 2008). Here, we use the metabolic sulfur flux model (Farquhar et al., 2007; Johnston et al., 2007) to investigate how the availability and the nature of the organic substrate alter the fluxes along each step of sulfate reduction and to predict the isotopic composition of intracellular sulfur species. In addition to

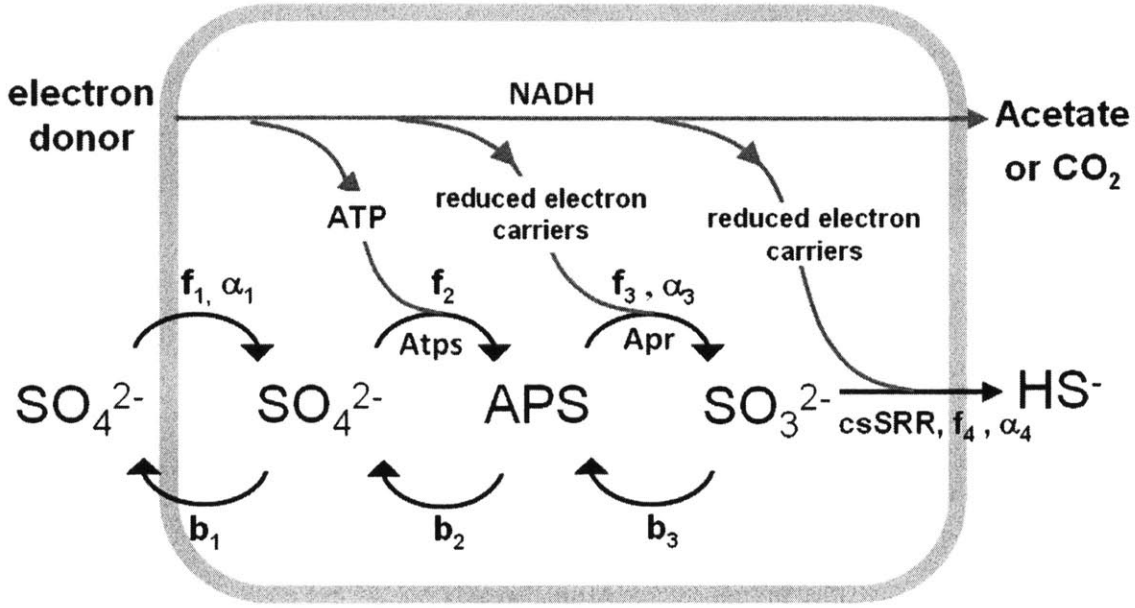

Figure 2.4. Schematic of biochemical pathways thought to influence the fractionation of sulfur isotopes during mSR. Grey box represents the cell wall, APS is adenosine-5'-phosphosulfate. Forward and backward mass flows among the reservoirs are shown as f_i and b_i (in e.g., moles/time), α represent isotope fractionation factors of enzymatic reactions thought to produce isotope fractionations. Reducing equivalents flow from the electron donor to sulfur through a series of carriers and enzymes (Rabus et al., 2006). The first enzymatic step in mSR is the transport of SO_4^{2-} into the cell, thought to involve only a small isotope effect (Rees, 1973). In the second step, ATP sulfurylase (Atps) activates SO_4^{2-} by consuming ATP (adenosine 5'-triphosphate) to form APS (e.g., Peck and LeGall, 1982; Akagi and Campbell 1962). APS is then reduced to sulfite by APS reductase (Apr) (Peck and LeGall, 1982) in a reaction that fractionates sulfur isotopes (Rees, 1973) and is thought to be reversible (Cypionka, 1995). Sulfite may be directly reduced to sulfide by dissimilatory sulfite reductase (Dsr). Alternatively, this reduction may proceed through trithionate ($S_3O_6^{2-}$) and thiosulfate ($S_2O_3^{2-}$) (Drake and Akagi, 1977; Fitz and Cypionka, 1990) or other sulfur intermediates (Cypionka et al., 1998). The actual importance of these intermediates and the biochemistry of their production remain debated (e.g., Rabus et al., 2006).

$^{34}S/^{32}S$ ratios, minor isotope fractionations can provide additional constraints on the reversibility of MSR (Farquhar et al., 2003; Ono et al., 2006; Johnston et al., 2007) because the mixing of different sulfur pools within the cell follows a linear relationship but the mass-dependent isotope fractionation of each step is defined by a power law (Young et al., 2002). Following Rees-Farquhar model (Rees, 1973; Farquhar et al., 2003; Farquhar et al., 2007), the field of steady state solutions for the overall sulfur isotope effect is constructed by assuming reversible fluxes at two branching points: the uptake of sulfate (with $\varphi_1 = f_1/b_1$) and the reduction of sulfate to sulfite (with $\varphi_3 = f_3/b_3$), respectively (Figs. 2.4 and 2.5A) (*See details in* Appendix A).

During growth on lactate in batch culture, the coupling of csSRR and the isotopic data predicts that the intracellular pools of sulfate and sulfite pools are enriched in ^{34}S (i.e., positive $\delta^{34}S$ values, Fig. 2.5B). This reflects the isotope mass-balance principle when the export of H_2S slightly depleted in ^{34}S compared to the initial sulfate exceeds the loss of intracellular SO_4^{2-} enriched in ^{34}S. Due to the enrichment of intracellular ^{34}S, the overall isotope fractionation is small (6.4‰). A considerably more reversible uptake and reduction of sulfate should occur during the growth on hexose sugars (Fig. 2.5B). During growth on glucose, the sulfate inside the cell should be only slightly (3.5‰) enriched in ^{34}S relative to sulfate in the medium because of the significant backflow of sulfate across the cell membrane (99%) (Fig. 2.5B). Furthermore, about half of the sulfite should be reoxidized to sulfate (Fig. 2.5B). Notably, maximum φ_3 calculated for our experimental conditions (50%, Fig. 2.5C) is considerably lower than the theoretical maximum of ~100%, when maximum isotope effects are expected to occur (Brunner and Bernasconi, 2005; Wortmann et al. 2007). This discrepancy between the theoretical maxima and observations indicates that even more reversible sulfate reduction is possible, although it has not been attained in pure culture. The consistency of slope between φ_1 and φ_3 (Fig. 2.5C) for most data points suggests that the nature of the electron donor regulates both branching points in a correlated manner. This applies to growth on almost all substrates and to both batch and continuous cultures.

The current metabolic model of MSR, which assumes a single step reduction between sulfite and sulfide, can accommodate most of the ($^{34}\varepsilon$, ^{33}E) measurements in this study (Fig. 2.5A). However, the inclusion of one more intermediate sulfur redox species in the model (Fig. 2.5D) expands the solution field to accommodate all ($^{34}\varepsilon$, ^{33}E) measurements. These intermediate steps

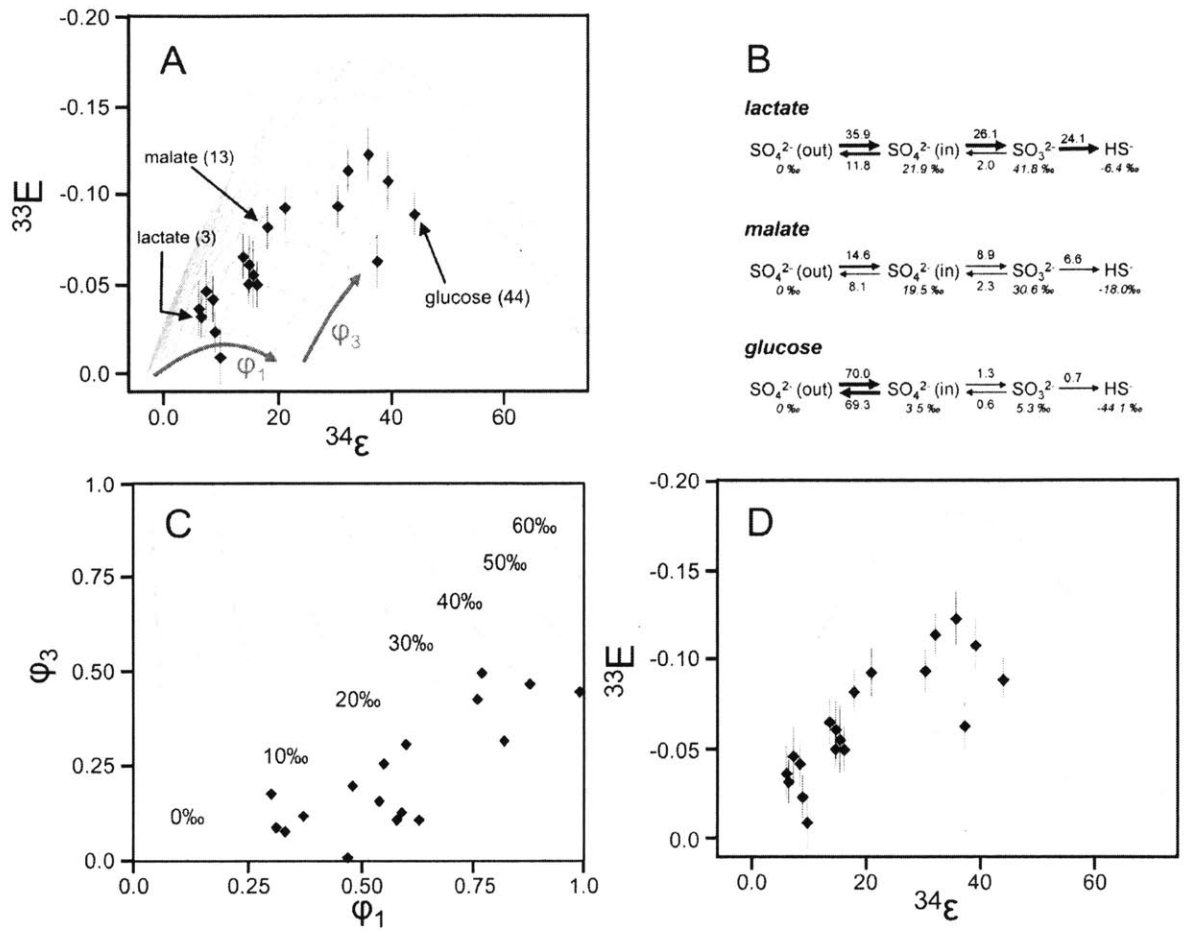

Figure 2.5. Plot of $^{34}\varepsilon$ vs. ^{33}E and the application of metabolic flux model to sulfur isotope effects produced by DMSS-1. (A) Solution field of the model compared to the experimental data from this study. The model is used to estimate the reversibility at two crucial steps in microbial sulfate reduction pathway: ϕ_1, the reversibility of sulfate uptake, and ϕ_3, the reversibility of the reduction of sulfate to sulfite. Black arrows show the model calculation for three electron donors and sampling dates for the flux calculation, shown in (B). (B) Fluxes of sulfur along each step of sulfate reduction (fmol/cell/day) and steady state $\delta^{34}S$ values of each sulfur pool (normalized to sulfate in the medium). The results are shown for three representative electron donors. (C) Reversibilities of sulfate uptake (ϕ_1) and the reduction of sulfate to sulfite (ϕ_3) associated with data points shown in (A) (except for two data points out of the solution field). Solid lines represent $^{34}\varepsilon$ as a function of both reversibilities. Note that even the largest isotope fractionations measured in this study are associated with values of ϕ_3 only about a half of the theoretical maximum. (D) $^{34}\varepsilon$ and ^{33}E plotted in the solution field of the model of MSR with three reversible steps (e.g., Brunners and Bernasconi, 2005). This model assumes that the reduction of sulfite to an undetermined species and the reduction of this species to sulfide fractionate equally (24‰). Solid lines represent the solution to the model with two reversible steps, broken lines show the expanded solution network with three reversible steps.

in sulfate reduction should be more important when the intracellular redox potential is high (Seki and Ishimoto, 1979). This may occur when microbial growth is limited by the supply rate of organic electron donor (i.e., slow dilution rate, Matin and Gottschal, 1976), but biochemical mechanisms that control the reversibility of individual steps during MSR remain poorly understood.

2.5.3. Correlation of csSRR to the Magnitude of S-isotope Effect

Since Harrison and Thode (1958) reported the correlation between $^{34}\varepsilon$ and the rate of sulfate reduction per unit biomass, many studies of MSR have attempted to correlate $^{34}\varepsilon$ and csSRR. Early studies growing *D. desulfuricans* on organic electron donors identified the inverse relationship between csSRR and $^{34}\varepsilon$ (Kaplan and Rittenberg, 1964; Chambers et al., 1975), but recent studies questioned this correlation both in single species grown under different conditions, and across different species (Detmers et al., 2001; Canfield et al., 2006; Johnston et al., 2007; Mangalo et al. 2007). Detmers et al. (2001) proposed a test by comparing the fractionations produced by a single strain grown on different substrates. Kleikemper et al. (2004) found the inverse relation between csSRR and $^{34}\varepsilon$ for a complete oxidizer, PRTOL1, grown on 5 different organic substrates, but questioned its statistical significance ($p=0.05$) (Fig. 2.6). Our results clearly demonstrate that $^{34}\varepsilon$ decreases with the increasing csSRR both during the growth of DMSS-1 on seven different organic electron donors (Figs. 2.3 and 2.6), and when its growth rate is regulated by the supply of a single electron donor. The latter results are consistent with those reported from *Desulfovibrio desulfuricans* (Chambers et al., 1975) and *Thermodesulfatator indicus* (Hoek et al., 2006) (Fig. 2.6). The comparison of the relationship between $^{34}\varepsilon$ and csSRR in different species shows that each of these species occupies the different region in the $^{34}\varepsilon$/csSRR diagram. Thus, the "species effect" may be most obvious in the slope of the relationship between csSRR and $^{34}\varepsilon$.

Not only do our measurements and modeling results show a correlation between $^{34}\varepsilon$ and csSRR, but they also show that even the individual steps in the MSR model (φ_1 and φ_3, respectively) correlate with csSRR (Fig. 2.7), accounting for the apparent correlation between csSRR and $^{34}\varepsilon$. This correlation is not readily apparent from metabolic modeling studies, which suggest that the magnitude of isotope fractionation inherently depends on the ratio of forward

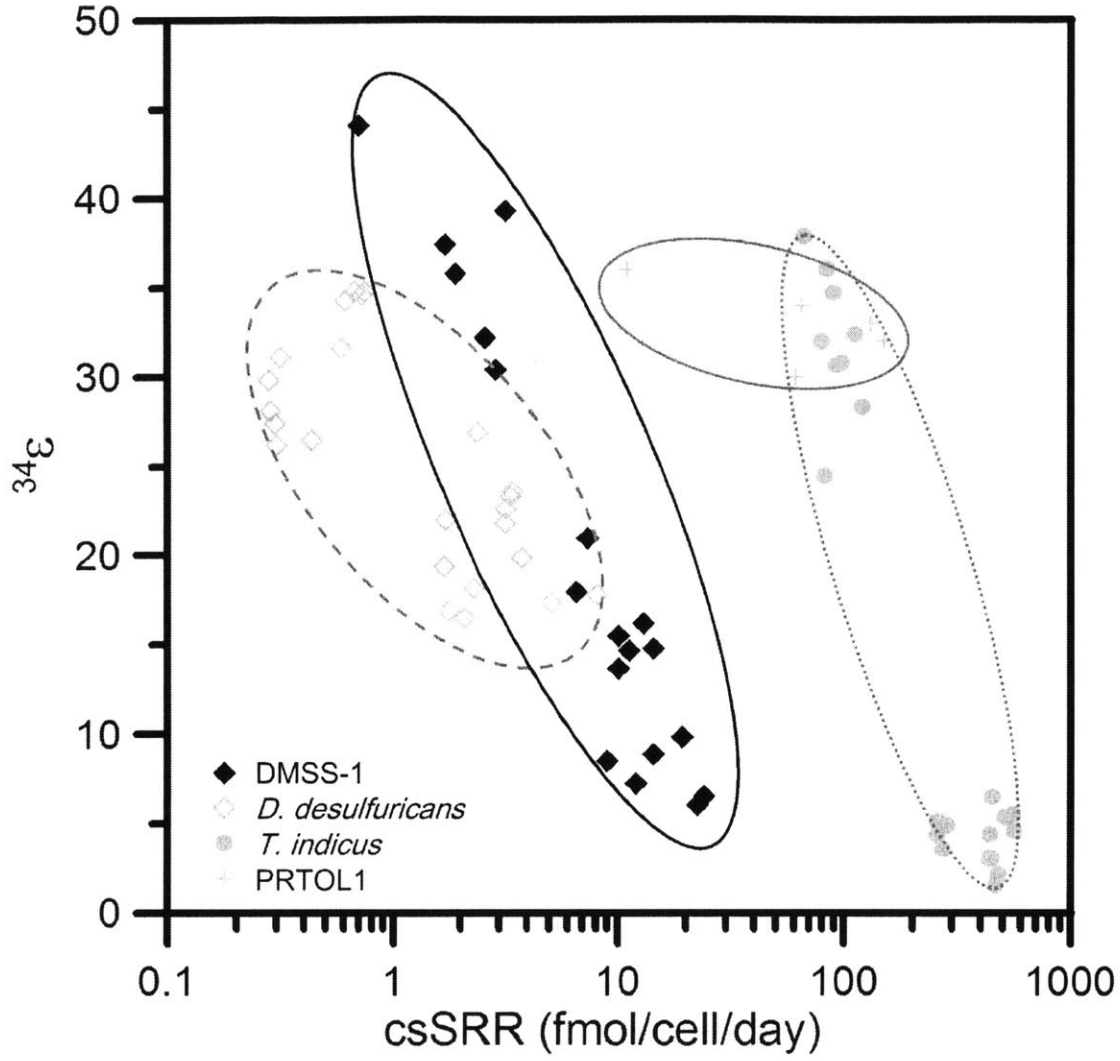

Figure 2.6. Variations in $^{34}\varepsilon$ and csSRR induced by either the availability or the nature of the electron donor, reported in this study and previously published data from actively growing cultures (Chambers et al., 1975; Kleikemper et al., 2004; Hoek et al., 2006).

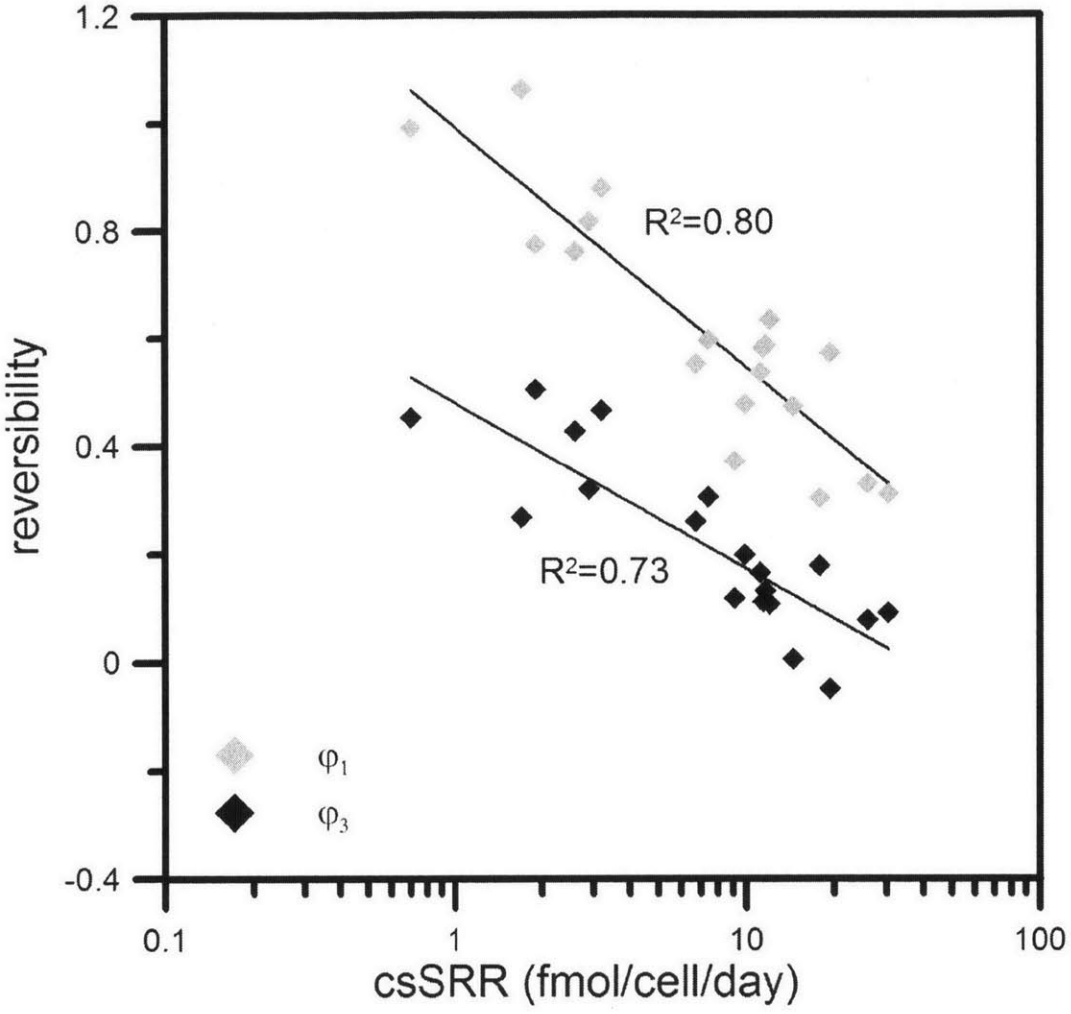

Figure 2.7. Correlation of the estimated reversibilities of the sulfate uptake (ϕ_1) and the reduction of sulfate to sulfite (ϕ_3) to csSRR.

and backward reactions of each step in MSR (reversibility) rather than the net forward flow (csSRR) (Fig. 2.4, Rees, 1973, Brunner and Bernasconi, 2005). How these correlations change with varying temperature, species, and the concentration of sulfate remains to be evaluated.

2.5.4. Fractionation of $^{33}S/^{32}S$ as a Unique Tracer of S-disproportionation

Recent studies have suggested that the minor isotope fractionation factor (^{33}E or $^{33}\lambda$) can be used to distinguish between the isotopic signatures of MSR and microbial S-disproportionation (MSD) in modern (Zerkle et al., 2010) and ancient environments (Johnston et al, 2005b). These suggestions are grounded in the distinct ranges of $^{33}\lambda$ values produced by MSR and MSD in pure culture studies (Farquhar et al., 2003; Johnston et al., 2005a; Johnston et al., 2007): from 0.5077 to 0.5125 for MSR, and from 0.5145 to 0.5187 for MSD, respectively. DMSS-1 produces $^{33}\lambda$ values from 0.5086 to 0.5141, which expands the range of $^{33}\lambda$ for MSR toward that for MSD (Fig. 2.8), although $^{33}\lambda$ values associated with $^{34}\varepsilon$ values larger than 44‰ from pure cultures of SRM remain to be determined. The range of ($^{34}\varepsilon$, $^{33}\lambda$) measured in DMSS-1 cultures is also in agreement with the values produced by natural populations of microbes incubated in chemically undefined mud, where MSD is assumed not to play a large role (Farquhar et al., 2008). The expanded range of minor isotope fractionations from our study is comparable to some natural ^{33}S-isotope signatures. For example, sulfur isotope fractionations between dissolved sulfate and sulfide in modern euxinic environments (Green Lake, Lago di Cadagno, and Cariaco Basin) yield high $^{34}\varepsilon$ values (> 30‰) and associated $^{33}\lambda$ values from 0.5112 to 0.5136 (Canfield et al., 2010; Li et al., 2010; Zerkle et al., 2010). These natural values exceed the range of isotope fractionations previously reported for pure cultures of sulfate reducing microbes, but overlap with the range of $^{34}\varepsilon$ and $^{33}\lambda$ measured in this study and do not overlap with the range of MSD alone (Fig. 2.8).

Models of global S-cycling based on the distinct ranges of $^{34}\varepsilon$ and $^{33}\lambda$ values for MSR and MSD are also used to track the relative contribution of these two microbial processes through the geologic time (Johnston et al., 2005b). In the absence of oxidative recycling of sulfur, the model that includes an expanded range of $^{34}\varepsilon$ and $^{33}\lambda$ values for MSR (Fig. 2.9) accommodates almost 50% of all sedimentary sulfate data points from the Proterozoic to the Cambrian (Johnston et al., 2005b). The insights from the DMSS-1 cultures are thus able to account for 25% more isotopic

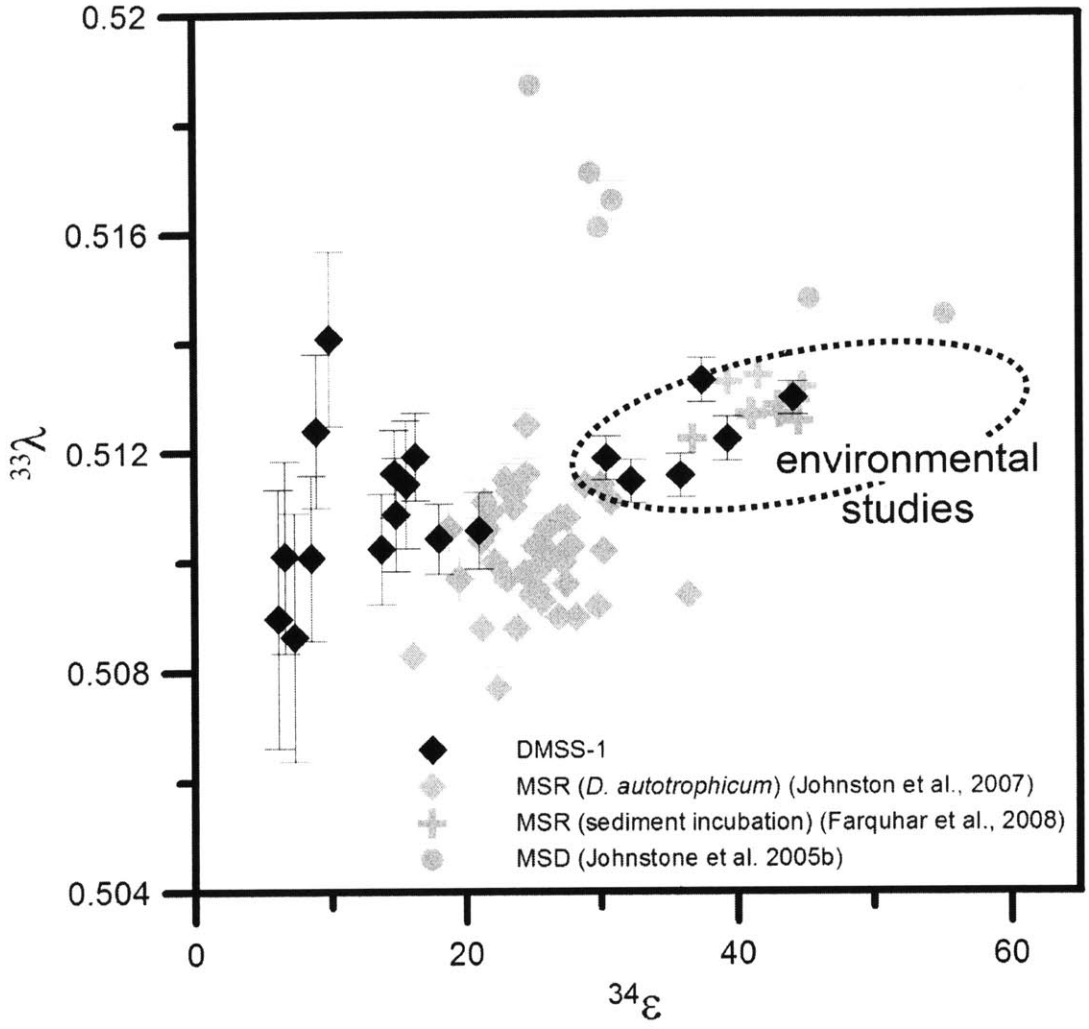

Figure 2.8. Comparison of $^{34}\varepsilon$ and $^{33}\lambda$ values produced by DMSS-1 with those reported by previous studies (Johnston et al., 2005b; Johnston et al., 2007; Farquhar et al., 2008) and those derived from the reported measurements of dissolved sulfide and sulfate in modern euxinic environments (Green Lake, Lago di Cadagno, and Cariaco Basin) (Canfield et al., 2010; Li et al., 2010; Zerkle et al., 2010).

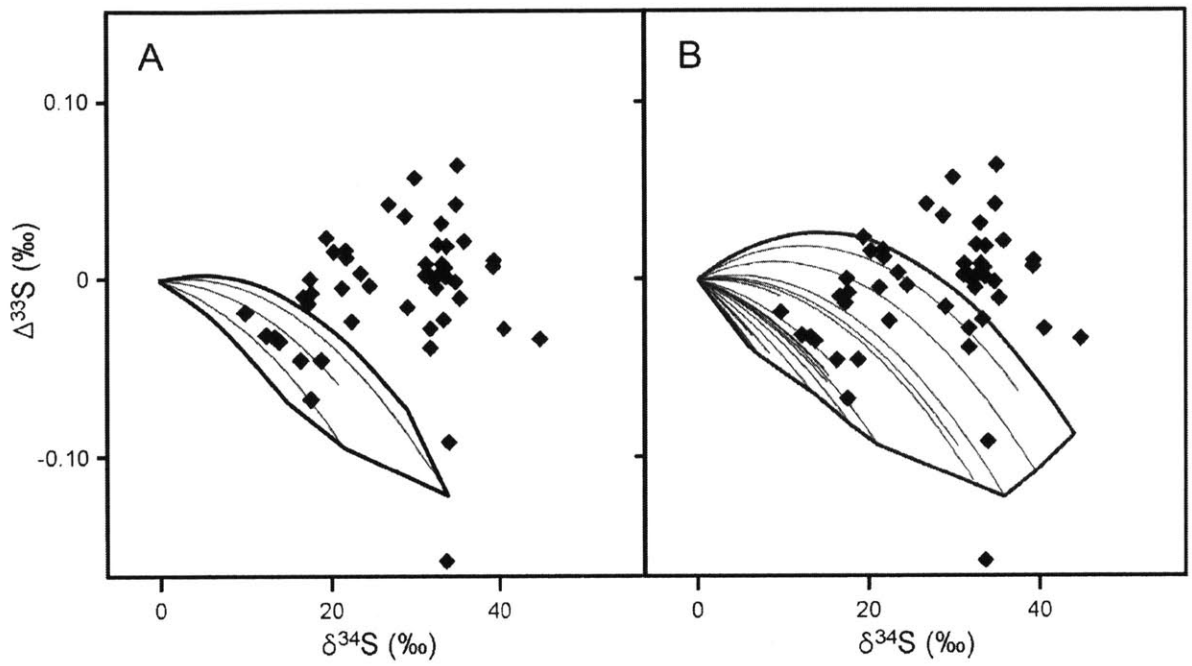

Figure 2.9. $\delta^{34}S$ and $\Delta^{33}S$ ($=\delta^{33}S - 1000\cdot((\delta^{34}S/1000 + 1)^{0.515} - 1)$) of seawater sulfate proxies from 2 to 0.5 Ga (black diamond) and the range of $\delta^{34}S$ and $\Delta^{33}S$ of seawater sulfate predicted based on the steady-state global sulfur cycle model including only MSR without MSD (solid lines) (Johnston et al., 2005a). (A) Steady state solutions calculated for the isotope fractionations previously reported from MSR (Johnston et al., 2005a). (B) Extended solution field with data presented in this study.

data points than previously thought. MSD and oxidative recycling of sulfur can account for the remaining data points. However, an apparent positive relationship between $^{34}\varepsilon$ and $^{33}\lambda$ in our study (Fig. 2.8) suggests that natural MSR producing extremely large $^{34}\varepsilon$ (Wortmann et al., 2001) may be associated with $^{33}\lambda$ values that are indistinguishable from those currently attributed to MSD, possibly accommodating all sedimentary sulfate data. This study thus increases the range of sulfur isotope effects attributable to MSR alone and reduces the range unambiguously indicative of MSD in both modern and ancient environments.

2.6. Conclusions

DMSS-1, a recently isolated marine sulfate reducing bacterium, degrades various organic compounds to acetate and CO_2 and yields $^{34}\varepsilon$ values ranging from 6.1 to 44.1 per mil. These $^{34}\varepsilon$ values, produced during active growth in the presence of non-limiting sulfate, span almost the entire range of S-isotope fractionations previously reported in pure culture experiments. This result demonstrates that the availability and the nature of the electron donor may influence the range of $^{34}\varepsilon$ in culture and in nature as much or more than the presence or absence of completely oxidizing strains. Sulfur isotope fractionation is larger in the presence of refractory organic compounds that support only slow growth rates (e.g., glucose and fructose) and at the very low supply rate of the electron donor. Increasing $^{34}\varepsilon$ values exhibit a positive correlation with declining csSRR, confirming observations by previous researchers. DMSS-1 fractionates minor sulfur isotopes, producing ^{33}E values ranging from -0.009 ‰ to -0.125 ‰. The use of multiple sulfur isotopes in the model of metabolic fluxes of sulfur shows that the loss of sulfate from the cell and the intracellular reoxidation of reduced sulfur species contribute unequally, but in a correlated manner, to the increase in isotope effects. When MSR produces sulfides that are not very depleted, the model of metabolic fluxes predicts the presence of intracellular sulfate and sulfite that are enriched in ^{34}S. During the production of the largest S-isotope effects, the flow of sulfate out of the cell should be almost as large as the intake of sulfate and about 50% of sulfite should be reoxidized intracellularly, but ^{34}S of the internal sulfate and sulfite should not be very enriched. DMSS-1 produces large $^{34}\varepsilon$ coupled with moderate ^{33}E under conditions that preclude extracellular disproportionation of sulfur. These ($^{34}\varepsilon$, ^{33}E) values significantly expand the range of isotope effects produced by MSR alone and reduce the range that is thought to unambiguously indicate MSD in ancient and modern sediments.

Appendix A. Multiple Sulfur Isotope Modeling

Initially developed by Rees (1973), the isotope fractionation model predicted a maximum fractionation of ~ 46‰, but later modifications (Brunner and Bernasconi, 2005) predicted even larger (up to ~ 70‰) fractionations during MSR. According to these models, the overall fractionation factor between sulfide and sulfate ($\alpha_{overall}$) depends not only on the magnitude of isotope effects that are intrinsic to each enzymatic reaction (α_1, α_3, and α_4) but also on the relative rates of forward (f_1, f_2, and f_3) and backward (b_1, b_2, and b_3) mass flows associated with each reaction (Fig. 2.4) (e.g., Northrop, 1975; Hayes, 2001).

Following the Rees-Farquhar model (Rees, 1973; Farquhar et al., 2003), the steady state solution for the overall sulfur isotope effect ($\alpha_{overall}$) during MSR with two branching points is described by Farquhar et al., (2007):

$$\alpha_{overall} = \frac{\alpha_1\alpha_3\alpha_4}{\varphi_1[\varphi_3(1-\alpha_4)+\alpha_4(1-\alpha_3)]+\alpha_3\alpha_4} \quad (10)$$

where, α is the fractionation factors $(^{34}S/^{32}S)_{pathway}/(^{34}S/^{32}S)_{pool}$, φ_1 is b_1/f_1 and φ_3 is b_3/f_3. In this model, one branching point describes the competition between the flow of sulfate into the cell (f_1) and the flows of sulfate and sulfide out of the cell (b_1 and f_4). The other branching point describes the competition between the oxidative and reductive flows in the cell: f_3, f_4, and b_3 (Farquhar et al., 2003). Hence, φ_1 represents the reversibility of sulfate uptake and φ_3 represents the reversibility of the reduction of sulfate to sulfide. The parameter α_i corresponds to the kinetic isotope effects intrinsic to each enzymatic reaction. This equation predicts that an overall isotope effect is determined by the reversibility of each step, which is a ratio between backward and forward flows in each step, rather than csSRR which is a net forward flow. Eq. 10 can be solved by assigning values to α_1, α_2, and α_3. Only f_3 and f_4 (Fig. 2.4) are thought to produce significant isotope effects (> 20 per mil) of the magnitude α_3 and α_4, respectively (Rees, 1973). Rees (1973) assumed a small inverse isotope effect for sulfate uptake (α_1 = 1.003). However, the reverse reactions (i.e., b_3 and b_4) are generally assumed not to produce any isotope effects (Rees, 1973; Farquhar et al., 2003; Johnston et al., 2007). The values of α_3 and α_4 are constrained by the experimental results and/or thermodynamic estimates of equilibrium fractionation factor (Rees, 1973; Brunner and Bernasconi, 2005; Johnston et al., 2007).

In addition to $^{34}S/^{32}S$ ratios, a multiple isotope system approach, initially proposed by Northrop (1975), can provide additional constraints on both φ_1 and φ_3 (Farquhar et al., 2003; Ono et al., 2006; Johnston et

al., 2007) because the mixing of different sulfur pools within the cell follows a linear relationship but the mass-dependent isotope fractionation of each step is defined by a power law (Young et al., 2002). The value of the exponent is set to 0.5147 for the low temperature equilibrium isotope fractionation between sulfate and sulfide (Farquhar et al., 2003).

$$^{33}\alpha_i = {}^{34}\alpha_i^{0.5147} \quad (11)$$

We solved Eqs. 7, 9, 10 and 11 for both reversibilities (φ_1 and φ_3) associated with the growth of DMSS-1 on various electron donors, assuming values for intrinsic fractionation factors α_3 and α_4 of 0.9756 and 0.9520, respectively, and assuming the absence of isotope effects associated with the reverse reactions (i.e., b_3 and b_4). These values for α_3 and α_4 represent equilibrium isotope effects at 20°C between sulfate and sulfide, and sulfite and sulfide, respectively (Farquhar et al., 2003). Plotted in the solution field of Eq. 10 and 11, our data ($^{34}\varepsilon$ and ^{33}E) can be semi-quantitatively interpreted in the light of fluxes of sulfate in and out of the cell and the oxidative fluxes of sulfur species in the cell (Fig. 2.5A) (Farquhar et al., 2007).

Supplementary Material. Sequence Information of *Desulfovibrio* sp. clone DMSS-1

Sequences were deposited in GENbank, and accession numbers are JF968436 for 16S rRNA gene and JF968437 for dsrB subunit (dissimilatory sulfite reductase, subunit beta).

16S rRNA gene, partial sequence of Desulfovibrio sp. clone DMSS-1

LOCUS Seq1 1419 bp DNA linear

DEFINITION clone DMSS-1.

SOURCE Desulfovibrio sp.

ORGANISM Desulfovibrio sp.

Bacteria; Proteobacteria; Deltaproteobacteria; Desulfovibrionales;

Desulfovibrionaceae; Desulfovibrio.

REFERENCE 1 (bases 1 to 1419)

AUTHORS Sim,M.S., Donovan,K., Templer,S.P., Ono,S. and Bosak,T.

TITLE Effect of electron donors on the fractionation of sulfur isotopes

JOURNAL Unpublished

REFERENCE 2 (bases 1 to 1419)

AUTHORS Templer,S.P., Bosak,T., Sim,M.S., Ono,S. and Donovan,K.

TITLE Direct Submission

JOURNAL Submitted (11-APR-2011) Earth, Atmospheric and Planetary Sciences,
Massachusetts Institute of Technology, 77 Massachusetts Avenue,
Cambridge, MA 02139, USA

COMMENT Bankit Comment: bankit1447291.
Bankit Comment: BankIt ID:1447291.
Bankit Comment: LocalID:Seq1.

FEATURES Location/Qualifiers

source 1..1419
/organism="Desulfovibrio sp."
/mol_type="genomic DNA"
/isolation_source="surface sediment from a tidal flat"
/db_xref="taxon:885"
/clone="DMSS-1"
/environmental_sample
/country="Cape Cod, Massachusetts, USA"
/note="[enrichment culture bacterial source]"

rRNA <1..>1419
/product="16S ribosomal RNA"

BASE COUNT 287 a 444 c 342 g 346 t

ORIGIN

1 ggcggctgcc ccccaaaggg ttggctcacc gacgtcgggt agaaccgact ttcgtggtgt
61 gacgggcggt gtgtacaagg cccgggaacg tattcaccct ggcatgctga tccaggatta
121 ctagcgattc caacttcatg cagtcgagtt gcagactgca atccggactg ggaggggctt
181 tttgggattg gcttggcctc gcggcgtagc tgccctttgt acccccccatt gtagtacgtg
241 tgtagccctg ggcgtaaggg ccatgatgac ttgacgtcgt ccccaccttc ctcccggttg

301 acccgggcag tctcgccaga gtgcccacca ttatgtgatg gcaactgaca ataagggttg

361 cgctcgttgc gggacttaac ccaacacctc acggcacgag ctgacgacag ccatgcagca

421 cctgtcactt ggttccccga agggcactct cctatctcta ggagattcca aggatgtcaa

481 acccaggtaa ggttcttcgc gttgcatcga attaaaccac atactccacc gcttgtgcgg

541 gcccccgtca attcctttga gtttcagcct tgcgaccgta ctccccaggc gggatgctta

601 atgcgttaac tgcggcaccg aaggtgaatc cccccgacac ctagcatcca tcgtttacag

661 cgtggactac cagggtatct aatcctgttt gctccccacg ctttcgtacc tcagcgtcag

721 tacctgtcca gatggccgcc ttcgccaccg gtgttcctcc tgatatctac ggatttcact

781 cctacaccag gaattccgcc atcctctcca ggactcaagc ctgtcagtat caagtgcaat

841 tcctcggttg agccgagggc tttcacacct gacttaacag gcagcctacg cacgctttac

901 gcccagtgat tccgattaac gcttgcacca tccgtattac cgcggctgct ggcacggatt

961 tagccggtgc ttcctctgaa ggtaccgtca aacatatgcg ctattaacac atatacattt

1021 cttcccttct gacagaggtt tacaacccga aagccttctt ccctcacgag gcgtcgctgc

1081 gtcagggttt cccccattgc gcaatattcc ccactgctgc ctcccgtagg agtctgggcc

1141 gtgtttcagt cccagtgtgg ctggtcatcc tctcaaacca gctactcatc gttgccttgg

1201 taggccgtta ccctaccaac aagctaatga gacgcgggcc catccagacg cggatgcata

1261 gtttagaggc acccttttcaa tcaaaataaa ttgattcgta tacggtatta gcagccgttt

1321 ccaactgtta tcccgatcgt ctgggcaggt agcccacgcg ttactcaccc gtacgccgct

1381 ctactaggct cccgaaggaa cttttctcgc acgactgca

//

Dissimilatory sulfite reductase, subunit A and B (*dsrAB*) of *Desulfovibrio* sp. clone DMSS-1

LOCUS Seq2 767 bp DNA linear

DEFINITION Desulfovibrio sp. clone DMSS-1, dissimilatory sulfite reductase alpha subunit (dsrA) and dissimilatory sulfite reductase beta subunit (dsrB) genes, partial cds.

SOURCE Desulfovibrio sp.

ORGANISM Desulfovibrio sp.

Bacteria; Proteobacteria; Deltaproteobacteria; Desulfovibrionales;

Desulfovibrionaceae; Desulfovibrio.

REFERENCE 1 (bases 1 to 767)

AUTHORS Templer,S.P., Sim,M.S., Donovan,K., Ono,S. and Bosak,T.

TITLE Effect of electron donors on the fractionation of sulfur isotopes

JOURNAL Unpublished

REFERENCE 2 (bases 1 to 767)

AUTHORS Templer,S.P., Sim,M.S., Donovan,K., Ono,S. and Bosak,T.

TITLE Direct Submission

JOURNAL Submitted (11-APR-2011) Earth, Atmospheric and Planetary Sciences,

Massachusetts Institute of Technology, 77 Massachusetts Avenue,

Cambridge, MA 02139, USA

COMMENT Bankit Comment: bankit1447386.

Bankit Comment: BankIt ID:1447386.

Bankit Comment: LocalID:Seq1.

FEATURES Location/Qualifiers

source 1..767

/organism="Desulfovibrio sp."

/mol_type="genomic DNA"

/isolation_source="surface sediment from a tidal flat"

/db_xref="taxon:885"

/clone="DMSS-1"

/environmental_sample

/country="Cape Cod, Massachusetts, USA"

/note="[enrichment culture bacterial source]"

gene 1..767

/gene="dsrA"

BASE COUNT 161 a 192 c 243 g 171 t

ORIGIN

1 cttctcgccg ttcagttcga ccttggtggg acgaatggcg gcggtggggc aggcagcgac

61 ggccagagga atttcgcaca ggttgtccag aacagcgtgg tccttcatgg gcggcttacg

121 gtgaatgccc aggaaggcga tgtcggagca gtgaaccgcg ccgcacatgt tcaggcagca

181 agccatggat acgcgcaacg gagcgggcag atccattttg ccgaagtggt cgaacagcac

241 gtccataacg gccttaacgg taccggaggc gtccgttgca ggcgtatggc agtgcaccca

301 accctgggtg tggacgatgt tcgtgatgga ggcgccggtt ccgccgatgg ggaacttgta

361 ggagccgccg gggaacttgc gggacagcag atcttctttc agaggagcca ctttgtcctt

421 gctgtccacc atgaactcga ggttgttacg agtggtgaag cgcaggtagc catcgcagta

481 cttgtcggcg atgtccataa cttcacgcat cagggtaacg gacatcaggc gggcagttgc

541 acaacggatg gtgtacactt cagcgccgct ttcagccacg tgcagcagaa tgccgggctc

601 cacgatttcg tggtatttcc atttaccgaa gttttccttg atgaccgggg gaagaaactg

661 atcgtatttc ttgggcccga tatcggaaat ccggttctcc atgggtttag cgggattgta

721 tcctgtggag ataaatgcca tggtatataa cctcccgtaa atttggg

//

References

Akagi J. M. and Campbell L. L. (1962) Studies on thermophilic sulfate-reducing bacteria III. *J. Bacteriol.* **84**, 1194-1201.

Barber R. T. (1968) Dissolved organic carbon from deep waters resists microbial oxidation. *Nature* **220**, 274-275.

Berner R. A. (1989) Biogeochemical cycles of carbon and sulfur and their effect on atmospheric oxygen over Phanerozoic time. *Global. Planet. Change* **1**, 97-122.

Bevington P. R. and Robinson D. K. (2002) *Data reduction and error analysis for the physical sciences*, McGraw-Hill, New York.

Bolliger C., Schroth M. H., Bernasconi S. M., Kleikemper J. and Zeyer J. (2001) Sulfur isotope fractionation during microbial sulfate reduction by toluene-degrading bacteria. *Geochim. Cosmochim. Acta* **19**, 3289-3298.

Bottcher M. E., Sievert S. M., and Keuver J. (1999) Fractionation of sulfur isotopes during dissimilatory reduction of sulfate by a thermophilic gram-negative bacterium at 60°C. *Arch. Microbiol.* **172**, 125-128.

Bruchert V., Knoblauch C. and Jorgensen, B. B. (2001) Controls on stable sulfur isotope fractionation during bacterial sulfate reduction in Arctic sediments. *Geochim. Cosmochim. Acta* **65**, 763-776.

Brunner, B. and Bernasconi S. M. (2005) A revised isotope fractionation model for dissimilatory sulfate reduction in sulfate reducing bacteria. *Geochim. Cosmochim. Acta* **69**, 4759-4771.

Canfield D. E. (2001) Isotope fractionation by natural populations of sulfate-reducing bacteria. *Geochim. Cosmochim. Acta* **65**, 1117-1124.

Canfield D. E. (2004) The evolution of the Earth surface sulfur reservoir. *Am. J. Sci.* **304**, 839-861.

Canfield D. E. and Farquhar J. (2009) Animal evolution, bioturbation, and the sulfate concentration of the oceans. *PNAS* **106**, 8123-8127.

Canfield, D. E., Farquhar, J., and Zerkle A. L. (2010) High isotope fractionations during sulfate reduction in a low-sulfate euxinic ocean analog. *Geology* **38**, 415-418.

Canfield D. E., and Teske A. (1996) Late Proterozoic rise in atmospheric oxygen concentration inferred from phylogenetic and sulphur-isotope studies. *Nature* **382**, 127-132.

Chambers L. A., Trudinger P. A. (1979) Microbiological fractionation of stable sulfur isotopes: A review and critique. *Geomicrobiol. J.* **1**, 249-293.

Chambers L. A., Trudinger P. A., Smith J. W. and Burns M. S. (1975) Fractionation of sulfur isotopes by continuous cultures of *Desulfovibrio desulfuricans*. *Can. J. Microbiol.* **21**, 1602-1607.

Cline J. D. (1969) Spectrophotometric determination of hydrogen sulfide in natural water. *Limnol. Oceanogr.* **14**, 454-458.

Cord-Ruwisch R., Kleintz W. and Widdel F. (1986) Sulfatreduzierende Bakterien in einem Erdölfeld - Arten und Wachstumsbedingungen (Abstract in English). *Erdöl Erdgas Kohle* **102**, 281-289

Cypionka H. (1995) Solute transport and cell energetics. In *Sulfate-reducing Bacteria* (ed. L. L. Barton). Plenum, New York.

Cypionka H., Smock A. M. and Bottcher M. E. (1998) A combined pathway of sulfur compound disproportionation *in Desulfovibrio desulfuricans*. *FEMS Microbiol. Lett.* **166**, 181-186.

Davidson M. M., Bisher M. E., Pratt L. M., Fong J., Southam G., Pfiffner S. M., Reches Z. and Onstott T. C. (2009) Sulfur isotope enrichment during maintenance metabolism in the thermophilic sulfate-reducing bacterium *Desulfotomaculum putei*. *Appl. Environ. Microbiol.* **75**, 5621-5630.

Detmers J., Bruchert V., Habicht K. and Kuever J. (2001) Diversity of sulfur isotope fractionations by sulfate reducing prokaryotes. *Appl. Environ. Microbiol.* **67**, 888-894.

Drake H. L. and Akagi J. M. (1977) Bisulfite reductase of *Desulfovibrio vulgaris*: Explanation for product formation. *J. Bacteriol.* **132**, 139-143.

Fareleira P., LeGall J., Xavier A. V. and Santos H. (1997) Pathways for utilization of carbon reserves in *Desulfovibrio gigas* under fermentative and respiratory conditions. *J. Bacteriol.* **179**, 3972-3980.

Farquhar J., Canfield D. E., Masterson A., Bao H. and Johnston D. (2008) Sulfur and oxygen isotope study of sulfate reduction in experiments with natural populations from Fællestrand, Denmark. *Geochim. Cosmochim. Acta* **72**, 2805-2821.

Farquhar J., Johnston D. T., Wing B. A. (2007) Implications of conservation of mass effects on mass-dependent isotope fractionations: Influence of network structure on sulfur isotope phase space of dissimilatory sulfate reduction. *Geochim. Cosmochim. Acta* **71**, 5862-5875.

Farquhar J., Johnston D. T., Wing B. A., Habicht K. S., Canfield D. E., Airieau S. and Thiemens M. H. (2003) Multiple sulphur isotopic interpretations of biosynthetic pathways: implications for biological signatures in the sulphur isotope record. *Geobiology* **1**, 27-36.

Fitz R. M. and Cypionka H. (1989) A study on electron transport-driven proton translocation in *Desulfovibrio desulfuricans*. *Arch. Microbiol.* **152**, 369-376.

Fry, B. (1991) Stable isotope diagram of freshwater foodwebs. *Ecology* **72**, 2293-2297.

Garrels R. M. and Lerman A. (1981) Phanerozoic cycles of sedimentary carbon and sulfur. *PNAS* **78**, 4652-4656.

Goldhaber M. B., and Kaplan I. R. (1975) Controls and consequences of sulfate reduction rates in recent marine sediments. *Soil Sci.* **119**, 42-55.

Hayes J. M. (2001) Fractionation of carbon and hydrogen isotopes in biosynthetic processes. *Rev. Mineral. Geochem.* **43**, 225-277.

Habicht K. S. and Canfield D. E. (1997) Sulfur isotope fractionation during bacterial sulfate reduction in organic-rich sediments. *Geochim. Cosmochim. Acta* **61**, 5351-5361.

Harrison, A. G. and Thode H. G. (1958) Mechanism of the bacterial reduction of sulphate from isotope fractionation studies. *Trans. Faraday Soc.* **54**, 84-92.

Hoek J., Reysenbach A., Habicht K. S. and Canfield D. E. (2006) Effect of hydrogen limitation and temperature on the fractionation of sulfur isotopes by a deep-sea hydrothermal vent sulfate-reducing bacterium. *Geochim. Cosmochim. Acta* **70**, 5831-5841.

Jeanloz R. W. (1967) The chemical structure of the cell wall of gram-positive bacteria. *Pure. Appl. Chem.* **14**, 57-70.

Johnston D. T., Farquhar J. and Canfield D. E. (2007) Sulfur isotope insights into microbial sulfate reduction: when microbes meet model. *Geochim. Cosmochim. Acta* **71**, 3929-3947.

Johnston D. T., Farquhar J., Wing B. A., Kaufman A. J., Canfield D. E. and Habicht K. S. (2005a) Multiple sulfur isotope fractionations in biological systems: A case study with sulfate reducers and sulfur disproportionators. *Am. J. Sci.* **305**, 645-660.

Johnston D. T., Wing B. A., Farquhar J., Kaufman A. J., Strauss H., Lyon T. W., Kah L. C. and Canfield D. E. (2005b) Active microbial sulfur disporportionation in the Mesoproterozoic. *Science* **310**, 1477-1479.

Jorgensen B. B. (1982) Mineralization of organic matter in the sea bed-the role of sulphate reduction. *Nature* **296**, 643-645.

Kaplan I. R. and Rittenberg S. C. (1964) Microbiological fractionation of sulphur isotopes. *J. Gen Microbiol.* **34**, 195-212.

Kemp A. L. W. and Thode H. G. (1968) The mechanism of bacterial reduction of sulphate and of sulphite from isotope fractionation studies. *Geochim. Cosmochim. Acta* **32**, 71-91.

Kleikemper J., Schroth M. H., Bernasconi S. M., Brunner B. and Zeyer J. (2004) Sulfur isotope fractionation during growth of sulfate reducing bacteria on various carbon sources. *Geochim. Cosmochim. Acta* **68**, 4891-4904.

Kremer D. R. and Hansen T. A. (1987) Glycerol and dihydroxyacetone dissimilation in *Desulfovibrio* strains. *Arch. Microbiol.* **147**, 249-256.

Kremer D. R., Nienhuis-Kuiper H. E., Timmer C. J. and Hansen T. A. (1989) Catabolism of malate and related dicarboxylic acids in various *Desulfovibrio* strains and the involvement of an oxygen-labile NADPH dehydrogenase. *Arch. Microbiol.***151**, 34-39.

Lane D. J. (1991) 16S/23S rRNA sequencing. In *Nucleic acid techniques in bacterial systematics* (eds. E. Stackebrant and M. Goodfellow). Academic Press, Chichester, UK, pp. 115-175.

Li X., Gilhooly W. P., Zerkel A. L., Lyons T. W., Farquhar J., Werne J. P., Varela R., and Scranton M. I. (2010) Stable sulfur isotopes in the water column of the Cariaco Basin. *Geochim. Cosmochim. Acta* **74**, 6764-6778.

Mangalo M., Einsiedl F., Meckenstock R. U. and Stichler W. (2008) Influence of the enzyme dissimilatory sulfite reductase on stable isotope fractionation during sulfate reduction. *Geochim. Cosmochim. Acta* **71**, 4161-4171.

Mangalo M., Meckenstock R. U., Stichler W. and Einsiedl F. (2007) Stable isotope fractionation during bacterial sulfate reduction is controlled by reoxidation of intermediates. *Geochim. Cosmochim. Acta* **71**, 4161-4171.

Matin A. and Gottschal J. C. (1976) Influence of dilution rate on NAD(P) and NAD(P)H concentrations and ratios in a *Pseudomonas* sp. grown in continuous culture. *J. Gen Microbiol.* **94**, 333-341.

Matz C. and Jurgens K. (2005) High motility reduces grazing mortality of planktonic bacteria. *Appl. Envion. Microbiol.* **71**, 921-929.

Muyzer G., de Waal E. C. and Uitterlinden A. G. (1993) Profiling of complex microbial populations by denaturing gradient gel electophoresis analysis of polymerase chain reaction-amplified genes encoding for 16S rRNA. *Appl. Environ. Microbiol.* **59**, 695-700.

Newberry C. J., Webster, G., Cragg B. A., Parkes R. J., Weightman A. J., and Fry J. C. (2004) Diversity of prokaryotes and methanogenesis in deep subsurface sediments from the Nankai Trough, Ocean Drilling Program Leg 190. *Environ. Microbiol.* **6**, 274-287.

Northrop D. B. (1975) Steady-state analysis of kinetic isotope effects in enzymatic reactions. *Biochemistry* **14**, 2644-2651.

Ono S., Wing B., Rumble D. and Farquhar J. (2006) High precision analysis of all four stable isotope of sulfur (^{32}S, ^{33}S, ^{34}S and ^{36}S) at nanomole levels using a laser fluorination isotope-ratio-monitoring gas chromatography-mass spectrometry. *Chem. Geol.* **225**, 30-39.

Okabe S., Nielsen P. H. and Characklis W. G. (1992) Factors affecting microbial sulfate reduction by *Desulfovibrio desulfuricans* in continuous culture: limiting nutrients and sulfide concentration. *Biotechnol. Bioeng.* **40**, 725-734.

Peck H. D. and LeGall J. (1982) Biochemistry of dissimilatory sulfate reduction. *Philos. Trans. R. Soc. Lond. Ser. B* **298**, 443-466.

Peterson B. J., Howarth R. W. and Garritt R. H. (1986) Sulfur and carbon isotopes as tracers of salt-marsh organic matter flow. *Ecology* **67**, 865-874.

Postgate J. R. (1984) *The sulphate-reducing bacteria*, Cambridge University Press, Cambridge.

Rabus R., Hansen T. A. and Widdel F. (2006) Dissimilatory sulfate- and sulfur- reducing prokaryotes. In *The Prokaryotes* (eds M. Dworkin, S. Falkow, E. Rosenberg, K. H. Schleifer and E. Stackbrandt). Springer-Verlag, New York.

Rees C. E. (1973) A steady-state model for sulphur isotope fractionation in bacterial reduction processes. *Geochim. Cosmochim. Acta* **37**, 1141-1162.

Reichenbecher W., and Schink B. (1997) *Desulfovibrio inopinatus*, sp. nov., a new sulfate-reducing bacterium that degrades hydroxyhydroquinone (1,2,4-trihydroxybenzene). *Arch. Microbiol.* **168**, 337-344.

Rudnicki M. D., Elderfield H. and Spiro B. (2001) Fractionation of sulfur isotopes during bacterial sulfate reduction in deep ocean sediments at elevated temperatures. *Geochim. Cosmochim. Acta* **65**, 777-789.

Seki, Y., and Ishimoto, M., 1979. Catalytic Activity of the Chromophore of Desulfovirdin, Sirohydrochlorin, in sulfite reduction in the presence of iron. *J. Biochem.* **86**, 273-276.

Strauss S. Y. (1997) Floral characters link herbivores, pollinators, and plant fitness. *Ecology* **78**, 1640-1645.

Thauer R. K., Jungermann K. and Decker K. (1977) Energy concervation in chemotrophic anaerobic bacteria. *Bacteriol. Rev.* **41**, 100-180.

Thode H. G., Monster J., and Dunford H. B. (1961) Sulphur isotope geochemistry. *Geochim. Cosmochim. Acta* **25**, 158-174.

Vu B., Chen M., Crawford R. J., and Ivanova E. P. (2009) Bacterial extracellular polysaccharides involved in biofilm formation. *Molecules* **14**, 2535-2554.

Wagner M., Roger A. J., Flax J. L., Brusseau G. A., and Stahl D.A. (1998) Phylogeny of dissimilatory sulfite reductases supports an early origin of sulfate respiration. *J. Bacteriol.* **180**, 2975-2982.

Webester G., Parkes R. J., Cragg B. A., Newberry C. J., Weightman A. J. and Fry J. C. (2006) Prokaryotic community composition and biochemical processes in deep subseafloor sediments for the Peru Margin. *FEMS Microbiol. Ecol.* **58**, 65-85.

Widdel F. and Bak F. (1992) Gram-negative mesophilic sulfate-reducing bacteria. In The Prokaryotes (eds A. Balows, H. G. Trueper, M. Dworkin, W. Harder and K. H. Schleifer), Springer, New York, pp. 3352-3378.

Widdel F., Kohring G. W. and Mayer F. (1983) Studies on dissimilatory sulfate-reducing bacteria that decomposed fatty acids. III. Characterization of the filamentous gliding *Desulfonema limocola* gen. nov. sp. nov., and *Desulfonema magnum* sp. nov. *Arch. Microbiol.* **134**, 286-294.

Widdel F., and Rabus R. (2001) Anaerobic biodegradation of saturated and aromatic hydrocarbons. *Curr. Opin. Biotech.* **12**, 259-276.

Wortmann U. G., Chernyavsky B. M. (2007) Effect of evaporite deposition on Early Cretaceous carbon and sulphur cycling. *Nature* **446**,654-656.

Wortmann U. G., Chernyavsky B., Bernasconi S. M., Brunner B., Bottcher M. E., and Swart P. K. (2007) Oxygen isotope biogeochemistry of pore water sulfate in the deep biosphere: Dominance of isotope exchange reactions with ambient water during microbial sulfate reduction (ODP Site 1130). *Geochim. Cosmochim. Acta* **71**, 4221-4232.

Wortmann U. G., Bernasconi S. M. and Bottcher M. E. (2001) Hypersulfidic deep biosphere indicates extreme sulfur isotope fractionation during single-step microbial sulfate reduction. *Geology* **29**, 647-650.

Young E. D. (2002) Kinetic and equilibrium mass-dependent isotope fractionation laws in nature and their geochemical and cosmochemical significance. *Geochim. Cosmochim. Acta* **66**, 1095-1104.

Zerkle A. L., Kamyshny A., Kump L. R., Farquhar J., Oduro H. and Arthur M. A. (2010) Sulfur cycling in a stratified euxinic lake with moderately high sulfate: Constraints from quadruple S isotopes. *Geochim. Cosmochim. Acta* **74**, 4953-4970.

3. Large sulfur isotope fractionation does not require disproportionation

3.1 Abstract

The composition of sulfur isotopes in sedimentary sulfides and sulfates traces the sulfur cycle throughout Earth history. In particular, depletions of ^{34}S in sulfide larger than 47‰ often serve as a proxy for the disproportionation of intermediate sulfur species in addition to sulfate reduction. Here, we demonstrate that a pure, actively growing culture of a marine sulfate reducing bacterium can deplete ^{34}S by up to 66‰ during sulfate reduction alone and in the absence of an extracellular oxidative sulfur cycle. Therefore, similar magnitudes of sulfur isotope fractionation in sedimentary rocks do not unambiguously record the presence of other sulfur-based metabolisms or the stepwise oxygenation of Earth's surface environment during the Proterozoic.

3.2 Results and Discussion

Dissimilatory microbial sulfate reduction (MSR) utilizes sulfate (SO_4^{2-}) as an electron acceptor and simple organic compounds or hydrogen as electron donors, producing sulfide that is depleted in heavy isotopes of sulfur (^{33}S, ^{34}S, and ^{36}S) relative to the starting sulfate. For more than 2.5 billion years of Earth history, this biological process has controlled the partitioning of sulfur isotopes between sedimentary sulfides and sulfates, leaving a sedimentary S-isotope record that is commonly used to track the geochemical cycling of sulfur, the oceanic budgets of oxidants, the evolution of microbial metabolisms and the levels of atmospheric oxygen through geologic history (*1*, *2*, *3*).

All interpretations of this geobiological record have drawn heavily on more than five decades of systematic studies of sulfur isotope effect produced by MSR under controlled laboratory conditions. Although previous environmental studies and models suspected that MSR alone could produce a sulfur isotope offset between sulfides and sulfates ($\delta^{34}S_{sulfate\text{-}sulfide}$, *4*) as large as ~ 75‰ (*5*, *6*, *7*, *8*), growth and chemical conditions that lead toward such large offsets remain poorly understood. On the other hand, laboratory culture studies of MSR have not reported sulfur isotope effects larger than 47‰ under chemically and biologically defined reproducible conditions (Fig. 3.1). Large $\delta^{34}S_{sulfate\text{-}sulfide}$ values commonly measured in nature (Fig. 3.1) were thus attributed to a combination of MSR, extracellular oxidative recycling of sulfur by abiotic or microbial processes, and microbial sulfur disproportionation (MSD) (*2*, *9*). This oxidative recycling model, applied to the temporal record of $\delta^{34}S_{sulfate\text{-}sulfide}$ values, is

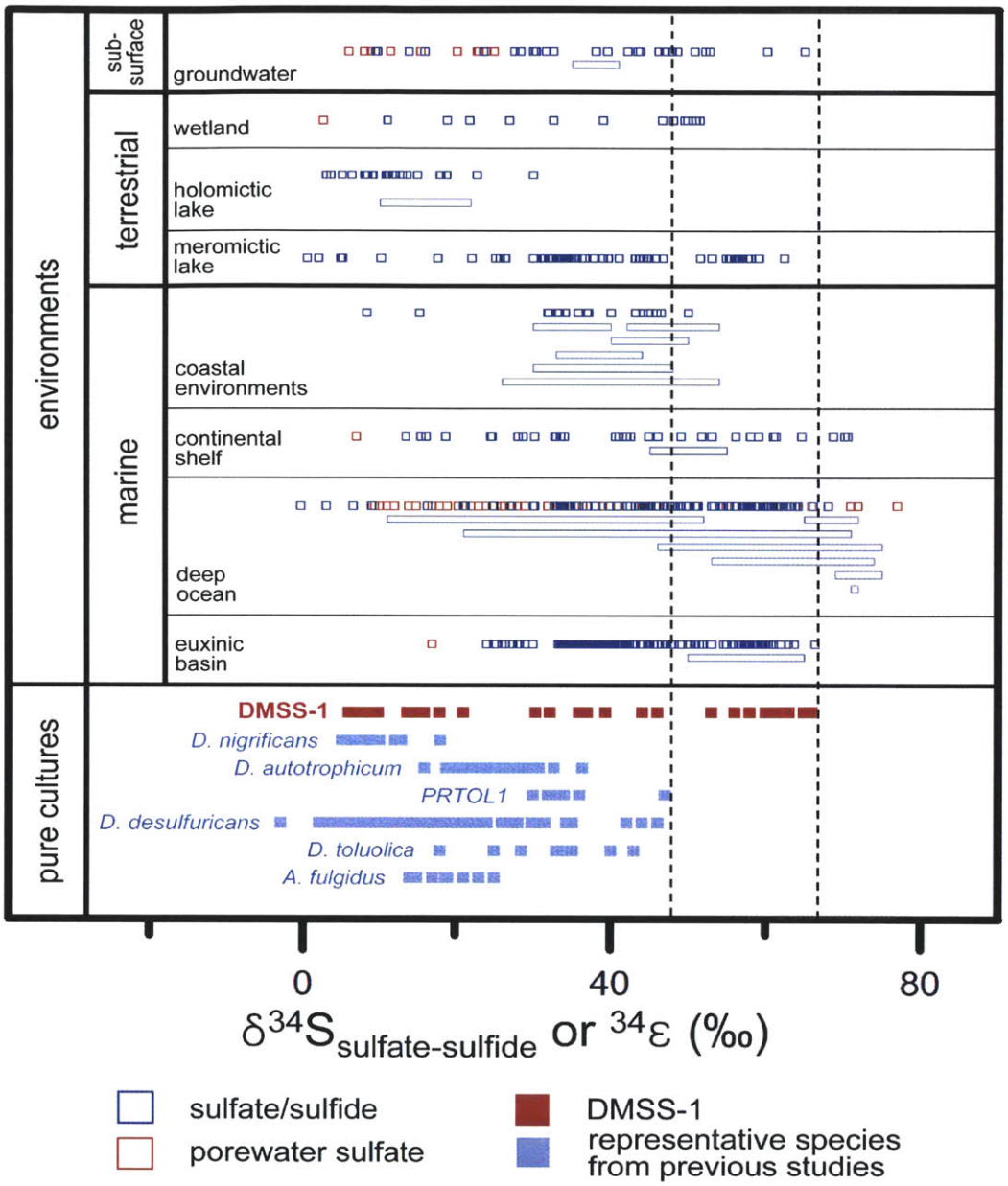

Figure 3.1. Fractionations of ^{34}S reported by studies of environmental samples ($\delta^{34}S_{sulfate\text{-}sulfide}$ or $^{34}\varepsilon$) and pure cultures of 44 different sulfate reducing microbes ($^{34}\varepsilon$). Isotope fractionations in environmental samples were estimated using dissolved sulfate and sedimentary or dissolved sulfide, or calculated from the concentration and the isotope composition of pore water sulfate. Each point in culture studies represents a different growth condition. Dashed black lines indicate the expanded range of ^{34}S fractionations by MSR (this study). Gray box outlines the equilibrium isotope effects between sulfate and sulfide with varying temperatures (0 ~ 40°C). Complete lists of references, data and criteria are available in Tables 3.S1 and 3.S2.

used to track the evolution of more oxidized conditions and the progressive oxygenation of Earth's surface environment (*2*, *10*, *11*, *12*, *13*).

We isolated a sulfate reducing δ-Proteobacterium (*Desulfovibrio* sp., DMSS-1) from marine coastal sediments from Cape Cod, MA (*14*), where $\delta^{34}S_{sulfate\text{-}sulfide}$ exceeds 50‰ (*15*). This microbe couples the reduction of sulfate with the incomplete oxidation of various organic substrates including fructose and glucose (*14*), producing a wide range of isotope enrichment factors ($^{34}\varepsilon$) from 6.1‰ to 65.6‰ (Fig. 3.1). Fractionations by DMSS-1 expand the range of $^{34}\varepsilon$ and $^{33}\lambda$ (*4*) values produced by MSR, accommodating most S-isotope fractionations observed in modern environments (Table 3.1, Fig. 3.1 and Fig. 3.2). Very slow growth of DMSS-1 in batch cultures grown on glucose as an electron donor and carbon source produces $^{34}\varepsilon$ values larger than 47‰ [Table 3.1, (*16*)]: the $^{34}\varepsilon$ values during the early exponential growth exceed 60‰, decreasing down to 44‰ at the very end of experiment (Table 3.1). Decreasing $^{34}\varepsilon$ values are accompanied by an increasing growth rate and cell yields, and a different reaction stoichiometry (*16*). Because DMSS-1 can ferment glucose in the absence of sulfate, different stoichiometries during the early and the late exponential growth suggest that DMSS-1 ferments some glucose during the early exponential growth (*16*). Conditions producing large and constant $^{34}\varepsilon$ (>47‰) values can be maintained indefinitely in continuous-flow cultures, where sulfate and glucose are the only available oxidant and reductant, respectively (Table 3.1). The production of large $^{34}\varepsilon$ values cannot be attributed to MSD coupled with the extracellular oxidation of sulfide to intermediate sulfur species (e.g., thiosulfate, sulfur, or sulfide), because other potential oxidants are absent from the defined culture medium (*16*). By proving that MSR alone can generate sulfides extremely depleted in ^{34}S even in the absence of extracellular oxidative recycling, our findings bridge the long-standing discrepancy between the ranges of sulfur isotope effects observed in laboratory cultures and geologic environments (Fig. 3.1).

One may ask whether large sulfur isotope effects produced by a single sedimentary microbe are truly representative of the natural environment. However, it is similarly unclear whether previous culture studies of MSR are representative of conditions conducive to large isotope fractionations in the environment, because most of these studies investigated MSR during growth on simple organic acids (e.g., lactate) and hydrogen and only rarely attained very slow growth rates and cell-specific sulfate reduction rates (csSRR) (*16*). Here, slow growth rates and csSRR are attained by growing DMSS-1 on glucose. This is not a conventional substrate for sulfate reducing microbes but is a common building block in biofilms (*17*) and storage polymers in some sulfate reducers (*18*), and a common monosaccharide in the ocean (*19*).

	experiments	f	$^{34}\varepsilon_{SR}$	$^{33}\varepsilon_{SR}$	$^{33}\lambda_{SR}$
batch cultures	10 mM glucose / 21 mM sulfate	0.99	62.6±0.3	32.7±0.1	0.5135±0.0002
		0.99	65.6±0.3	34.3±0.1	0.5142±0.0002
		0.99	65.2±0.3	34.1±0.1	0.5144±0.0002
	8.5 mM glucose / 21 mM sulfate	0.91	58.5±0.3	30.5±0.1	0.5137±0.0003
		0.93	59.7±0.4	31.1±0.2	0.5138±0.0002
		0.87	57.6±0.4	30.0±0.2	0.5135±0.0002
		0.81	53.0±0.4	27.6±0.2	0.5135±0.0003
		0.70*	44.1±0.4*	22.9±0.2*	0.5130±0.0003*
	10 mM glucose / 21 mM sulfate (+ amino acids)	0.96	55.9±0.4	29.1±0.2	0.5133±0.0004
		0.93	62.1±0.3	32.4±0.1	0.5144±0.0002
	1 mM glucose / 21 mM sulfate	0.99	58.4±0.3	30.4±0.1	0.5131±0.0003
	10 mM glucose / 2 mM sulfate	0.85	61.1±0.4	31.9±0.2	0.5133±0.0002
	1 mM glucose / 2 mM sulfate	0.90	45.9±0.4	23.8±0.2	0.5131±0.0003
chemostat (0.08 day^{-1})	10 mM glucose / 21 mM sulfate		52.6±0.3	27.4±0.1	0.5134±0.0005

Table 3.1. Sulfur isotope effects during the growth of DMSS-1 on glucose. f is the fraction of remaining sulfate. Solid horizontal lines indicate separate experiments. Individual numbers within solid lines represent cultures inoculated at the same time and grown simultaneously in identical growth media, but in separate bottles. Calculated $^{34}\varepsilon$ values vary depending on the growth stage. The largest and the smallest* $^{34}\varepsilon$ values were always found during the early and the late exponential growth, respectively. Errors were propagated from analytic uncertainties of isotope analysis and sulfide concentration measurement. *, data from (14).

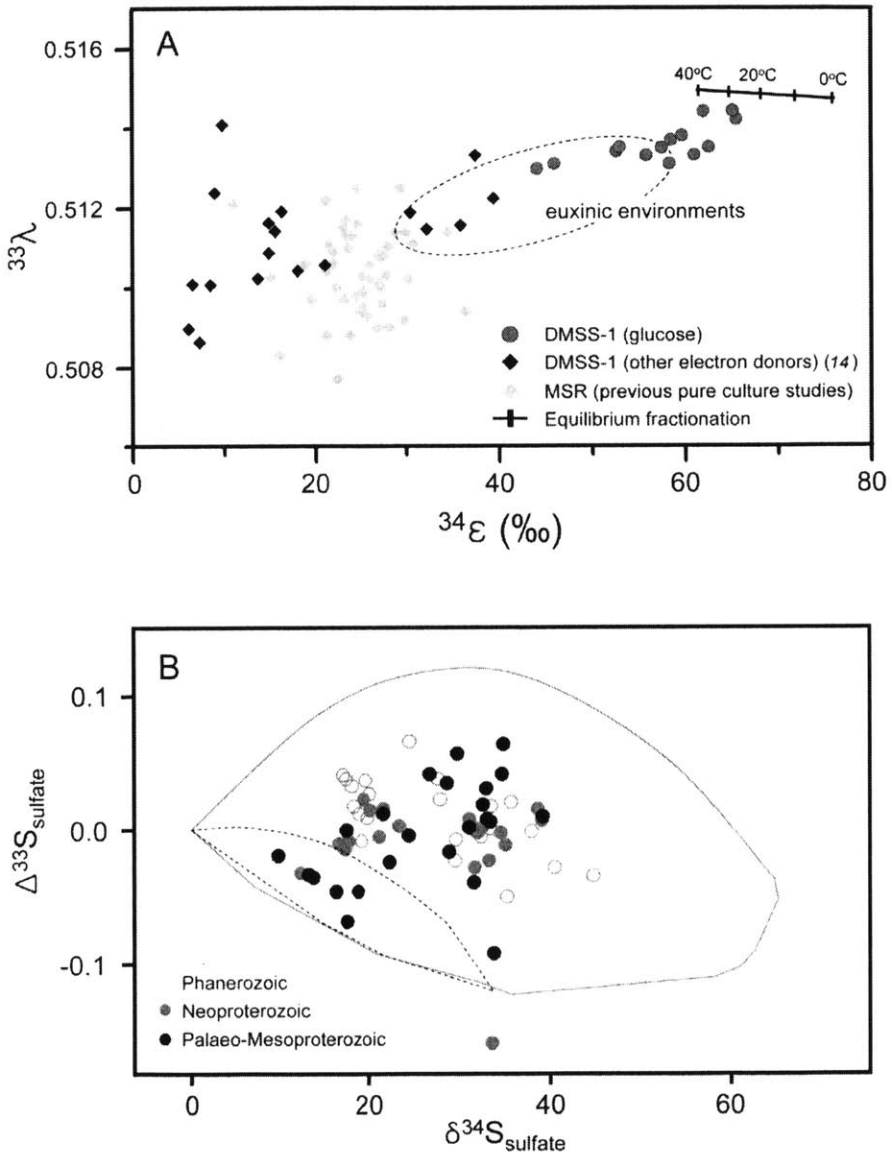

Figure 3.2. (A) Comparison of $^{34}\varepsilon$ and $^{33}\lambda$ values in this study to the values reported by previous culture studies (*23*, *34*) and to the range ($^{34}\varepsilon$, $^{33}\lambda$) from coexisting dissolved sulfide and sulfate in modern euxinic environments (Green Lake, Lago di Cadagno, and Cariaco Basin) (*8*, *27*, *35*). (B) $\delta^{34}S$ and $\Delta^{33}S$ (*4*) of seawater sulfate proxies (round symbols) from 2 to 0.2 Ga standardized to the Vienna Canyon Diablo Troilite (*11*, *32*). Predicted range of $\delta^{34}S$ and $\Delta^{33}S$ values of seawater sulfate based on the steady-state global sulfur cycle model including only MSR without MSD, constrained by the previous range of $^{34}\varepsilon$ and $^{33}\lambda$ values for MSR (*11*) (dashed line) or the expanded range reported in this study (solid line).

Sulfate reducing microbes accomplish the eight-electron reduction of sulfate to sulfide in a stepwise and reversible manner (*7*, *20*). The overall isotope effects between sulfate and sulfide thus depend both on the ratio between forward and backward fluxes at each intermediate step and on the isotope effect intrinsic to each transfer flux (*20*, *21*). The largest isotope effect is expected when sulfate reduction pathway operates in a highly reversible manner, leading to near equilibrium conditions (*7*). Accordingly, the largest $^{34}\varepsilon$ values produced by MSR should approach the equilibrium isotope effect between dissolved sulfate and sulfide, calculated to 68±2‰ at 20°C (*22*). This upper boundary is also supported by the relationship among multiple isotopes of sulfur. As $^{34}\varepsilon$ approaches the equilibrium value, so does $^{33}\lambda$ (Figure 3.2A), whereas smaller $^{34}\varepsilon$ are associated with smaller $^{33}\lambda$, as expected for the kinetic isotope effects in multiple isotope systems (*23*). Our estimate for the largest $^{34}\varepsilon$ is close to the apparent upper boundary for the values of $\delta^{34}S_{sulfate\text{-}sulfide}$ in nature (Fig. 3.1). In contrast, models that include oxidative recycling do not necessarily limit the values of $\delta^{34}S_{sulfate\text{-}sulfide}$ to the equilibrium value [Fig. 2 in (*9*)].

Models of S-isotope effects produced by a combination of MSR and MSD predict that the largest $\delta^{34}S_{sulfate\text{-}sulfide}$ should occur in areas of intense sulfur redox cycling and significant MSD. Although these processes demonstrably occur in modern coastal environments (*9*, *24*), large (> 47‰) $\delta^{34}S_{sulfate\text{-}sulfide}$ values are not reported frequently in these settings (Fig. 3.1). Large $\delta^{34}S_{sulfate\text{-}sulfide}$ values are instead commonly reported from deep-sea sediments, where the extremely slow microbial metabolisms are attributed to the limited availability and the poor reactivity of organic substrates (*25*, *26*). The diversity of microbes and growth conditions that generate natural $\delta^{34}S_{sulfate\text{-}sulfide}$ values larger than 47 ‰ remains to be determined, but the overall scarcity of sulfides exhibiting $\delta^{34}S_{sulfate\text{-}sulfide}$ > 47‰ over geologic history (*2*) thus might be simply related to the lack of preservation of deep-sea sediments. Euxinic basins also exhibit a wide range of $\delta^{34}S_{sulfate\text{-}sulfide}$ values that commonly exceed 47‰ and $^{33}\lambda$ values larger than those previously attributed to MSR (Fig. 3.2A). These $\delta^{34}S_{sulfate\text{-}sulfide}$ and $^{33}\lambda$ values have been used as an indication of the contribution of MSD to the cycling of sulfur in modern euxinic environments (*27*). However, the combined isotopic signatures of $^{34}\varepsilon$ and $^{33}\lambda$ produced by DMSS-1 can explain nearly all observations from modern euxinic settings (Fig. 3.2A) and demonstrate that neither $^{34}\varepsilon$ nor $^{33}\lambda$ unambiguously indicates MSD in modern environments.

The earliest values of $\delta^{34}S_{sulfate\text{-}sulfide}$ larger than 50‰ occur in a 1.2 Ga old non-marine environment (*13*), and may have become more widespread in marine environments after ~ 700 Ma (*28*) or even later (*10*, *12*). Grounded in the assumption that $^{34}\varepsilon$ values larger than 47‰ do not occur during MSR alone, this temporal trend was attributed to various mechanisms including: the growth of the marine sulfate reservoir (*29*), the increasing importance of disproportionation (*11*), the progressive oxygenation of the oceans (*2*),

and the advent of bioturbating organisms close to the Precambrian/Cambrian boundary (*30*). However, given that DMSS-1 in the presence of just 2 mM sulfate produces $^{34}\varepsilon$ values of 61.1‰, i.e., outside the limit previously attributed to MSR alone (*2*, *11*), MSR alone could have produced similar S-isotope signatures after a moderate increase in the size of marine sulfate reservoir (2 mM) during the mid-Mesoproterozoic (*31*).

In addition to ^{34}S (*2*), ^{33}S record has been used to show significant contribution of MSD to the global sulfur cycle as early as 1300 Ma (*11*, *32*). This constraint is based on model estimates for sulfur isotope compositions ($\delta^{34}S$ and $\Delta^{33}S$) of proxies for seawater sulfate (Fig. 3.2B). However, the input parameters for this model include the relatively small ranges of $^{34}\varepsilon$ and $^{33}\lambda$ values from previous laboratory experiments (*11*). When the same box model is solved with new expanded ranges of $^{34}\varepsilon$ and $^{33}\lambda$ values produced by DMSS-1, all but one sample of Phanerozoic and Proterozoic sedimentary sulfates (*11*, *32*) are consistent with the global sulfur cycle including only MSR without MSD (Fig. 3.2B). Therefore, ^{33}S isotope signatures in sedimentary records do not clearly indicate sulfur disproportionation in the ancient oceans (*2*, *9*, *11*).

Because the fractionation of sulfur isotopes between sulfate and sulfide can exceed 50‰ even if sulfide is not reoxidized outside of the cell and at an environmental scale, more Proterozoic samples exhibiting a large $\delta^{34}S_{sulfate\text{-}sulfide}$ may be found. Any temporal changes in the sulfur isotope record during this time could reflect the changing nature of organic material that fueled sulfate reduction, rather than measure the extent of oxygenated areas in oceans. The relative contributions of MSR alone and of the environmental-scale oxidative recycling toward large present and past natural fractionations of S-isotope ratios now remain to be evaluated.

3.3. Supporting Materials

3.3.1. Literature Data Used to Construct Figure 3.1

environment		location	material and method	isotope fractionation (‰)	ref.
subsurface	Groundwater	Bahamian blue holes	sulfate/sulfide	47 ~ 49	49
		Canadian River alluvium	porewater sulfate	23	50
		Dogger geothermal aquifer	sulfate/sulfide	35 ~ 41	51
		Edwards aquifer	sulfate/sulfide	38	52
		Floridan ground water	sulfate/sulfide	65	52
		Fuhrberger Field	sulfate/sulfide	10	53
		Ground water around Dead Sea	sulfate/sulfide	30	54
		Karstic groundwater, Franconian Alb	porewater sulfate	6 ~ 11	55
		Lincolnshire Aquifer	sulfate/sulfide	30 ~ 60	56
		MSL15	sulfate/sulfide	16	57
		MSL17	sulfate/sulfide	14	57
		Murray Basin	porewater sulfate	24	58
		oil-contaminated aquifer in Studen, Switzerland	porewater sulfate	20 ~ 23	59
		Owens Dry Lake	sulfate/sulfide	24 ~ 53	60
		phenol contaminated aquifer	sulfate/sulfide	9	61
		south-central Canada	porewater sulfate	16	62
		TSL	porewater sulfate	25	63
terrestrial	wetland	Everglades	sulfate/sulfide	39 ~ 51	64
		New Jersey Pinelands	porewater sulfate	3	65
		New Jersey Pinelands	sulfate/sulfide	27	65
		Okefenokee swamp	sulfate/sulfide	11 ~ 33	64
	holomictic lake	Adirondack Mountains lakes	sulfate/sulfide	10 ~ 22	66
		Canadice lake	sulfate/sulfide	19	67
		Cliff lake	sulfate/sulfide	12	67
		Crystal lake	sulfate/sulfide	9	67
		Dart lake	sulfate/sulfide	3	67
		ELA lake 240	sulfate/sulfide	4	67
		Lake Chany	sulfate/sulfide	11 ~ 23	68
		Lake Hufeisensce	sulfate/sulfide	8 ~ 14	69
		Lake Ontario	sulfate/sulfide	30	70
		Lake Steisslingen	sulfate/sulfide	18	71
		Linsley pond	sulfate/sulfide	8 ~ 11	72
		Mares lake	sulfate/sulfide	13	67
		Mountain lake	sulfate/sulfide	12	67

		MT.Tom Pond	sulfate/sulfide	9	72
		Queechy lake	sulfate/sulfide	5	72
		Trout Bsain 2	sulfate/sulfide	11	67
		Trout North	sulfate/sulfide	6	67
	meromictic lake	Bird lake	sulfate/sulfide	5	67
		Black Kirchier	sulfate/sulfide	10	73
		Conesus lake	sulfate/sulfide	18	67
		Great Kirchier	sulfate/sulfide	2	73
		Green lake	sulfate/sulfide	56 ~ 59	72
		Green lake	sulfate/sulfide	55 ~ 58	74
		Green lake	sulfate/sulfide	49 ~ 57	27
		Gull lake	sulfate/sulfide	5	67
		Heart lake	sulfate/sulfide	0	67
		Jellyfish lake	sulfate/sulfide	22 ~ 41	75
		Lago di Cadagno	sulfate/sulfide	31 ~ 45	8
		Lake Mogil'noe	sulfate/sulfide	56 ~ 62	76
		Lake Mogil'noe	sulfate/sulfide	32 ~ 47	77
		Lake Vanda	sulfate/sulfide	30	78
		Lake Vanda	sulfate/sulfide	35	79
		Mahoney Lake (salty)	sulfate/sulfide	52 ~ 53	80
		Sakovo	sulfate/sulfide	27	73
		Trout Basin 3	sulfate/sulfide	5	67
marine	coastal environments	Great Sippewissett Salt Marsh, Cape Cod	sulfate/sulfide	50	15
		Jade Bay	sulfate/sulfide	26~54	81
		Logten Lagoon	sulfate/sulfide	37	82
		Newport Marsh	sulfate/sulfide	32 ~ 45	83
		Orinoco Delta	sulfate/sulfide	8 ~ 15	84
		Saint Lucia, Lesser Antilles	sulfate/sulfide	42 ~ 54	85
		Sapelo Island	sulfate/sulfide	30 ~ 50	86
		Shark Bay	sulfate/sulfide	33 ~ 44	87
		Solar Lake	sulfate/sulfide	40	82
		Solar Lake	sulfate/sulfide	37 ~ 46	88
		Spencer Gulf	sulfate/sulfide	30 ~ 48	89
		Watson and Callaway Bayou	sulfate/sulfide	40 ~ 46	90
		Weddewarden	sulfate/sulfide	32 ~ 33	88
	continental shelf	Aarhus Bay	sulfate/sulfide	52 ~ 61	88
		Baltic Sea	sulfate/sulfide	14 ~ 33	91
		Black Hole, Long Island Sound	sulfate/sulfide	41	9
		Black sea	sulfate/sulfide	65 ~ 71	88

	Brandford Bay	sulfate/sulfide	42 ~ 43	72
	Captian Key	sulfate/sulfide	41 ~ 46	92
	Friends of Anoxic Mud, Long Island Sound	sulfate/sulfide	49	9
	Long Island Sound	sulfate/sulfide	33 ~ 34	72
	Makirina Bay	sulfate/sulfide	49 ~ 53	93
	Marina Del Rey Harbor	sulfate/sulfide	33	94
	Northwest Control, Long Island Sound	sulfate/sulfide	58	9
	Oregon Shelf	porewater sulfate	7	95
	Sachem, Long Island Sound	sulfate/sulfide	34	9
	Western Svalbard	sulfate/sulfide	45 ~ 55	96
deep sea	Aleutian Trench	porewater sulfate	10 ~ 72	95
	Astoria Fan	porewater sulfate	58	95
	Bahama Ridge	porewater sulfate	38	97
	Bermuda Rise	porewater sulfate	39	97
	Blake Ridge	porewater sulfate	12 ~ 62	97
	Blake Ridge	porewater sulfate	11	98
	Caribbean	porewater sulfate	33	95
	Carmen Basin	porewater sulfate	60	99
	Cascadia Basin	porewater sulfate	77	5
	Central Altantic	porewater sulfate	27	95
	E. Caroline Basin	porewater sulfate	55	97
	East Cortez Basin	sulfate/sulfide	57	94
	Eastern Equatorial Pacific	porewater sulfate	14 ~ 40	100
	Eastern Mediterranean	porewater sulfate	47 ~ 64	101
	Gulf of Mexico	porewater sulfate	9 ~ 26	102
	hyper sulfidic deep biosphere	sulfate/sulfide	65 ~ 72	6
	Japan Sea	porewater sulfate	28 ~ 41	97
	Juan de Fuca Ridge	porewater sulfate	44 ~ 50	97
	Long Basin, California	sulfate/sulfide	68	94
	North Atlantic Ridge	sulfate/sulfide	9 ~ 64	103
	North Pacific	porewater sulfate	41 ~ 56	95
	North Pacific	porewater sulfate	17 ~ 29	97
	northeastern Arabian Sea	sulfate/sulfide	47 ~ 66	104
	Ontong Java	porewater sulfate	19	97
	Oregon Slope	porewater sulfate	22	95
	Peru Margin	porewater sulfate	18 ~ 23	100
	Peru margin	sulfate/sulfide	27 ~ 55	105
	Peru Slope	porewater sulfate	11	97
	Peru Trench	porewater sulfate	32	97
	Pescadero Basin	sulfate/sulfide	49 ~ 60	99
	San Diego Trough	sulfate/sulfide	16 ~ 54	83
	Santa Barbara Basin	sulfate/sulfide	0 ~ 44	83
	Santa Catalina Basin	sulfate/sulfide	33 ~ 55	83
	Santa Monica Basin	sulfate/sulfide	7 ~ 36	83

	Southwest Pacific	porewater sulfate	9 ~ 48	106
	Southwest Pacific	sulfate/sulfide	11 ~ 75	106
	Western Atlantic	sulfate/sulfide	57 ~ 68	107
	Western Mediterranean	porewater sulfate	25 ~ 71	108
	Western Pacific	sulfate/sulfide	25 ~ 57	109
euxinic basin	Baltic Sea	sulfate/sulfide	24 ~ 46	91
	Black Sea	sulfate/sulfide	43 ~ 58	110
	Black Sea	sulfate/sulfide	57 ~ 61	111
	Black sea	sulfate/sulfide	58 ~ 66	88
	Black sea	sulfate/sulfide	62	112
	Cariaco Basin	porewater sulfate	17	95
	Cariaco Basin	sulfate/sulfide	50 ~ 65	113
	Cariaco Basin	sulfate/sulfide	52	112
	Cariaco Basin	sulfate/sulfide	52 ~ 55	35
	Framvaren Fjord	sulfate/sulfide	36 ~ 47	114
	Gotland Deep	sulfate/sulfide	46 ~ 50	115
	Kiel Bay, Baltic Sea	sulfate/sulfide	52 ~ 61	116
	Mariager Fjord	sulfate/sulfide	30 ~ 42	117

Table 3.S1. S-isotope fractionation in modern environments. Isotope fractionations were estimated using dissolved sulfate and sedimentary or dissolved sulfide, or calculated from the concentration and the isotope composition of pore water sulfate. Wetland: swamps, bogs, and peats. Coastal environments: salt marshes, tidal flats, deltas, and lagoons. Continental slope denotes the boundary of continental shelf. Localities beyond the continental shelf are classified as deep sea. This table does not include isotope data from hydrothermal or acidic environments, where abiotic processes can be as significant as microbial processes.

strain	$^{34}\varepsilon$ (‰)	electron donor	references
A. fulgidus Strain Z	14 ~ 25	lactate	118, 119
ASv20	14 ~ 21	acetate	118, 120
	8	lactate	120
ASv26	20 ~ 21	acetate	120
D. acetoxidans	18	acetate	118
	24	formate	121
D. arctica	6	lactate	118
D. autotrophicum	16 ~ 36	butyrate	34, 118
	14	H_2	118
D. baarsii	23	butyrate	118
D. baculatum	13	lactate	118
D. balticum	23	butyrate	118
D. desulfuricans	24	dextrose	122
	8 ~ 46	ethanol	122, 123
	24	glucosamine	122
	3 ~ 14	H_2	122, 123
	-3 ~ 35	lactate	47, 121, 122, 123, 124, 125, 126, 127
	19	mannose	122
	19 ~ 20	mucin	122
D. elongatus	6	propionate	118
D. geothermicum	13	lactate	118
D. gibsoniae	28	butyrate	118
D. halophila	8	pyruvate	118
D. halophilus	2	lactate	118
D. hydrogenovorans	5	acetate	121
	6	formate	118
D. joergensenii	26	pyruvate	118
D. lacustre	19	ethanol	118
D. magnum	42	benzoate	118
D. marinus	7	propionate	118
D. nigrificans	5 ~ 18	lactate	125, 128
D. oceanense	22	acetate	118
D. orientis	4 ~ 11	lactate	118
D. oxyclinae	5	lactate	118
D. phenolica	37	benzoate	118
D. profundus	4	lactate	118
D. psychrophila	4	lactate	118
D. putei	10 ~ 21	lactate	129
D. redbaense	11	lactate	118
D. salexigens	5 ~ 11	lactate	125
D. sapovorans	17	lactate	118
D. thermocisternum	15	lactate	118

D. toluolica	29	benzoate	118
	18~ 43	toluene	130, 131
D. variabilis	15	benzoate	118
D. vulgaris	8 ~ 10	lactate	125
Desulfococcus sp.	16	pyruvate	118
Desulfovibrio sp. strain X	5	lactate	118
DMSS-1	14 ~ 16	ethanol	14
	30 ~ 39	fructose	14
	44 ~ 66	glucose	this study, 14
	9 ~ 10	glycerol	14
	6 ~ 37	lactate	14
	16 ~ 18	malate	14
	7 ~ 8	pyruvate	14
LSv514	6	lactate	120
LSv54	6 ~ 10	lactate	120
PRTOL1	32	acetate	132
	30	benzoate	132
	33	phenylpropionate	132
	36	pyruvate	132
	32 ~ 47	toluene	130
T. commune	5	lactate	118
T. indicus	4 ~ 32	H_2	133
T. yellowstonii	17	lactate	118
TRM1	40	toluene	121

Table 3.S2. S-isotope fractionations in pure cultures of sulfate reducing microbes utilizing different electron donors.

3.3.2. Materials and Methods

3.3.2.1. Culture Experiments

DMSS-1 was enriched and isolated from marine coastal sediments in Cape Cod, Massachusetts, USA (*14*).The isolated bacterium, DMSS-1, reduces sulfate to sulfide using various organic compounds or hydrogen as electron donors, ferments glucose, and disproportionates thiosulfate (Table 3.S3). The growth of DMSS-1 was determined either by measuring the optical density at 660 nm (OD660) or by microscopic counts of cells stained by SYTOX-Green nucleic acid stain (Invitrogen S7020, Paisley, UK).

DMSS-1 was grown in a chemically defined medium consisting of (per liter): $NaHCO_3$, 9g; Na_2SO_4, 3g (for 21 mM sulfate) or 0.3g (for 2 mM sulfate); KH_2PO_4, 0.2g; NH_4Cl, 0.3g; NaCl 21g; $MgCl_2 \cdot 6H_2O$, 3g; KCl, 0.5g; $CaCl_2 \cdot 2H_2O$, 0.15g; resazurin 1 mg, 1 ml of trace element solution SL-10 (*36*), 10 ml of vitamin solution described as a part of DSMZ medium 141 (DSMZ, Braunschweig, Germany: Catalogue of strains 1993), and 1 ml of selenium stock solution (0.4mg of Na_2SeO_3 per 200 ml of 0.01N NaOH). Sodium ascorbate (1.5 g per liter) was added as the reducing agent. Glucose was used both as an electron donor and as a carbon source. The medium was titrated to pH 7.5 and prepared anaerobically under 80% N_2/20% CO_2. Amino acid mix (*37*) was added to some cultures to test the effect of recycled nitrogen and carbon on S-isotope effects. The ability of DMSS-1 to disproportionate thiosulfate was tested in the same basal medium containing 10 mM thiosulfate and 3 mM acetate, in the absence of other organic electron donors. The ability of DMSS-1 to disproportionate elemental sulfur was tested in the medium modified after Finster et al. (*38*).

The flow-through culture was continuously gassed by 80% N_2/20% CO_2 to buffer the pH and to strip the sulfide. Sulfide was sampled by bubbling through a 0.18 M zinc acetate solution. The basal medium containing 10 mM glucose and 21 mM sulfate was prepared as described above and pumped into and out of a 500 ml reactor by a peristaltic pump at a rate of 38 ml/day. Sulfide and effluent from the flow-through culture were sampled after one month and the steady state was confirmed by measuring the cell density, sulfide production rate, and the isotope composition of the sulfide produced in the reactor.

3.3.2.2. Measurements of Cell Densities and Chemical Concentrations

Sulfide concentration was measured by a modified methylene blue assay (*39*). Cell growth was monitored by measuring the optical density at 630 nm and by microscopic counts of cells stained by SYTOX-Green nucleic acid stain (Invitrogen S7020, Paisley, UK) using a Zeiss Axio Imager M1 epifluorescence microscope (Carl Zeiss, Thornwood, NY, USA). The concentration of glucose was

metabolism	substrate	growth
sulfate respiration	acetate	-
	acetylglucosamine	-
	ascorbate	-
	ethanol	+
	fructose	+
	galactose	-
	glucose	+
	glucuronic acid	-
	glycerol	++
	hydrogen/acetate	+
	lactate	++
	malate	+
	maltose	-
	mannose	-
	pyruvate	++
	succinate	-
	sucrose	-
disproportionation	elemental sulfur	-
	thiosulfate	+
fermentation	glucose	+

Table 3.S3. Growth of DMSS-1 on various organic and inorganic substrates. ++, cell density more than doubled in one week; +, cell density at least doubled in two weeks; -, no growth [cell density either decreased or remained unchanged within the limit of experimental error (15 %) over the course of one month].

determined by a colorimetric glucose assay kit (Sigma, GAHK20-KT, MO, USA). The concentration of acetate was determined in the anion form by an ion chromatograph (DX500, Dionex, Sunnyvale, CA). All colorimetric and optical density measurements were performed using a Synergy2 microplate reader (BioTek U.S., Winooski, VT).

3.3.2.3. Measurements of S-isotopes

Sulfide from batch cultures was extracted by acidifying the culture medium with 6 N HCl at 80°C under nitrogen gas for two hours. Sulfide produced during the distillation was precipitated as ZnS in a Zn-acetate solution (0.18 M). After the extraction of sulfide, sulfate in the remaining medium was reduced to sulfide in the reaction with 30 ml of the reducing agent (mixture of HI, H_3PO_2 and HCl, *40*). Samples were boiled and purged by N_2 gas for two hours. After volatile products were passed through a condenser and a trap containing distilled water, sulfide was collected in the Zn-acetate trap. Sulfide from continuous culture was collected directly by passing the effluent gas through a sulfide trap containing a 0.18 M Zn-acetate solution. Sulfate was extracted from a 2-3 ml sample of the effluent as described above. ZnS was converted to Ag_2S by the addition of $AgNO_3$ and the incubation at 70 °C for one day. Ag_2S was centrifuged, washed with distilled water three times and dried at 70 °C. The Ag_2S samples were allowed to react with an excess of fluorine gas for more than 5 hours at 300°C, and the produced SF_6 was purified by gas chromatography. The purified SF_6 was transferred into an isotope-ratio mass spectrometer for multiple sulfur isotope measurements in the dual inlet mode (*41*).

3.3.2.4. Data Processing

Specific growth rates of DMSS-1 (day^{-1}) during the late or the early exponential growth phase were calculated as the slopes of linear regression of natural log of cell density. Growth yield (number of cells/mol of reduced SO_4^{2-}) during the same interval was calculated as the ratio of the increase in the number of cells and of the sulfate consumed (that equals to sulfide produced). The average cell-specific sulfate reduction rates (csSRR) were calculated from the specific growth rate and the growth yield:

$$csSRR\ (mole \cdot cell^{-1} \cdot time^{-1}) = \frac{specific\ growth\ rate\ (time^{-1})}{growth\ yield\ (cell \cdot mole^{-1})} (1)$$

Isotope fractionation factors (α) for batch culture experiments are calculated using the Rayleigh distillation equation:

$$\alpha = -\frac{1}{\ln f_r} \ln\left(1 + \frac{(1-f_r)}{f_r} \frac{\delta_{\Delta p} + 1000}{\delta_r + 1000}\right) \quad (2)$$

where, f_r is the fraction of the remaining reactant, $\delta_{\Delta p}$ is the sulfur isotope composition (^{33}S or ^{34}S) of sulfide produced during the incubation, and δ_r is the sulfur isotope composition of sulfate at the end of incubation. Inocula were degassed and washed three times by centrifugation and resuspension in sterile fresh medium to remove the carry-over of sulfide. This was done in all but one set of experiments (second set with 8.5 mM glucose/21 mM sulfate, Table 3.S4). Isotopic compositions and the concentrations of the sulfide carry-over in these experiments were measured in the inocula and the isotope mass-balance was used to derive $\delta_{\Delta p}$.

Isotope fractionation factors in continuous cultures at the steady state were calculated according to:

$$^{x}\alpha = \frac{\delta^{x}S_{HS} + 1000}{\delta^{x}S_{SO_4} + 1000} \quad (3)$$

where, x is 33 or 34.

Isotope enrichment factor is defined as:

$$^{x}\varepsilon = 1000 \cdot (1 - {}^{x}\alpha) \quad (4)$$

$^{33}\lambda$ values, used to characterize the mass-dependent fractionation during sulfate reduction, are defined as:

$$^{33}\lambda = \frac{\ln(^{33}\alpha)}{\ln(^{34}\alpha)} \quad (5)$$

To estimate errors for $^{34}\varepsilon$ and $^{33}\lambda$ values, errors from isotope analysis (0.1‰ for $\delta^{33}S$, 0.2‰ for $\delta^{34}S$, and 0.01‰ for $\delta^{33}S - 0.515 \cdot \delta^{34}S$) and sulfide concentration measurement (±5%) were propagated according to the methods described by Bevington and Robinson (*42*).

3.3.3. Growth of DMSS-1 on Glucose

To determine how DMSS-1 reduces sulfate and grows on glucose, we conducted control experiments. DMSS-1 does not grow when glucose is omitted from the medium, indicating that DMSS-1 does not couple the reduction of sulfate with the oxidation of some alternative electron donor in the basal

	experiments	f	sulfide (mM)	sulfide $\delta^{33}S$	sulfide $\delta^{34}S$	remaining sulfate $\delta^{33}S$	remaining sulfate $\delta^{34}S$
batch cultures	10 mM glucose / 21 mM sulfate	0.99	0.2	-32.74	-62.68	0.09	0.26
		0.99	0.2	-34.24	-65.45	0.20	0.45
		0.99	0.2	-34.13	-65.23	0.12	0.28
		0.91	1.9	-30.01	-57.59	1.95	3.76
	8.5 mM glucose / 21 mM sulfate	1.00	0.1#	-30.01#	-57.59#		
		0.93	1.5	-30.75	-58.95	1.51	2.93
		0.87	2.8	-28.72	-55.17	3.50	6.76
		0.81	4.1	-25.54	-49.13	5.19	10.06
		0.70*	6.3*	-19.96*	-38.56*	7.48*	14.48*
	10 mM glucose / 21 mM sulfate (+ amino acids)	0.96	0.9	-28.62	-54.95	1.10	2.18
		0.93	1.5	-31.42	-60.18	2.25	4.34
	1 mM glucose / 21 mM sulfate	0.99	0.2	-29.90	-57.39	0.67	1.36
	10 mM glucose / 2 mM sulfate	0.85	0.3	-28.94	-55.59	5.68	11.03
	1 mM glucose / 2 mM sulfate	0.90	0.2	-22.79	-43.94	2.32	4.49
continuous ($0.08\ day^{-1}$)	10 mM glucose / 21 mM sulfate			-27.25	-52.26		
				-28.54	-54.65		
				-27.81	-53.41	-0.45	-0.83

Table 3.S4. Isotopic compositions of sulfide produced during the growth of DMSS-1 and of sulfate remaining in the medium. Measured isotope compositions are presented as $\delta^{x}S$ values normalized to VCDT (Vienna-Canyon Diablo Troilite). f is the fraction of remaining sulfate. *, data from (*14*). #, Isotope composition and concentration of the initial sulfide was measured in the inoculum. The carry-over of sulfide only occurred in the set of experiments with 8.5 mM glucose/21 mM sulfate. Cell inocula used in all other experiments were washed in sterile medium.

medium. In turn, the concentration of glucose in sterile, uninoculated medium remains constant for more than two months (Fig. 3.S1), showing that the breakdown of this sugar requires the presence of DMSS-1 cells. These control experiments confirm that DMSS-1 grows on glucose, and not on other components of the basal medium, or on some products of the abiotic breakdown of glucose. DMSS-1 does not grow on glucose derivatives acetylglucosamine and glucuronic acid, but can grow by coupling the reduction of sulfate with the oxidation of fructose.

Main products of the oxidation of monosaccharide coupled with sulfate reduction in some *Desulfobulbus, Desulfotomaculum,* and *Desulfovibro* species are acetate and CO_2 (*43*, *44*, *45*). The ratios of glucose consumed to sulfide produced and of glucose consumed to acetate produced during the growth of these microbes on glucose are 1 and ½ , respectively.

$$C_6H_{12}O_6 + SO_4^{2-} \rightarrow 2CH_3COO^- + 2CO_2 + H_2S + 2H_2O \quad (6)$$

The measured ratio of glucose to sulfide is 2.8 ± 0.2 in the early exponential phase in batch cultures, and 5.6 ± 0.3 in continuous cultures of DMSS-1 (Table 3.S5). This differs from the ratio of 1, predicted by Eq. 6. This discrepancy suggests that some electrons derived by the oxidation of glucose are not directed to the sulfate reduction system but are transferred into the production of other organic products or hydrogen. This is consistent with the ability of DMSS-1 to ferment glucose (Table 3.S3) and the reports of similar decoupling between carbon and sulfur metabolisms in other glucose-utilizing sulfate reducing bacteria (*45*, *46*). In turn, the stoichiometry of the reaction integrated over the late vegetative growth in batch culture [1.1±0.1 for glucose/sulfide, and 1.9±0.1 for acetate/sulfide (Table 3.S5)] is consistent with Eq. 6 and suggests that any intermediate products of glucose oxidation are fully oxidized to acetate and CO_2 during late growth stage. The metabolic and stoichiometric differences between early and later exponential growth in batch culture are accompanied by lower cell yields (per sulfate reduced) and higher csSRR during early exponential growth (Table 3.S5). The stoichiometry, growth rates and growth yields during the growth of DMSS-1 in continuous culture are similar to those during early exponential growth in batch culture (Table 3.S5). These conditions can be maintained indefinitely in continuous culture, because the initial metabolic products are continuously diluted or degassed.

The physiological differences during growth in batch culture are accompanied by a change in isotope enrichment factor ($^{34}\varepsilon$). This factor exceeds 60‰ during the initial stages of growth on glucose but decreases to 44‰ at the end of experiment (Table. 3.1).

Overall, DMSS-1 grows and reduces sulfate more slowly when it oxidizes glucose than during the oxidation of other organic substrates (*14*). Only one previous study (*47*) reports isotope fractionation at

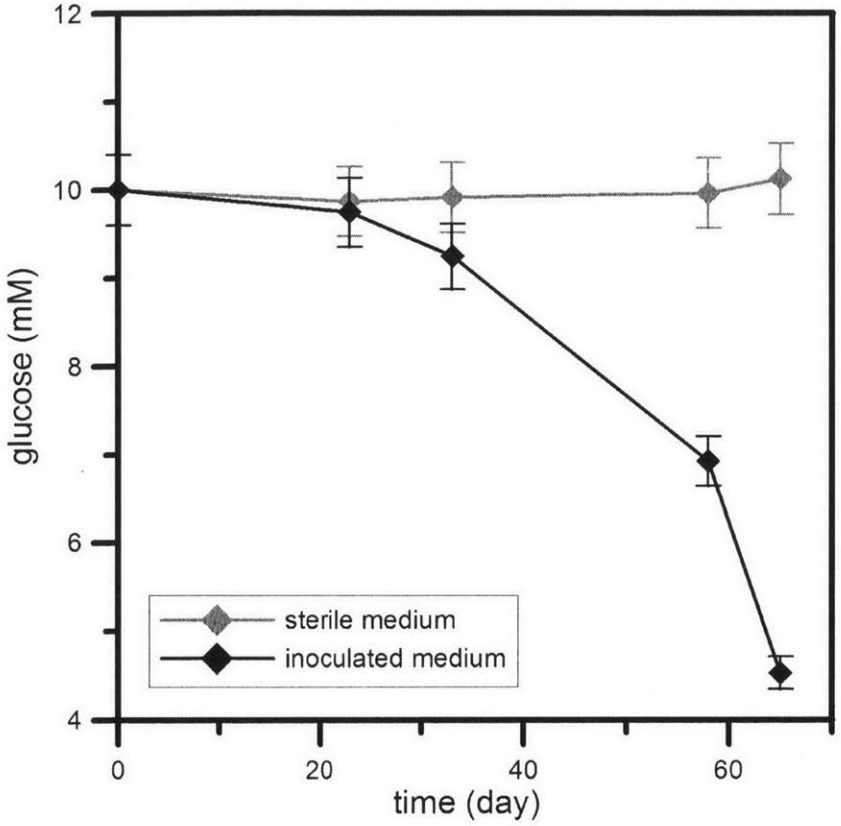

Figure 3.S1. Concentration of glucose in sterile medium (grey diamonds) and medium containing DMSS-1 (black diamonds). Error bars indicate the analytic uncertainty of the measurement of glucose concentrations (±4%).

experiments		growth rate (day^{-1})	growth yield (10^6cells/μmole SO_4^{2-})	csSRR (fmole HS^- /cell/day)	glucose/sulfide	acetate/sulfide
batch cultures	early growth	0.08±0.01	73±12	1.1±0.2	2.8±0.2	5.3±0.3
	entire growth	0.12±0.00*	160±25*	0.7±0.1*	1.1±0.1	1.9±0.1
continuous cultures		0.08	51±8	1.6±0.2	5.6±0.4	-

Table 3.S5. Growth rates, yields and the stoichiometry of glucose, acetate, and sulfide in cultures of DMSS-1 grown on glucose. *, data from (*14*).

comparable growth rates and csSRRs. The same study reported the largest isotope fractionation (35‰) among other eight studies using the same strain (*Desulfovibrio desulfuricans*) and substrate (lactate) (Table 3.S2). However, much slower csSRRs are estimated for natural environments, ranging from 4×10^{-7} ~ 9×10^{-3} fmol/cell/day in deep sea sediments (*25*) to 8×10^{-3} ~ 8×10^{-2} fmol/cell/day in coastal sediments (*48*).

References and Notes

1. R. M. Garrels, A. Lerman, *PNAS* **78**, 4652 (1981).
2. D. E. Canfield, A. Teske, *Nature* **382**, 127 (1996).
3. R. A. Berner, S. T. Petsch, *Science* **282**, 1426 (1998).
4. $\delta^{34}S_{sulfate\text{-}sulfide}$ is the depletion of ^{34}S in sulfide relative to sulfate source (e.g., seawater sulfate for marine environments) ($\approx\delta^{34}S_{sulfate}$-$\delta^{34}S_{sulfide}$). $\delta^{x}S$ values are defined as $\delta^{x}S=1000\cdot[(^{x}S/^{32}S)_{sample}/(^{x}S/^{32}S)_{standard}-1]$, where x is 33 or 34. $\Delta^{33}S=\delta^{33}S-1000\cdot[(\delta^{34}S/1000+1)^{0.515}-1]$. $^{x}\varepsilon=1000\cdot[1-(^{x}S/^{32}S)_{sulfide}/(^{x}S/^{32}S)_{sulfate}]$ and $^{33}\lambda=\ln[(^{33}S/^{32}S)_{sulfide}/(^{33}S/^{32}S)_{sulfate}]/\ln[(^{34}S/^{32}S)_{sulfide}/(^{34}S/^{32}S)_{sulfate}]$, where $(^{x}S/^{32}S)_{sulfide}$ and $(^{x}S/^{32}S)_{sulfate}$ are the instantaneous S-isotope ratios of sulfide and the remaining sulfate, respectively.
5. M. D. Rudnicki, H. Elderfield, B. Spiro, *Geochim. Cosmochim. Acta* **65**, 777 (2001).
6. U. G. Wortmann, S. M. Bernasconi, M. E. Böttcher, *Geology* **29**, 647 (2001).
7. B. Brunner, S. M. Bernasconi, *Geochim. Cosmochim. Acta* **69**, 4759 (2005).
8. D. E. Canfield, J. Farquhar, A. L. Zerkle, *Geology* **38**, 415 (2010).
9. D. E. Canfield, B. Thamdrup, *Science* **266**, 1973 (1994).
10. M. T. Hurtgen, M. A. Arthur, G. P. Halverson, *Geology* **33**, 41 (2005).
11. D. T. Johnston *et al.*, *Science* **310**, 1477 (2005).
12. D. A. Fike *et al.*, *Nature* **444**, 744 (2006).
13. J. Parnell *et al.*, *Nature* **468**, 290 (2010).
14. M. S. Sim *et al.*, *in revision for Geochim. Cosmochim. Acta.*
15. B. J. Peterson, R. W. Howarth, R. H. Garritt, *Ecology* **67**, 865 (1986).
16. Further details are available in the supporting material on *Science* Online.
17. B. Vu *et al.*, *Molecules* **14**, 2535 (2009).
18. J. M. Stams *et al.*, *Arch. Microbiol.* **136**, 54 (1983).
19. K. Mopper *et al.*, *Mar. Chem.* **10**, 55 (1980).
20. C. E. Rees, *Geochim. Cosmochim. Acta* **37**, 1141 (1973).
21. D. B. Northrop, *Ann. Rev. Biochem.* **50**, 103 (1981).
22. The range reflects values derived either by the extrapolation from high temperature (> 200°C) or by theoretical calculations (*33*) assuming pH=7. The equilibrium isotope fractionation factor between aqueous H_2S and HS^- is ~6‰.
23. J. Farquhar *et al.*, *Geobiology* **1**, 27 (2003).
24. B. B. Jørgensen, *Science* **249**, 152 (1990).
25. S. D'Hondt, S. Rutherford, A. J. Spivack, *Science* **295**, 2067 (2002).
26. B. B. Jørgensen, A. Boetius, *Nat. Rev. Micro.* **5**, 770 (2007).
27. A. L. Zerkle et al., *Geochim. Cosmochim. Acta* **74**, 4953 (2010).
28. G. M. Ross, J. D. Bloch, H. R. Krouse, *Precambrian Res.* **73**, 71 (1995).
29. J. M. Hayes, I. B. Lambert, H. Strauss, in *The Proterozoic Biosphere: A Multidisciplinary Study*, J. W. Schopf, C. Klein, Eds. (Cambridge Univ Press, Cambridge, UK, 1992), pp 129-132.
30. D. E. Canfield, J. Farquhar, *PNAS* **106**, 8123 (2009).
31. L. C. Kah, T. W. Lyons, T. D. Frank, *Nature* **431**, 834 (2004).

32. N. Wu *et al.*, *Geochim. Cosmochim. Acta* **74**, 2053 (2010).
33. T. Otake, A. C. Lasaga, H. Ohmoto, *Chem. Geol.* **249**, 357 (2008).
34. D. T. Johnston, J. Farquhar, D. E. Canfield, *Geochim. Cosmochim. Acta* **71**, 3929 (2007).
35. X. Li *et al.*, *Geochim. Cosmochim. Acta* **74**, 6764 (2010).
36. F. K. Widdel, G. W. Kohring, F. Mayer, *Arch. Microbiol.* **134**, 286-294 (1983).
37. A. G. Argawal, M. V. Gastel, W. Gartner, W. Lubitz, *J. Phys. Chem. B* **110**, 8142-8150 (2006).
38. K. Finster, W. Liesack, B. Thamdrup, *Appl. Environ. Microbiol.* **64**, 119-125 (1998).
39. J. D. Cline J. D. (1969), *Limnol. Oceanogr.* **14**, 454-458 (1969).
40. H. G. Thode, J. Monster, H. B. Dunford, *Geochim. Cosmochim. Acta* **25**, 158-174 (1961).
41. S. Ono, B. Wing, D. Johnston, J. Farquhar, D. Rumble, *Geochim. Cosmochim. Acta.* **70**, 2238-2252 (2006).
42. P. R. Bevington, D. K. Robinson, *Data reduction and error analysis for the physical sciences*, McGraw-Hill, New York (2002).
43. R. Cord-Ruwisch, B. Ollivier B., J. L. Garcia, *Curr. Microbiol.* **13**, 285-289 (1986).
44. G. Zellner, P. Messner, H. Kneifel, J. Winter J., *Arch. Microbiol.* **152**, 329-334 (1989).
45. A. Sass, H. Rutters, H. Cypionka, H. Sass, *Arch. Microbiol.* **177**, 468-474 (2002).
46. J. M. Akagi, G. Jackson G., *Appl. Microbiol.* **15**, 1427-1430 (1967).
47. L. A. Chambers *et al.*, *Can. J. Microbiol* **21**, 1602 (1975).
48. K. Sahm *et al.*, *Environ. Microbiol.* **1**, 65-74 (1999).
49. S. H. Bottrell et al., *Appl. Geochem.* **6**, 97-103 (1991).
50. M. L. W. Tuttle, G. N. Breit, I. M. Cozzarelli, *Chem. Geol.* **265**, 455-467 (2009).
51. C. Fouillac, A. Fouillac, A. Criaud, *Appl. Geochem.* **5**, 415-427 (1990).
52. R. Rye *et al.*, *Geochim. Cosmochim. Acta* **45**, 1941-1950 (1981).
53. O. Strebel, J. Böttcher, P. Fritz, *J. Hydrol.* **121**, 155-172 (1990).
54. I. Gavrieli *et al.*, *Earth Planet Sc. Lett.* **186**, 199-213 (2001).
55. F. Einsiedl, B. Mayer, *Environ. Sci. Technol.* **39**, 7118-7125 (2005).
56. S. H. Bottrell *et al.*, *Chem. Geol.* **169**, 461-470 (2000).
57. M. J. Spence *et al.*, *J. Contam. Hydrol.***79**, 67-88 (2005).
58. S. Dogramaci *et al.*, *Appl. Geochem.* **16**, 475-488 (2001).
59. M. H. Schroth *et al.*, *J. Contam. Hydrol.* **51**, 179-195 (2001).
60. J. Ryu *et al.*, *Chem. Geol.* **229**, 257-272 (2006).
61. M. J. Spence *et al.*, *J. Contam. Hydrol.* **53**, 285-304 (2001).
62. W. Robertson, S. Schiff, *J. Hydrol.* **158**, 123-134 (1994).
63. K. Knöller *et al.*, *Environ. Sci. Technol.* **40**, 3879-3885 (2006).
64. F. T. Price, D. J. Casagrande, *Int. J. Coal Geol.* **17**, 1-20 (1991).
65. K. W. Mandernack *et al.*, *Geochim. Cosmochim. Acta* **64**, 3949-3964 (2000).
66. B. Fry, *Biogeochemistry* **2**, 329-343 (1986).
67. B. Fry *et al.*, in *Geochemical Transformation of Sedimentary Sulfur*, A. Vairavamurthy, M. A. A. Schoonens, Eds. (American Chemical Society, 1995), pp. 397-410.
68. H. Doi *et al.*, *Hydrobiologia* **529**, 227-237 (2004).
69. G. Asmussen, G. Strauch G., *Water Air Soil Poll.* **108**, 271-284 (1998).
70. J. T. Nriagu, R. D. Coker, *Limnol. Oceanogr.* **21**, 485-489 (1976).
71. B. Mayer, L. A. Schwark, *Chem. Geol.* **161**, 315-337 (1999).
72. N. Nakai, M. Jensen, *Geochim. Cosmochim. Acta* **28**, 1893-1912 (1964).
73. M. V. Ivanov, *The Global Biogeochemical Sulphur Cycle*, John Wiley & Sons (1983).
74. B. Fry, *Limnol. Oceanogr.* **31**, 79-88 (1986).
75. A. L. Bates *et al.*, *Chem. Geol.* **106**, 63-76 (1993).
76. M. V. Ivanov *et al.*, *Microbiology* **70**, 583-593 (2001).
77. V. M. Gorlenko, M. B. Vainstein, V. I. Kachalkin, *Arch. Hydrobiol.* **81**, 475-492 (1978).
78. K. Purdy *et al.*, *Antarct. Sci.* **13**, 393-399 (2001).

79. N. Nakai *et al.*, *Geochem. J.* **9**, 7-24 (1975).
80. J. Overmann *et al.*, *Limnol. Oceanogr.* **41**, 147-156 (1996).
81. M. E. Böttcher *et al.*, *Continental Shelf Research* **20**, 1749-1769 (2000).
82. K. S. Habicht, D. E. Canfield, *Geochim. Cosmochim. Acta* **61**, 5351-5361 (1997).
83. I. Kaplan, K. Emery, S. Rotenberg, *Geochim. Cosmochim. Acta* **27**, 297-331 (1963).
84. H. G. Thode, A. G. Harrison, J. Monster, *Bull. Amer. Assoc. Petrol. Geol.* **44**, 1809-1817 (1960).
85. T. C. Ku *et al.*, *Mar. Geol.* **249**, 184-205 (2008).
86. B. J. Peterson, R. W. Howarth, *Limnol. Oceanogr.* **32**, 1195-1213 (1987).
87. J. Bauld, L. A. Chambers, G. W. Skyring, *Aust. J. Mar. Freshwater Res.* **30**, 753-764 (1979).
88. D.T. Johnston *et al.*, *Geobiology* **6**, 425-435 (2008).
89. L. Chambers, *Geochim. Cosmochim. Acta* **46**, 721-728 (1982).
90. V. Brüchert, *Geochim. Cosmochim. Acta* **62**, 1567-1586 (1998).
91. A. Y. Lein, *Eco. Bull.* **35**, 441-461 (1983).
92. T. Ku *et al.*, *Geochim. Cosmochim. Acta* **63**, 2529-2546 (1999).
93. S. Lojen *et al.*, *Sci. Total Environ.* **327**, 265-284 (2004)
94. I. R. Kaplan, in *Stable Isotopes in Sedimentary Geology*, M. R. Arthur et al., Eds. (SEPM, 1983), pp. 2-1-2-108.
95. G. E. Claypool, thesis, Los Angeles, Univ, California. (1974).
96. V. Brüchert, C. Knoblauch, B. B. Jørgensen, *Geochim. Cosmochim. Acta* **65**, 763-776 (2001).
97. G. E. Claypool, In *Geochemical Investigations in Earth and Space Science*, R. J. Hill et al., Eds. (Geochem. Soc., 2004), pp. 59-65.
98. G.E. Claypool, C. N.Threlkeld, in *Initial reports of the Deep Sea Drilling Project* **76**, R. E. Sheridan et al., Eds. (U. S. Government Printing Office, Washington, 1983), pp. 391-402.
99. M. B. Goldhaber, I. R. Kaplan, I.R. *Mar. Chem.* **9**, 95-143 (1980).
100. M. E. Böttcher *et al.*, *Proc. ODP, Sci. Results* **201**, 1-21 (2001).
101. M. E. Böttcher, H. -J. Brumsack, G. J. De Lange, *Proc. ODP, Sci. Results* **160**, 365-373 (1998).
102. P. Aharon, B. Fu, *Geochim. Cosmochim. Acta* **64**, 233-246 (2000).
103. H. R. Krouse, H. M. Brown, In *Initial Reports of the Deep Sea Drilling Project* 37, F. Aumento et al., Eds. (U.S. Government Printing Office, Washington, 1977), pp. 621-623.
104. A. Lückge et al., *Mar. Geol.* **158**, 1-13 (1999).
105. J. Mossmann *et al.*, *Geochim. Cosmochim. Acta* **55**, 3581-3595 (1991).
106. M. E. Böttcher *et al.*, *Mar. Geol.* **205**, 249-260 (2004).
107. H. Puchelt, H. W. Hubberten, In *Initial Reports of the Deep Sea Drilling Project* 51, 52, 53, Pt. 2, T. Donnelly et al., Eds. (U.S. Government Printing Office, Washington, 1980), pp. 1145-1148.
108. M. E. Böttcher, S. M. Bernasconi, H. J. Burmsack, *Proc. ODP, Sci. Results* **160**, 365-373 (1999).
109. J. C. Alt, J. W. Burdett, *Proc. ODP, Sci. Results* **129**, 283-294 (1992).
110. T. W. Lyons, *Geochim. Cosmochim. Acta* **61**, 3367-3382 (1997).
111. R. E. Sweeney, I. R. Kaplan, *Mar. Chem.* **9**, 145-152 (1980).
112. B. Fry *et al.*, *Deep-Sea Res. I* **38**, S1003-S1019 (1991).
113. J. P. Werne *et al.*, *Chem. Geol.* **195**, 159-179 (2003).
114. K. W. Mandernack, H. R. Krouse, J. M. Skei, *Chem. Geol.* **195**, 181-200 (2003).
115. J. Sternbeck, G. Sohlenius, *Chem. Geol.* **135**, 55-73 (1997).
116. M. Hartmann, H. Nielsen H., *Geol. Rundsch.* **58**, 621–655 (1969).
117. K. B. Sørensen, D. E. Canfield, D.E., *Geochim. Cosmochim. Acta* **68**, 503-515 (2004).
118. J. Detmers *et al.*, *Appl. Environ. Microbiol.* **67**, 888-894 (2001).
119. K. S. Habicht *et al.*, *Appl. Environ. Microbiol.* **71**, 3770-3777 (2005).
120. V. Brüchert, C. Knoblauch, B. B. Jørgensen, *Geochim. Cosmochim. Acta* **65**, 763-776 (2001).
121. M. Mangalo *et al.*, *Geochim. Cosmochim. Acta* **71**, 4161-4171 (2007).
122. A. L. W. Kemp, H. G. Thode, *Geochim. Cosmochim. Acta* **32**, 71-91 (1968).
123. I. R. Kaplan, S. C. Rittenberg, *J. Gen. Microbiol.* **34**, 195-212 (1964).

124. A. G. Harrison, H. G. Thode, *Trans. Faraday Soc.* **54**, 84-92 (1958).
125. R. McCready, *Geochim. Cosmochim. Acta* **39**, 1395-1401 (1975).
126. D. E. Canfield, C. A. Olesen, R. P. Cox, *Geochim. Cosmochim. Acta* **70**, 548-561 (2006).
127. M. Mangalo *et al.*, *Geochim. Cosmochim. Acta* **72**, 1513-1520 (2008).
128. M. E. Böttcher, S. M. Sievert, J. Kuever, *Arch. Microbiol.* **172**, 125-128 (1999).
129. M. M. Davidson *et al.*, *Appl. Environ. Microbiol.* **75**, 5621-5630 (2009).
130. C. Bolliger *et al.*, *Geochim. Cosmochim. Acta* **65**, 3289-3298 (2001).
131. K. Knöller *et al.*, *Environ. Sci. Technol.* **40**, 3879-3885 (2006).
132. J. Kleikemper *et al.*, *Geochim. Cosmochim. Acta* **68**, 4891-4904 (2004).
133. J. Hoek *et al.*, *Geochim. Cosmochim. Acta* **70**, 5831-5841 (2006).

4. Effect of Iron and Nitrogen on S-isotope Fractionation during Microbial Sulfate Reduction

4.1. Abstract

Microbial sulfate reduction utilizes sulfate as an electron acceptor and produces sulfide that is depleted in heavy isotopes of sulfur relative to sulfate. This process controls much of the distribution of sulfur isotopes in sedimentary sulfides and sulfates. Sulfur isotope fractionation is commonly used to trace the biogeochemical cycling of sulfur and its coupling to other essential elements such as carbon, nitrogen, and phosphorous. This study investigates the relationship between the availability of iron and reduced nitrogen and the magnitude of S-isotope fractionation during microbial sulfate reduction by DMSS-1, a marine sulfate reducing bacterium. Iron limitation increases S-isotope fractionation by about 50% relative to iron-replete cultures, whether grown on lactate or malate. This increase in S-isotope fractionation is accompanied by a decrease in the cytochrome c content and csSRR, implying that iron may affect S-isotope fractionation through enzymes that couple carbon and sulfur catabolism. Indeed, iron deficiency and the varying availability or chemistry of an electron donor yield very similar relationship between csSRR and 34ε. In contrast to iron, nitrogen limitation increases both csSRR and S-isotope fractionation. The energy and reducing power required for nitrogen fixation may be responsible for this opposite trend. Nitrogen and iron limitation may lead to large observed S-isotope effects in the water column of some euxinic lakes and seas, and anoxic sediments under a highly productive photic zone.

4.2. Introduction

Microbial sulfate reduction (MSR) is an anaerobic respiration process that utilizes sulfate as an electron acceptor. This process remineralizes organic carbon in anaerobic marine sediments and drives a global biogeochemical sulfur cycle (Canfield and Raiswell, 1999; Bottrell and Newton, 2006). Among the four stable isotopes of sulfur in nature (^{32}S, ^{33}S, ^{34}S, and ^{36}S), MSR preferentially utilizes lighter S-isotopes, producing sulfide that is depleted in heavy isotopes relative to the reactant sulfate. This isotope fractionation between sulfate and sulfide has been widely used to trace the biogeochemical cycling of sulfur and carbon (Strauss, 1997; Canfield, 2001a). Numerous studies have characterized S-isotope fractionation in pure and mixed cultures of sulfate-reducing microbes (Kaplan and Rittenberg, 1964;

Chambers et al., 1975; Habicht and Canfield 1997; Bolliger et al., 2001; Canfield, 2001b; Detmers et al., 2001; Hoek et al., 2006; Kleikemper et al., 2004; Johnston et al., 2005; Sim et al., 2011a; Sim et al., 2011b) and demonstrated a correlation between sulfate reduction rates and the magnitude of S-isotope fractionation (Kaplan and Rittenberg, 1964; Chambers et al., 1975; Hoek et al., 2006; Kleikemper et al., 2004; Sim et al., 2011a). However, links between environmental variables and physiological mechanisms that control sulfate reduction rates within cells deserve further attention.

Because all respiration processes use a terminal electron donor and acceptor, most studies have focused on the influence of sulfate (electron acceptor) and organic substrates (electron donor) on S-isotope fractionation. The magnitude of S-isotope fractionation during MSR decreases as sulfate concentrations fall below 200 μM (Harrison and Thode, 1958; Canfield, 2001a; Habicht et al., 2002 and 2005). On the other hand, MSR yields higher fractionations when limited by the low concentration of organic electron donors or coupled with the oxidation of refractory organic compounds (Kaplan and Rittenberg, 1964; Chambers et al., 1975; Sim et al., 2011a and 2011b). Doubtless, both electron donor and acceptor influence the magnitude of isotope fractionation, but it is unclear how this happens in the cell because sulfate reducing microbes do not translocate electrons from the organic substrate directly to the terminal electron acceptor, sulfate. Instead, the rates of electron transfer depend on a number of enzymes and electron carriers (Keller and Wall, 2011; Pereira et al., 2011). Thus, any alterations in the electron transfer chain may ultimately influence the magnitude of S-isotope fractionation by changing the coupling between the electron donor and sulfate.

Alterations to the electron transfer chain may arise from environmental limitations. Iron is an important cofactor in many enzymes and electron carriers in microbial electron transfer chains, including hydrogenases, ferredoxin or cytochromes. Iron deficiency impacts The synthesis and function of these enzymes and carriers in various microbes (Waring and Werkman, 1944; Hubbard et al., 1986; Cotter et al., 1992), including sulfate-reducing bacteria (Postgate, 1965). Therefore, one of the likely consequences of iron limitation is the reduction of respiratory energy conservation (Harder and Dijkhuizen, 1983). The cellular energy and redox budgets also change if some of the reducing equivalents generated by the oxidation of organic substrates are diverted toward metabolic processes such as nitrogen fixation, as would be expected during nitrogen limitation. This limitation impacts general protein synthesis, and not just the respiration machinery. To the best of our knowledge, previous studies have not investigated the effect of iron and other nutrient limitations on S-isotope fractionation during MSR.

Here we report the effect of Fe- and N-limitation on the physiology of a marine sulfate reducing bacterium, DMSS-1, and the resulting S-isotope fractionation. Though these two limitations likely

impact different cellular processes, both influence S-isotope effects. The potential significance of both limitations and their accompanying S-isotope fractionations are discussed in an environmental context.

4.3. Methods

Organism and growth medium. DMSS-1, a sulfate reducing bacterium isolated from marine coastal sediments (Sim *et al.*, 2011a), was grown in a chemically defined medium consisting of (per liter): $NaHCO_3$, 9 g; Na_2SO_4, 3 g; KH_2PO_4, 0.2 g; NaCl 21g; $MgCl_2 \cdot 6H_2O$, 3 g; KCl, 0.5 g; $CaCl_2 \cdot 2H_2O$, 0.15 g; resazurin 1 mg, 1 ml of trace element solution SL-10 omitting $FeCl_2$ (Widdel *et al.*, 1983), 10 ml of vitamin solution described as a part of DSMZ medium 141 (DSMZ, Braunschweig, Germany: Catalogue of strains 1993), 1 ml of selenium stock solution (0.4 mg of Na_2SeO_3 per 200 ml of 0.01N NaOH). The concentrations of iron and ammonium in the basal medium before the addition of ammonium and iron stock solutions were determined by ICP-OES (ActLab, Ontario, Canada) and a fluorometric method (Holmes *et al.*, 1999), respectively (with 0.7 μM and 0.5 μM detection limits for iron and ammonium, respectively). Regular (control) growth medium contained 10 ml of anaerobic NH_4Cl stock solution (3 g/100 ml water), and 1 ml of $FeCl_2 \cdot 4H_2O$ stock solution (150 mg $FeCl_2 \cdot 4H_2O$ in 100 ml of 0.25% HCl). In limitation experiments, the ammonium and iron stock solutions were serially diluted by 10 times with anaerobic water and 0.25% HCl, respectively, before the addition to the basal medium. Sodium ascorbate (1 g per liter) was added as a reducing agent. Cultures contained either lactate or malate as electron donors and carbon sources. The medium was titrated to pH 7.5 and sterilized anaerobically under 80% N_2/20% CO_2.

Culture experiments. DMSS-1 was incubated in batch cultures containing different concentrations of iron or ammonium. Culture bottles (165 mL) containing sterile media (100 ml) were inoculated with washed cells. The cells were washed three times by anaerobic centrifugation and resuspension in a fresh medium that lacked both iron and ammonium to eliminate carryover of sulfide, iron and ammonium. Growth (optical density, cell counts, and protein) and sulfide concentrations were monitored every day for lactate-grown cultures and every other day for malate-grown cultures. Sulfide concentration was measured in 200 μL culture samples fixed by 1 ml of 0.05 M Zn–acetate solution by a modified methylene blue assay (Cline, 1969). Growth was monitored by measuring the optical density at 630 nm using the Synergy2 Biotek microplate reader, (BioTek, VT, USA) and by microscopic counts of cells stained by SYTOX-Green nucleic acid stain (Invitrogen S7020, Paisley, UK) using a Zeiss Axio Imager M1 epifluorescence microscope (Carl Zeiss, Thornwood, NY, USA). At the end of each incubation, 20 ml of 1 M Zn-acetate were added to terminate microbial activity and to precipitate dissolved sulfide as

zinc sulfide. These samples were stored at 4°C until the extraction of sulfur and the subsequent isotope analysis.

Nitrogenase activity. Nitrogenase activity was determined in actively-growing cultures of DMSS-1, using a modified acetylene reduction technique (Dilworth, 1966). Acetylene gas (20±1 μmole) was injected into a set of culture bottles containing 10 ml of ammonium-free medium, and the bottles were subsequently inoculated with washed cells. One bottle was sacrificed every two days to monitor ethylene production from acetylene. H_2S was removed from the headspace by adding 1 ml of 1 M zinc acetate solution, and 0.5 ml of the headspace gas was withdrawn using a gas-tight syringe. The gas sample was analyzed by a gas chromatography (Shimadzu GC-2014) equipped with FID detector and a packed column (Carboxene-1000, 60/80 mesh). Procedural and analytical reproducibility was 8%. Ethylene production was monitored in parallel control sterile media and cultures, both containing 5.6 mM ammonium.

Cytochrome spectra. Reduced and oxidized cytochrome spectra and the difference between the two were obtained using the whole cell method (Hubbard *et al.*, 1986; Johnston *et al.*, 2008). Cells were harvested from 45 ml of the culture by centrifugation at 3000 g for 15 min. The supernatant was discarded and the cells were resuspended in 1 ml of phosphate buffered saline solution (PBS; 50mM phosphate buffer, and 350 mM NaCl). Cell suspensions were transferred into 1.5 ml microcentrifuge tubes and washed twice by centrifugation (13000 g, 3 min) and resuspension in PBS. Protein was determined using a Pierce BCA protein assay kit (Pierce, Rockfold, IL) with albumin standard, and the cells were resuspended in PBS at ~ 1.5mg protein/ml. The resuspended cultures were transferred into flat-bottom 96-well plates (200 μL), and oxidized or reduced by the addition of 20 μL of 30% H_2O_2 and 20 μL of freshly prepared 50 mg/ml sodium dithionite stock solution, respectively. After a 1-min incubation, the cells were shaken in the Synergy2 microplate reader (BioTek, VT, USA) for 10 seconds and optical absorptions measured in the 400 to 700 nm range at 2-nm intervals.

Isotope measurements. Sulfide and sulfate were extracted by acidifying the culture medium with 6 N HCl at 80°C under a flow of nitrogen gas for two hours. Sulfide produced during the distillation was precipitated as ZnS in a Zn-acetate solution (0.18 M). After the extraction of sulfide, sulfate in the remaining medium was reduced to sulfide with 30 ml of the reducing agent (mixture of HI, H_3PO_2 and HCl, Thode *et al.*, 1961). Samples were boiled and purged by N_2 gas for two hours. Volatile products were passed through a condenser and a trap containing distilled water, and sulfide was subsequently collected in a Zn-acetate trap. Sulfide from continuous culture was collected directly by passing the effluent gas through a sulfide trap containing a 0.18 M Zn-acetate solution. Sulfate was extracted from a

2-3 ml sample of the effluent as described above. ZnS was converted to Ag_2S by the addition of $AgNO_3$ and the incubation at 70°C for one day. Ag_2S was centrifuged, washed with distilled water three times and dried at 70°C. The Ag_2S samples reacted with an excess of fluorine gas for more than 5 hours at 300°C, and the produced SF_6 was purified by gas chromatography. Purified SF_6 was transferred into an isotope-ratio mass spectrometer for multiple sulfur isotope measurements in the dual inlet mode (Ono *et al.*, 2006). Sulfur isotopic compositions are reported using the conventional delta notation.

Data processing. Cellular growth yield during the vegetative phase was calculated as the ratio of the increase in the number of cells to the amount of sulfide produced. When not limited by iron or ammonium, the cells grow exponentially until they become limited by organic carbon (sulfate was supplied in excess). Cell-specific sulfate reduction rates (csSRR) during the exponential growth were calculated as:

$$csSRR = \frac{\ln(c_x) - \ln(c_1)}{t_x - t_1} \cdot \frac{[H_2S]_x - [H_2S]_1}{c_x - c_1} \quad (1)$$

where t_1 and t_x are the start of exponential growth and the time of sampling (in days), respectively, and C and $[H_2S]$ are cell densities (number of cells/ml) and sulfide concentrations at the time of sampling, respectively. When limited by iron and ammonium, DMSS-1 cells grew more slowly and not exponentially. The csSRR in these cultures was calculated simply by dividing the sulfide production rate by the time-weighted average of the cell density during the vegetative phase.

The isotope fractionation factor ($^x\alpha$) in the batch culture experiment was calculated using the modified Rayleigh distillation equation as previously described (Sim *et al.*, 2011a):

$$^x\alpha = -\frac{1}{\ln f_r} \ln\left(1 + \frac{(1-f_r)}{f_r} \frac{\delta_p + 1000}{\delta_r + 1000}\right) \quad (2)$$

where f_r is the fraction of the remaining sulfate, δ_r and δ_p are sulfur isotope compositions (^{33}S or ^{34}S) of sulfate remaining at the time of sampling (t_x) and sulfide produced by the day of sampling (t_x), respectively.

The isotope enrichment factor is defined as:

$$^x\varepsilon = 1000 \cdot (1 - {}^x\alpha) \quad (3)$$

In this definition, positive values represent the depletion of heavy isotopes in the product. To characterize the mass-dependent fractionation for sulfate reduction, ^{33}E values are calculated as:

$$^{33}\mathrm{E} = 1000 \cdot (^{33}\alpha - ^{34}\alpha^{0.515}) \quad (4)$$

For each calculation, errors from cell counts (±15%), sulfide concentration measurements (±5%), isotope analyses (0.1‰ for $\delta^{33}S$, 0.2‰ for $\delta^{34}S$, and 0.01‰ for $\delta^{33}S–0.515\cdot\delta^{34}S$) were propagated according to Bevington and Robinson (2002).

4.4. Results

DMSS-1 cultures limited by iron (< 1μM) and ammonium (< 0.3 mM) grew and produced sulfide more slowly than iron- and ammonium-replete cultures (Fig. 4.1). These effects of iron and ammonium limitation could be observed in cultures grown on malate or lactate (Figs. 4.1, 4.2). When cells grew on lactate, limitations by iron and ammonium reduced the cellular yield to one half and one fourth, respectively, relative to the control cultures (Fig. 4.2 and Table 4.1). The cell specific sulfate reduction rates (csSRRs) were lower in iron-limited cultures, but higher in nitrogen-limited cultures, respectively, relative to the control cultures (Fig. 4.2 and Table 4.1). When DMSS-1 coupled sulfate reduction with the oxidation of malate, it attained higher cell densities but exhibited slower csSRRs than during sulfate reduction coupled with the oxidation of lactate (Fig. 4.2 and Table 4.1). Iron limitation diminished both growth yield and csSRR by half, compared to the malate-fed controls. Limitation by ammonium reduced the growth yield to 20% of the control cultures, while accelerating the specific respiration rate (Fig. 4.2 and Table 4.1).

The growth of DMSS-1 in the absence of ammonium suggested that this organism could fix nitrogen and use it in biosynthesis. Production of ethylene by acetylene reduction was measurable within the micromole level in ammonium-limited cultures, but ethylene was not detected in ammonium-replete cultures and sterile control, indicating DMSS-1 fixed N_2 only when grown in ammonium-deficient medium (Fig. 4.3). Slower respiration by DMSS-1 in iron-limited cultures suggests that this metal may be impairing the function of respiratory proteins, rather than limiting the overall biosynthesis. Therefore, we examined how the iron limitation affected the content of cytochrome *c*, one of the essential proteins in electron transfer chains. Reduced *minus* oxidized spectra of iron-replete cells showed predominant peaks at 420-422, 523-524, and 552-553 nm, typical for *c*-type cytochromes (Fig. 4.4, Postgate and Cambell, 1966). These peaks were more than twice as large as in iron-replete cells relative to the iron-deficient cells (Fig. 4.4), confirming a reduced abundance of cytochrome *c* (per cell protein) in iron-limited cultures.

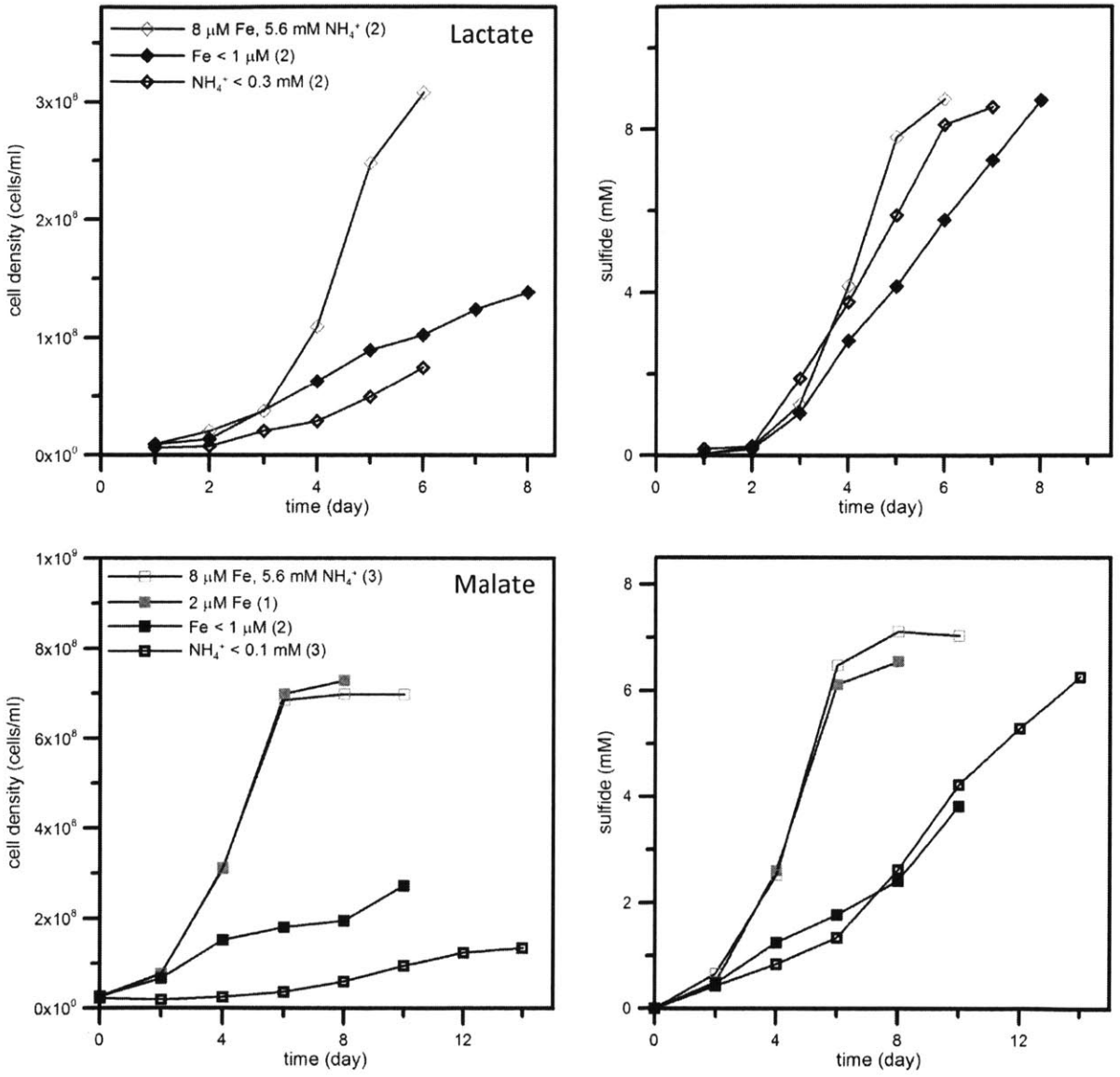

Figure 4.1. Effect of iron and nitrogen limitation on growth (left) and sulfide production (right) of DMSS-1 grown on lactate (upper panels) and malate (lower panels). Results are shown as the average of independent experiments carried out under the given condition, and the numbers in parentheses refer to the number of experiments.

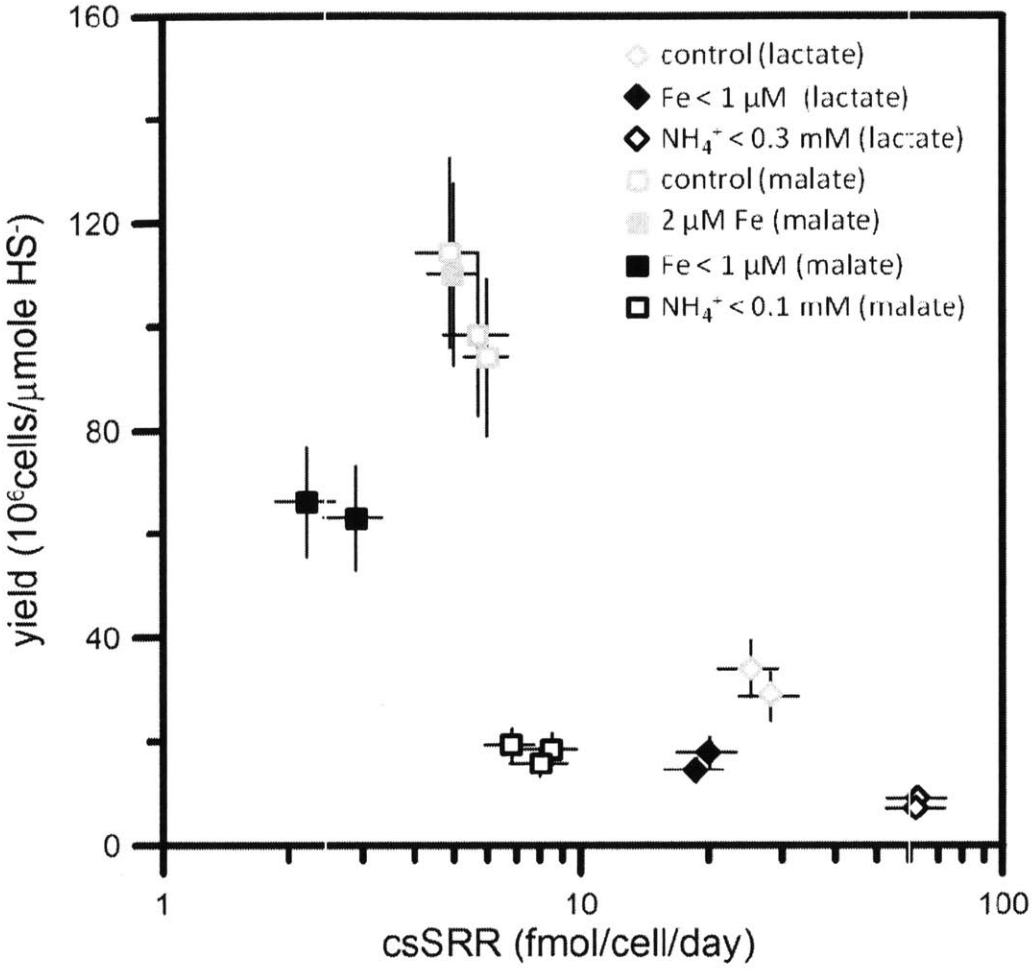

Figure 4.2. Effect of Fe and N limitation on DMSS-1 growth yields and csSRR. Both limitations reduced the growth yield. Iron deficiency decreased csSRR, while cells limited by ammonium respired faster than control cultures.

organic substrate	NH_4Cl (mM)	$FeCl_2$ (μM)	growth yield (10^6cells/μmole SO_4)	csSRR (fmol/cell/day)	$^{34}\varepsilon$ (‰)	^{33}E (‰)
lactate	5.6 mM	8	29 ± 5	28.2 ± 4.5	6.8 ± 0.2	0.033 ± 0.011
	5.6	8	34 ± 5	25.1 ± 4	7.0 ± 0.2	0.035 ± 0.011
	5.6	< 1	15 ± 2	18.7 ± 3	11.8 ± 0.3	0.032 ± 0.011
	5.6	< 1	18 ± 3	20.1 ± 3.2	10.3 ± 0.3	0.040 ± 0.011
	< 0.3	8	7 ± 1	62.4 ± 9.9	8.4 ± 0.3	0.031 ± 0.011
	< 0.3	8	9 ± 1	62.9 ± 9.9	7.8 ± 0.3	0.033 ± 0.011
malate	5.6	8	114 ± 18	4.9 ± 0.8	16.6 ± 0.3	0.077 ± 0.012
	5.6	8	94 ± 15	6 ± 0.7	19.0 ± 0.3	0.088 ± 0.012
	5.6	8	99 ± 16	5.7 ± 1	18.6 ± 0.3	0.067 ± 0.012
	5.6	2	110 ± 17	5 ± 0.6	17.5 ± 0.3	0.069 ± 0.012
	5.6	< 1	63 ± 10	2.9 ± 0.5	25.1 ± 0.3	0.085 ± 0.013
	5.6	< 1	66 ± 10	2.2 ± 0.3	29.0 ± 0.3	0.101 ± 0.013
	< 0.1	8	19 ± 3	6.8 ± 0.9	22.0 ± 0.3	0.110 ± 0.012
	< 0.1	8	16 ± 3	8 ± 1.2	23.0 ± 0.3	0.089 ± 0.012
	< 0.1	8	19 ± 3	8.5 ± 1.3	23.1 ± 0.3	0.092 ± 0.012

Table 4.1. Growth parameters and isotope fractionations in batch cultures containing different concentrations of iron and ammonium. Errors were propagated from analytic uncertainties of cell density, sulfide, and isotope measurements.

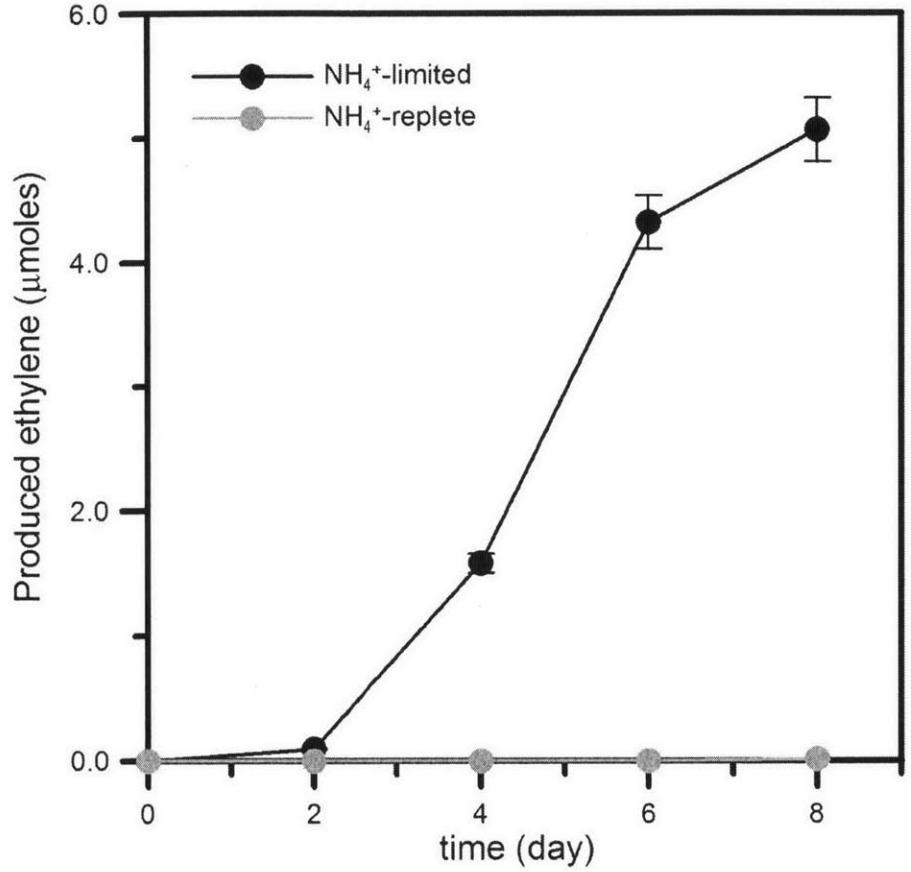

Figure 4.3. Production of ethylene by the reduction of acetylene in ammonium-limited medium (< 1 μM). Ethylene was not detected (<10 nmole) in cultures that contain 5.6 mM ammonium. Error bars indicate procedural and analytical reproducibility (± 5%).

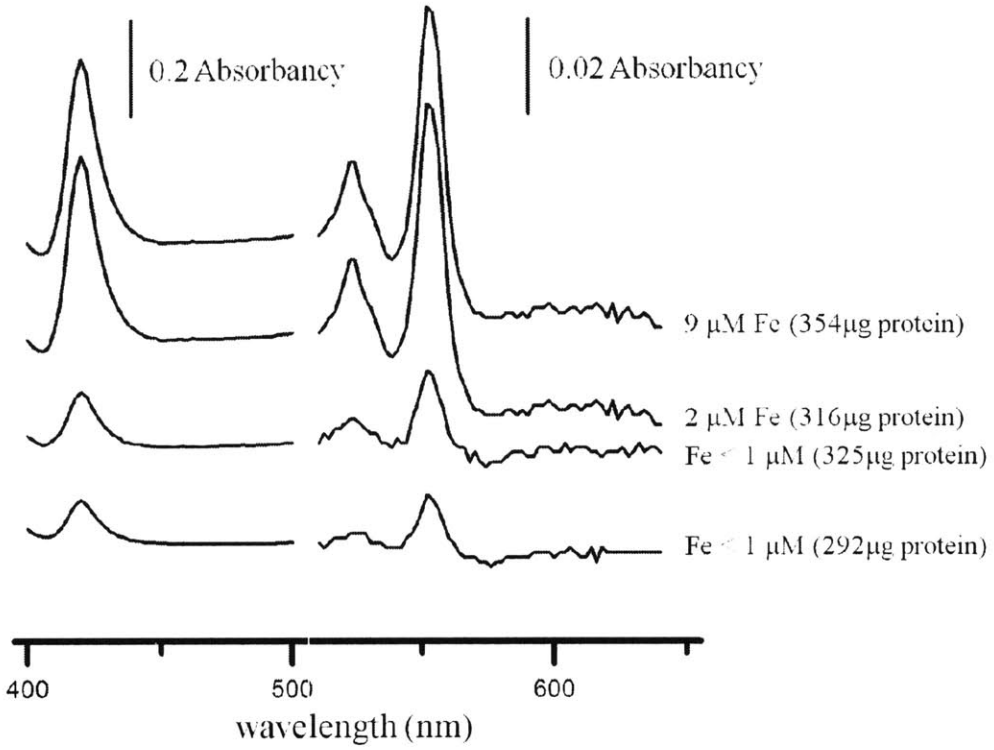

Figure 4.4. Reduced *minus* oxidized spectra of whole cells of DMSS-1 in 0.05M PBS. Three peaks typical for the absorption by cytochrome *c* were prominent in iron-replete cells, but small relative to the total signal when DMSS-1 was grown in iron-deficient media. All samples contained similar amounts of total protein.

Analyses of S-isotope ratios of sulfates and sulfides in DMSS-1 cultures limited by iron or nitrogen showed that both limitations increased the fractionation of S-isotopes (Table 4.1). The calculated enrichment factor ($^{34}\varepsilon$) in control cultures grown on lactate was 6.9 ± 0.2‰, as previously reported (Sim *et al.*, 2011). Iron-deficient cells grown on lactate fractionated $^{34}S/^{32}S$ up to 12‰, while limitation by ammonium increased the enrichment factors by only 1‰ with respect to the control cultures (Fig. 4.5 and Table 4.1). Overall larger fractionation factors associated with the growth on malate amplified the isotopic effects of limitations by iron and ammonium. Malate-fed, iron- and ammonium-replete cultures fractionated ^{34}S at 18±1‰, while limitations by ammonium and iron increased this enrichment factor to 23 and 29‰, respectively (Fig. 4.5 and Table 4.1). DMSS-1 fractionated triple isotope ratios ($^{32}S/^{33}S/^{34}S$) in a mass-dependent manner, yielding ^{33}E values that ranged from -0.031 to -0.040‰ and from -0.067 to -0.101‰ for lactate- and malate-fed cultures, respectively (Fig 4.6 and Table 4.1). The values of ^{33}E decreased with the decreasing concentrations of iron and ammonium in malate-grown cells, but remained rather constant in lactate-fed cultures.

4.5. Discussion

Iron limitation. Iron deficiency reduced the growth and sulfate reduction rates of DMSS-1, and led to increasing fractionation factors. A similar inverse relationship between csSRR and $^{34}\varepsilon$ was previously reported for DMSS-1 cultures, in which csSRR was a function of the electron donor and its concentration (Sim et al., 2011a, Fig. 4.7). These correlated and similar results are consistent with important roles of iron in MSR pathway. Although the mechanism of energy conservation by sulfate-reducing bacteria is not fully understood, H_2 cycling between cytoplasm and periplasm is thought to be involved in this process (Odom and Peck, 1981) (Fig. 4.8). In the H_2-cycling model, electrons generated by the oxidation of organic compounds react with protons to form H_2 in reactions catalyzed by various Fe-containing cytoplasmic hydrogenases. The resulting H_2 diffuses across the cytoplasmic membrane into the periplasm, where it is split into protons and electrons by periplasmic hydrogenases. Electrons return to the cytoplasm through cytochromes and transmembrane protein complexes, and are delivered to terminal reductases and used to reduce sulfate. The remaining protons generate proton motive force. This model requires both cytoplasmic and periplasmic hydrogenases, enzymes that invariably contain iron in their active site (Pereira *et al.*, 2011). The key electron carrier involved in H_2-cycling, a cytochrome *c*, is also a metalloprotein containing a heme prosthetic group (Postgate, 1956). Increasing genetic and biochemical evidence points to the presence of redundant electron transport chains, suggesting that hydrogen cycling may not be essential for the energy conservation in sulfate reducing bacteria (Keller and Wall, 2011). Nonetheless, because most of the redundant components involved in the electron transfer from lactate to

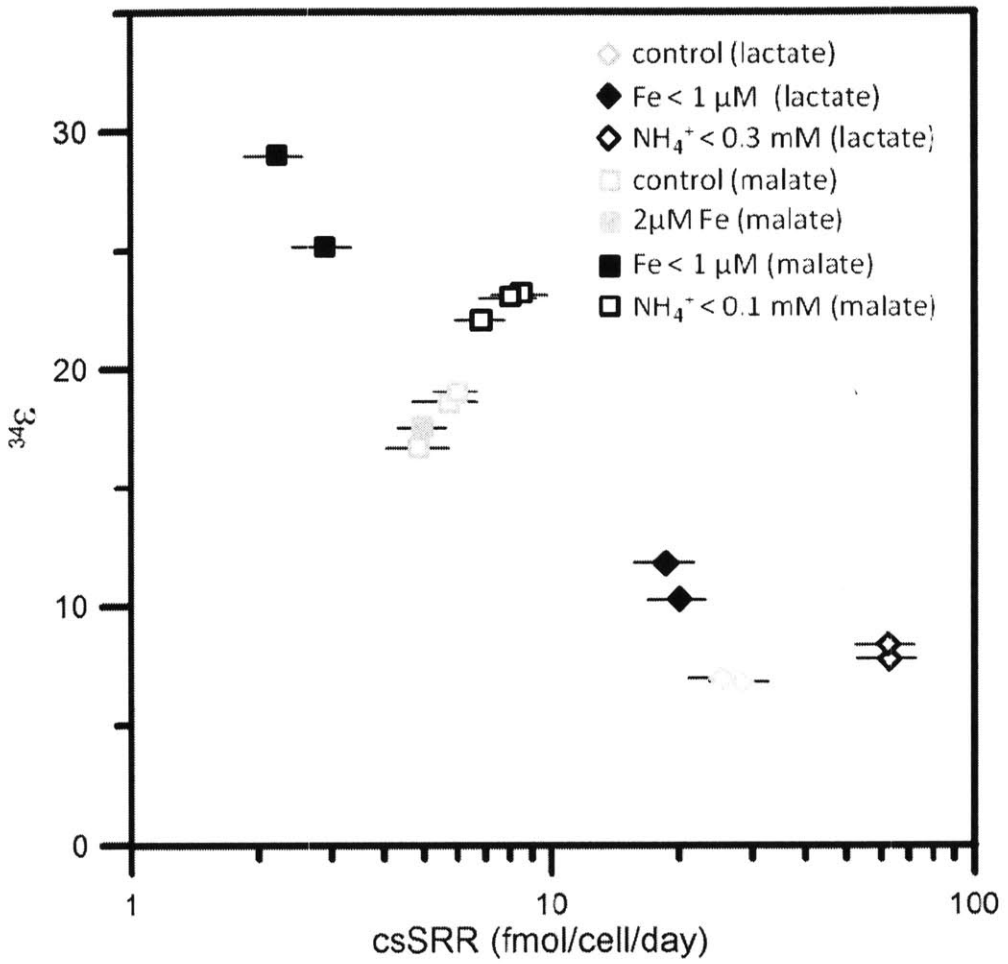

Figure 4.5. Relationship between S-isotope fractionation and csSRR in cultures limited by iron and nitrogen, respectively. Both limitations increased the magnitude of S-isotope fractionation, but the effect of iron deficiency was larger than that of ammonium limitation.

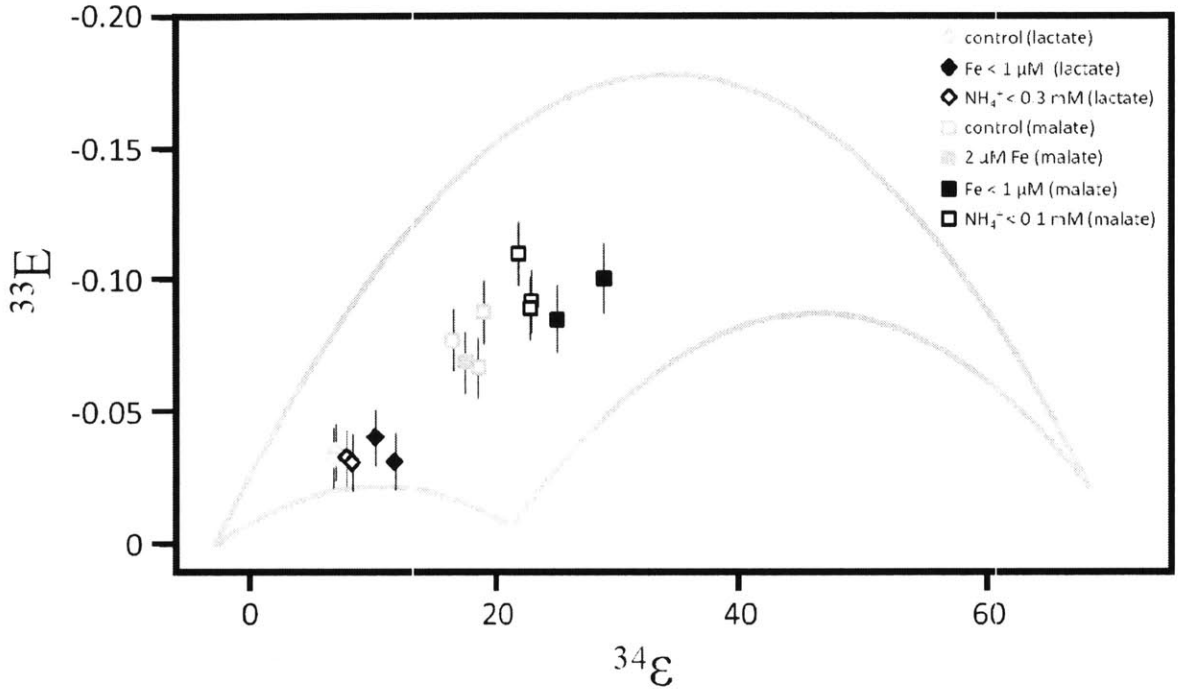

Figure 4.6. $^{34}\varepsilon$ and ^{33}E produced by DMSS-1. Measured multiple S-isotope fractionations can be accounted by the metabolic flux model for mass-dependent fractionation of S-isotopes during MSR (gray line) (Rees, 1973; Farquhar *et al.*, 2003; Sim *et al.*, 2011). The model assumes branching points in the pathway at the uptake of sulfate and the reduction of sulfate to sulfite, and enzymatic fractionation factors of 0.9756 and 0.952 for the reduction of APS to sulfite and that of sulfite to sulfide, respectively.

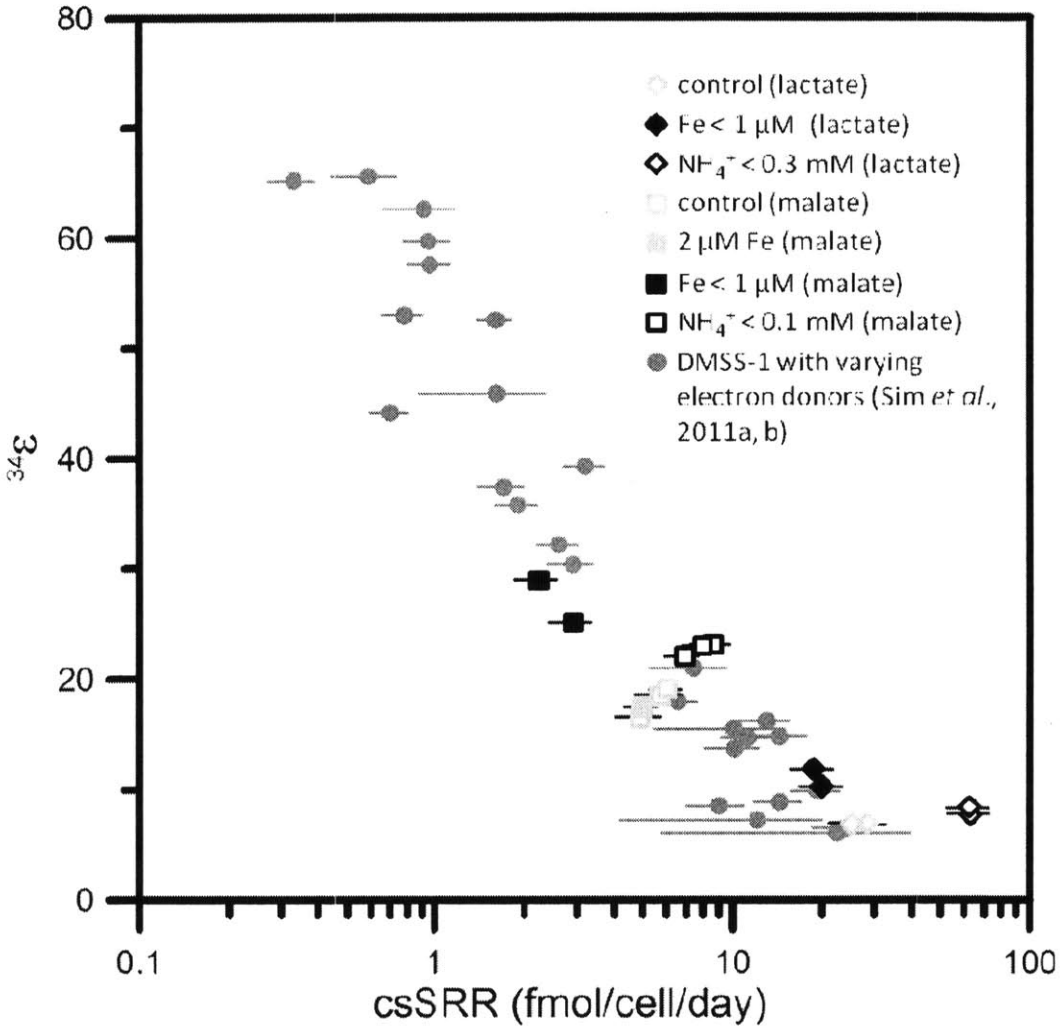

Figure 4.7. Variations in $^{34}\varepsilon$ and csSRR associated with the limitation by iron or ammonium (this study) and the availability or nature of the electron donor (grey circles, Sim et al., 2011a, 2011b).

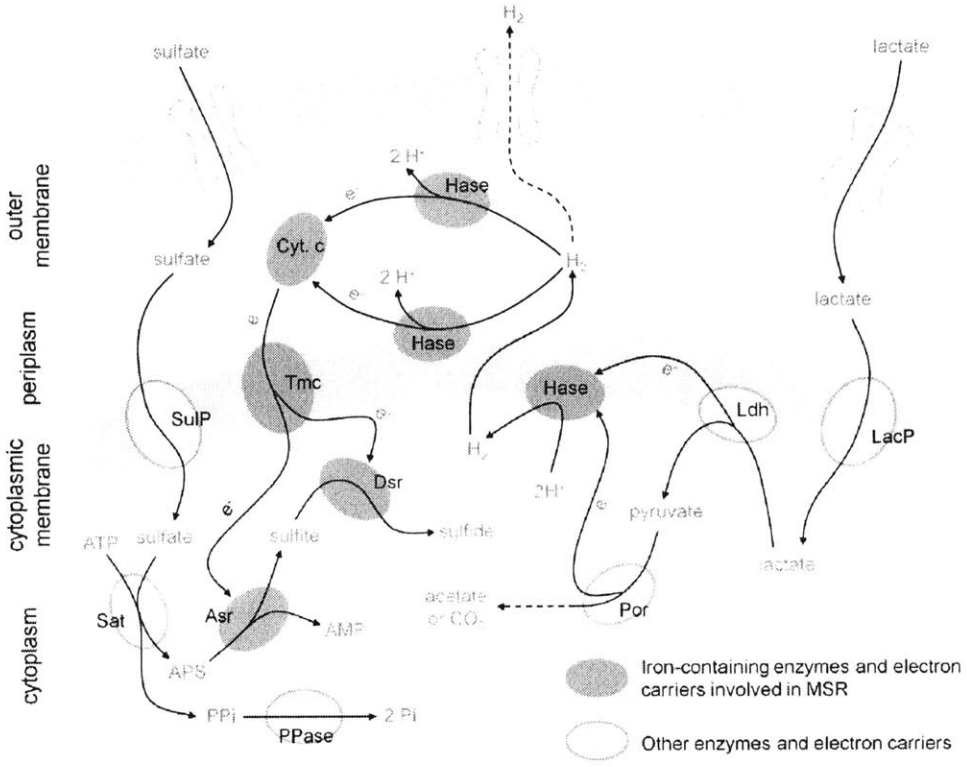

Figure 4.8. Schematic representation of electron flow during MSR in Gram-negative sulfate reducing bacteria that oxidize lactate. Some reducing equivalents may flow from the electron donor to sulfur through hydrogen cycling (Odom and Peck, 1981; Heidelberg et al., 2004). Many enzymes and electron carriers involved from the cytoplasm to the periplasm in this process contain iron in their active sites (Lampreia *et al.*, 1994; Rabus *et al.*, 2006). Iron limitation impairs the synthesis of cytochromes and hyrdrogenases, reducing the flow of electrons to sulfate reduction system. Abbreviations: LacP, lactate permease; Ldh, lactate dehydrogenase; Por, pyruvate-ferrodoxin oxidoreductase; Hase, hydrogenase; Cyt. *c*, cytochromes *c*; Tmc, transmembrane redox complex; SulP, sulfate permease; Sat, ATP sulfurylase; Asr, APS reductase; Dsr, dissimilatory sulfite reductase; PPase, pyrophosphate phosphatase.

sulfur contain iron (Pereira *et al.*, 2011), iron limitation should slow down the electron flow and impart an isotopic signature on sulfide. Our experiments strongly support that role of cytochrome *c* in electron transfer in DMSS-1 that reduces sulfate and oxidizes lactate or malate. In particular, the ratio of this metalloprotein to total protein decreases in iron-starved DMSS-1 cells (Fig. 4.4). This decrease of iron-dependent components of the respiratory chain likely impairs the flow of electrons from organic electron donors to sulfur and slows down the respiration.

The reduced flow of electrons to the sulfate reducing system would affect S-isotope fractionation. According to the reaction and isotope fractionation scheme for MSR initially developed by Rees (1973) and further modified by Brunner and Bernasconi (2005) (referred to as the RBB model), the MSR pathway consists of several enzymatic steps that are thought to be reversible. These steps include ATP sulfurylation, reduction of APS, and reduction of sulfite. The RBB model explains the overall S-isotope fractionation by considering both the ratios between forward and backward fluxes (reversibility) at each step, and the intrinsic isotope effects of these enzymatic steps. Because isotope effects at individual enzymatic steps depend on the difference between ground-state and transition-state structures in each reaction (O'Leary, 1989), which is unlikely to be altered by the nutrient availability itself, MSR operating in a more reversible manner should yield larger S-isotope effects. According to the RBB model, when DMSS-1 is limited by iron, the sulfate reducing pathway operates under more reversible conditions. Given that electrons are essential substrates for sulfate reduction, a slower flow of electrons to terminal reductases could slow down the forward reactions, increase the reversibility, and in turn, increase the overall fractionation. Our results show that this may be triggered by a deficiency in iron-dependent components of the respiratory chain.

Interestingly, iron deficiency and the varying availability or chemistry of an electron donor yield very similar relationship between csSRR and $^{34}\varepsilon$ (Fig. 4.7). This is consistent with the ability of both iron and electron donors to dictate the rate at which electrons are released from the donor (Brunner and Bernasconi, 2005; Sim *et al.*, 2011a and 2011b), whether at the very entry point, in the case of organic electron donors, or further downstream, in the case of iron. Limitations by other metals may similarly affect S-isotope fractionation during MSR: the ATP sulfurylase contains Co and Zn (Gavel *et al.*, 1998), and hydrogenases commonly contain Ni and Se, along with Fe at their active sites (Rabus *et al.*, 2006).

Ammonium limitation. Acetylene reduction assay confirms the ability of DMSS-1 to fix nitrogen when it grows in a nitrogen-limited medium (Fig. 4.3). This ability is also reported in other *Desulfovibrio* species (Riederer-Henderson and Wilson, 1970). Nitrogen limitation diminishes the growth yield of DMSS-1, while increasing the respiratory activity of each cell (Fig. 4.2). N_2 fixation is a metabolically

expensive process requiring 8 electrons and 16 ATP molecules (Postgate, 1982) and requires that a larger portion of energy generated by the respiratory activity be spent on nitrogen fixation rather than biosynthesis. Consequently, this decreases the growth yield.

Unlike the limitation by iron or organic compounds, which decreased csSRR and increased $^{34}\varepsilon$, nitrogen limitation increased both csSRR and $^{34}\varepsilon$ in DMSS-1 cultures (Fig. 4.7). The RBB model described above attributes the overall isotope fractionation during MSR to the reversibility and the intrinsic isotope effect of each enzymatic step. In the steady state, csSRR is equal to the difference between the forward and backward fluxes at any enzymatic steps. According to the RBB model, a faster respiration accompanied by a larger isotope fractionation requires a greater reversibility of MSR *and* a larger net forward flow. This requirement generates a testable hypothesis that links nitrogen fixation to sulfate reduction through the expression levels or concentrations of respiratory enzymes. For each enzymatic reaction in the MSR pathway, both forward and backward fluxes are proportional to the concentration of the enzyme catalyzing that reaction. As a result, the net forward flow is proportional to the concentration of respiratory enzymes, but the ratio between the two fluxes (reversibility) should not depend on the enzyme concentration in the cell. Proteins involved in the central energy metabolism and electron transport are upregulated during nitrogen fixation in the cynobacterium *Nostoc* sp. and the α-proteobacterium *Rhodopseudomonas palustris*, reflecting a high metabolic demand for nitrogen fixation (VerBerkmoes *et al.*, 2006; Stensjo *et al.*, 2007). We predict that nitrogen limitation similarly increases the concentration of respiratory enzymes in DMSS-1, thereby increasing csSRR. At the same time, N_2 fixation as an additional sink for reducing power, may reduce the electron flow to the MSR pathway, resulting in a moderate increase in S-isotope fractionation. This hypothesis can be explored byproteomic studies of nitrogen-replete and limited cultures of DMSS-1.

Environmental and geological significance. The effect of iron and nitrogen limitation on S-isotope fractionation can influence interpretations of sulfur isotope data in modern and ancient environments. The natural habitat of DMSS-1, a salt marsh, contains 10 - 60 μM of dissolved iron in the anoxic porewaters (Giblin and Howarth, 1984), i.e., at least two orders of magnitude more iron than the submicromolar levels limiting the growth of DMSS-1 under our experimental conditions. It is thus unlikely that these bacteria are iron limited in their natural habitat. Iron concentrations of reducing porewater are usually several to several tens of μM in the open ocean sediments (Klinkhammer, 1980; Sawlan and Murray, 1983; Winters and Buckley, 1986; Böttcher *et al.*, 2006) and several tens to several hundreds of μM in the coastal environments (King et al., 1982; Böttcher *et al.*, 2000) and in the euxinic Black Sea (Wijsman *et al.*, 2001). The relatively high concentrations of iron, produced by the reduction

of iron oxides and liberation of soluble iron into porewater, suggest that iron is not the key factor controlling the magnitude of microbial S-isotope fractionation in anoxic marine sediments. However, the situation may be different in the water column, where iron concentrations are commonly smaller. For example, iron concentration in the anoxic waters is lower than 0.3 μM in the Black Sea (Alkan and Tufekci, 2009) and lower than 0.5 μM in the Cariaco Basin (Li *et al.*, 2011). In modern marine environments, MSR is mostly restricted to anoxic sediments, but in some anoxic basins, sulfate reducing microbes thrive in the water column. For example, in the Black Sea, 10 ~ 50% of pyrite burial is attributed to sulfate reduction in the water column (Neretin *et al.*, 2001). The sub-micromolar concentrations of dissolved iron there may limit MSR and contribute to the production of sulfides depleted up to 60‰ (Sweeny and Kaplan, 1980; Fry *et al.*, 1991; Lyons, 1997). The same mechanism may have been relevant in the past ocean, particularly during times of oceanic euxinia (Trude, 2012) which would have expanded the habitat of sulfate reducing microbes from the sediments into the water column. This expansion might have diminished the overall availability of iron for marine sulfate reducing microbes, thereby increasing the magnitude of S-isotope fractionation. This hypothesis may explain some of the > 20‰ increase in S-isotopic difference between sedimentary sulfide and sulfate at the onset of the Cretaceous Oceanic Anoxic Event 2 (Adams *et al.*, 2010).

Ammonium ion liberated by the mineralization of organic matter provides a source of nitrogen to microbes in zones of sulfate reduction (Volkov and Rozanov, 2006; Schrum *et al.*, 2009), but sulfate reducers are also reported to contribute to N_2 fixation in some highly productive environments, including a wetland (Santruckova *et al.*, 2010), an intertidal microbial mat (Steppe and Paerl, 2002), and a seagrass-covered coastal lagoon (Welsh et al., 1996). All of these settings generally exhibit substantial rates of both N_2 fixation and sulfate reduction (Hines *et al.*, 1989; Steppe and Paerl, 2002; Pester *et al.*, 2010), suggesting that larger S-isotope fractionations may accompany high rates of sulfate reduction if sulfate reducers also fix N_2. Lake Cadagno, a meromictic lake in Switzerland may be an environment that meets the above conditions. In this lake, dense populations of anoxygenic phototrophic bacteria at the chemocline enrich the underlying monimolimnion and sediments with organic compounds accessible to sulfate reducing microbes (Del Don *et al.*, 2001), and sulfate reducing δ-Proteobacteria fix N_2 (Halm et al., 2009). Nitrogen fixation fueled by vigorous sulfate reduction may account for a part of the S-isotope difference between dissolved sulfate and sulfide, which is often as large as 45‰ (Canfield *et al.*, 2010). Nitrogen limitation may also contribute to the large S-isotope fractionation in areas characterized by low productivity, such as deep sea sediments (e.g. Rudnicki *et al.*, 2001). Organic compounds limit the growth and MSR in these settings, but the nitrogen requirement of microbial communities in deep sea

sediments may further increase $^{34}\varepsilon$, depending on the C/N ratio of the substrates used for growth (Anderson and Pondaven, 2003).

To the best of our knowledge, this is the first study to demonstrate the relationship between the availability of iron and reduced nitrogen and the magnitude of S-isotope fractionation during MSR. The marked effect of both nutrients on S-isotope fractionation underscores the need to better understand nutrient and metal requirements of sulfate-reducing microbes in nature. Improved constraints on microbial S-isotope fractionation will bring a stronger physiological perspective to the interpretation of S-isotope signatures. The emerging constraints on the physiological coupling among S, C, Fe, N, and other cycles show that controls on natural S-isotope signatures are complex, and may involve various limitations that extend beyond the availability and quality of organic carbon.

References

Adams DD, Hurtgen MT, Sageman BB. 2010. Volcanic triggering of a biogeochemical cascade during Oceanic Anoxic Event 2. Nat. Geosci. 3: 201-204.

Alkan N, Tüfekçi M. 2009. Distribution of dissolved forms of manganese and iron in the water column of the Southeastern Black Sea. Turk. J. Fish. Aquat. Sci. 9: 159-164.

Anderson TR, Pondaven P. 2003. Non-redfield carbon and nitrogen cycling in the Sargasso Sea: pelagic imbalance and export flux. Deep-Sea Res. I 50: 573-591.

Bevington PR, Robinson DK. 2002. Data reduction and error analysis for the physical sciences. McGraw-Hill, New York.

Bolliger C, Schroth MH, Bernasconi SM, Kleikemper J, Zeyer J. 2001. Sulfur isotope fractionation during microbial sulfate reduction by toluene-degrading bacteria. Geochim. Cosmochim. Acta 19: 3289-3298.

Bottrell SH, Newton R. 2006. Reconstruction of change in global sulfur cycling from marine sulfate isotopes. Earth Sci. Rev. 75: 59-83.

Böttcher ME, Hespenheide B, Llobet-Brossa E, Beardsley C, Larsen O, Schramm A, Wieland A, Böttcher G, Berninger U, Amann R. 2000. The biochemistry, stable isotope geochemistry, and microbial community structure of a temperate intertidal mudflat: an integrated study. Cont. Shelf Res. 20: 1749-1769.

Böttcher ME, Hetzel A, Brumsack H, Schipper A. 2006. Sulfur-iron-carbon geochemistry in sediments of the Demerara Rise. ODP Scientific Results 207: 1-23.

Brunner B, Bernasconi SM. 2005. A revised isotope fractionation model for dissimilatory sulfate reduction in sulfate reducing bacteria. Geochim. Cosmochim. Acta 69: 4759-4771.

Canfield DE. 2001a. Biogeochemistry of sulfur isotopes. Rev. Mineral. Geochem. 43: 607-636.

Canfield DE. 2001b. Isotope fractionation by natural populations of sulfate-reducing bacteria. Geochim. Cosmochim. Acta 65: 1117-1124.

Canfield DE, Farquhar J, Zerkle AL. 2010. High isotope fractionations during sulfate reduction in a low-sulfate euxinic ocean analog. Geology 38: 415-418.

Canfield DE, Raiswell R. 1999. The evolution of the sulfur cycle. Am. J. Sci. 299: 679-723.

Chambers LA, Trudinger PA, Smith JW, Burns MS. 1975. Fractionation of sulfur isotopes by continuous cultures of *Desulfovibrio desulfuricans*. Can. J. Microbiol. 21: 1602-1607.

Cline JD. 1969. Spectrophotometric determination of hydrogen sulfide in natural water. Limnol. Oceanogr. 14: 454-458.

Cotter PA, Darie S, Gunsalus RP. 1992. The effect of iron limitation on expression of the aerobic and anaerobic electron transport pathway genes in *Escherichia coli*. FEMS Microbiol. Lett. 79: 227-232.

Del Don C, Hanselmann KW, Peduzzi R, Bachofen R. 2001. The meromictic alpine Lake Cadagno: Orographical and biochemical description. Aquat. Sci. 63: 70-90.

Detmers J, Bruchert V, Habicht K, Kuever J. 2001. Diversity of sulfur isotope fractionations by sulfate reducing prokaryotes. Appl. Environ. Microbiol. 67: 888-894.

Dilworth MJ. 1966. Acetylene reduction by nitrogen-fixing preparations from *Clostridium pasteurianum*. Biochim. Biophys. Acta 127: 285-294.

Fry B, Jannasch HW, Molyneaux SJ, Wirsen C, Muramoto J, King S. 1991. Stable isotope studies of the carbon, nitrogen and sulfur cycles in the Black Sea and the Cariaco Trench. Deep-Sea Res. II 38: S1003-S1019.

Gavel OY, Bursakov SA, Calvete JJ, George GN, Moura JJ, Moura I. 1998. ATP sulfurylases from sulfate-reducing bacteria of the genus *Desulfovibrio*. A novel metalloprotein containing cobalt and zinc. Biochemistry 37: 16225-16232.

Giblin AE, Howarth RW. 1984. Porewater evidence for a dynamic sedimentary iron cycle in salt marshes. Limnol. Oceanogr. 29: 47-63.

Habicht KS, Canfield DE. 1997. Sulfur isotope fractionation during bacterial sulfate reduction in organic-rich sediments. Geochim. Cosmochim. Acta 61: 5351-5361

Halm H, Musat N, Lam P, Langlois R, Musat F, Peduzzi S, Lavik G, Schubert CJ, Singha B, LaRoche J, Kuypers MMM. 2009. Co-occurrence of denitrification and nitrogen fixation in a meromictic lake, Lake Cadagno (Switzerland). Environ. Microbiol. 11: 1945-1958.

Harder W, Dijkhuizen L. 1983. Physiological responses to nutrient limitation. Ann. Rev. Microbiol. 37: 1-23.

Harrison AG, Thode HG. 1958. Mechanism of the bacterial reduction of sulphate from isotope fractionation studies. Trans. Faraday Soc. 54: 84-92.

Heidelberg JF,Seshadri R,Haveman SA, Hemme CL, Paulsen IT, Kolonay JF, Eisen JA, Ward N, Methe B, Brinkac LM, Daugherty SC, Deboy RT, Dodson RJ, Durkin AS, Madupu R, Nelson WC, Sullivan SA, Fouts D, Haft DH, Delengut J, Peterson JD, Davidsen TM, Zafar N, Zhou L, Radune D, Dimitrov G, Hance M, Tran K, Khouri H, Gill J, Utterback TR, Feldblyum TV, Wall JD, Voordouw G, Fraser CM. 2004. The genome sequence of the anaerobic sulfate-reducing bacterium *Desulfovibrio vulgaris* Hildenborough. Nat.Biotechnol. 22: 554–559.

Hines ME, Knollmeyer SL, Tugel JB. 1989. Sulfate reduction and other sedimentary biogeochemistry in a northern New England salt marsh. Limnol. Oceanogr. 34: 578-590.

Hoek J, Reysenbach A, Habicht KS, Canfield DE. 2006. Effect of hydrogen limitation and temperature on the fractionation of sulfur isotopes by a deep-sea hydrothermal vent sulfate-reducing bacterium. Geochim. Cosmochim. Acta 70: 5831-5841.

Holmes RM, Aminot A., Kerouel R., Hooker BA, Peterson BJ .1999. A simple and precise method for measuring ammonium in marine and fresh water ecosystems. Can. J. Fish. Aquat. Sci. 56: 1801-1808.

Hubbard JAM, Lewandowska KB, Hughes MN, Poole RK. 1986. Effects of iron-limitation of *Escherichia coli* on growth, the respiratory chains and gallium uptake. Arch Microbiol. 146: 80-86.

Johnston DT, Farquhar J, Wing BA, Kaufman AJ, Canfield DE, Habicht KS. 2005. Multiple sulfur isotope fractionations in biological systems: A case study with sulfate reducers and sulfur disproportionators. Am. J. Sci. 305: 645-660.

Johnston WA, Huang W, de Voss JJ, Hayes MA, Gillam EM. 2008. Quantitative whole-cell cytochrome P450 measurement suitable for high-throughput application. J. Biomol. Screen. 13: 135-141.

Kaplan IR, Rittenberg SC. 1964. Microbiological fractionation of sulphur isotopes. J. Gen Microbiol. 34: 195-212.

Keller KL, Wall JD. 2011. Genetics and molecular biology of the electron flow for sulfate respiration in *Desulfovibrio*. Front. Microbio. 2:135.

King GM, Klug MJ, Wiegert RG, Chalmers AG. 1982. Relation of soil water movement and sulfide concentration to *Spartina alterniflora* production in a Georgia Salt Marsh. Science 218: 61-63.
Kleikemper J, Schroth MH, Bernasconi SM, Brunner B, Zeyer J. 2004. Sulfur isotope fractionation during growth of sulfate reducing bacteria on various carbon sources. Geochim. Cosmochim. Acta 68: 4891-4904.
Klinkhanmner GP. 1980. Early diagnosis in sediments from the eastern equatorial Pacific. II. Pore water metal results. Earth Planet. Sci. Lett. 49: 81-101.
Lamperia J, Pereira AS, Moura JJG. 1994. Adenylylsulfate reductase from sulfate-reducing bacteria. Methods Enzymol. 243: 241-260.
Li X, Gilhooly WP, Zerkel AL, Lyons TW, Farquhar J, Werne JP, Varela R, Scranton MI. 2010. Stable sulfur isotopes in the water column of the Cariaco Basin. Geochim. Cosmochim. Acta 74: 6764-6778.
Lyons TW. 1997. Sulfur isotopic trends and pathways of iron sulfide formation in upper Holocene sediments of the anoxic Black Sea. Geochim. Cosmochim. Acta 61: 3367-3382.
Neretin LN, Volkov II, Böttcher ME, Grinenko VA. 2001. A sulfur budget for the Black Sea anoxic zone. Deep-Sea Res. I 48: 2569-2593.
Odom JM, Peck HD Jr. 1981. Hydrogen cycling as a general mechanism for energy coupling in the sulfate reducing bacteria, *Desulfovibrio* sp. FEMS Microbiol. Lett. 12: 47-50.
O'Leary MH. 1989. Multiple isotope effects on enzyme-catalyzed reactions. Annu. Rev. Biochem. 58: 377-401.
Ono S, Wing B., Rumble D, Farquhar J. 2006. High precision analysis of all four stable isotope of sulfur (^{32}S, ^{33}S, ^{34}S and ^{36}S) at nanomole levels using a laser fluorination isotope-ratio-monitoring gas chromatography-mass spectrometry. Chem. Geol. 225: 30-39.
Pereira IAC, Ramos AR, Grein F, Marques MC, Marques da Silva S, Venceslau SS. 2011. A comparative genomic analysis of energy metabolism in sulfate reducing bacteria and archaea. Front. Microbiol. 2: 69.
Pester M, Bittner N, Deevong P, Wagner M, Loy A. 2010. A 'rare biosphere' microorganism contributes to sulfate reduction in a peatland. ISME J. 4: 1591-1602.
Postgate JR. 1956. Iron and synthesis of cytochrome c_3. J. Gen. Microbiol. 15: 186-193.
Postgate JR. 1982. The fundamental of nitrogen fixation. Cambridge University Press, Cambridge.
Postgate JR, Campbell LL. 1966. Classification of *Desulfovibrio* species, the non-sporulating sulfate-reducing bacteria. Bact. Rev. 30: 732-738.
Rabus R, Hansen TA, Widdel F. 2006. Dissimilatory sulfate- and sulfur- reducing prokaryotes. In The Prokaryotes (eds M Dworkin, S Falkow, E Rosenberg, KH Schleifer, E Stackbrandt). Springer-Verlag, New York.
Rees CE. 1973. A steady-state model for sulphur isotope fractionation in bacterial reduction processes. Geochim. Cosmochim. Acta 37: 1141-1162.
Rudnicki MD, Elderfield H, Spiro B. 2001. Fractionation of sulfur isotopes during bacterial sulfate reduction in deep ocean sediments at elevated temperatures. Geochim. Cosmochim. Acta 65: 777-789.
Santruckova H, Rejmankova E, Pivnickova B, Snyder JM. 2010. Nutrient enrichment in tropical wetlands: shifts from autotrophic to heterotrophic nitrogen fixation. Biochemistry 101: 295-310.
Sawlan JJ, Murray JW. 1983. Trace metal remobilization in the interstitial waters of red clay and hemipelagic marine sediments. Earth Planet. Sci. Lett. 64: 213-230.
Schrum HN, Spivack AJ, Kastner M, D'Hondt S. 2009. Sulfate-reducing ammonium oxidation: A thermodynamically feasible metabolic pathway in subseafloor sediment. Geology 37: 939-942.
Sim MS, Ono S, Donovan K, Templer SP, Bosak T. 2011a. Effect of electron donors on the fractionation of sulfur isotopes by a marine Desulfovibrio sp. Geochim. Cosmochim. Acta 75: 4244-4259.
Sim MS, Bosak T, Ono S. 2011b. Large sulfur isotope fractionation does not require disproportionation. Science 333: 74-77.

Stensjo K, Ow SY, Barrios-Llerena ME, Lindblad P, Wright PC. 2007. An iTRAQ-based quantitative analysis to elaborate the proteomic response of Nostoc sp. PCC 7120 under nitrogen fixing conditions. J. Proteome Res. 6: 621-635.

Steppe TF, Paerl HW. 2002. Potential N_2 fixation by sulfate-reducing bacteria in a marine intertidal microbial mat. Aquat. Microb. Ecol. 28: 1-12.

Strauss H. 1997. The isotopic composition of sedimentary sulfur through time. Palaeogeogr. Palaeoclimateol. Palaeoecol. 132: 97-118.

Sweeny RE, Kaplan IR. 1980. Stable isotope composition of dissolved sulfate and hydrogen sulfide in the Black Sea. Mar. Chem. 9: 145-152.

Thode HG, Monster J, Dunford HB. 1961. Sulphur isotope geochemistry. Geochim. Cosmochim. Acta 25: 158-174.

Treude, T. 2012. Biogeochemical reactions in marine sediments underlying anoxic water bodies. In Anoxia (eds. Altenbach A, Bernhard JM, Seckbach J). Springer, Netherlands, pp. 17-38.

VerBerkmoes NC, Shah M, Lankford PK, Pelletier DA, Strader MB, Tabb DL, McDonald WH, Barton JW, Hurst GB, Hauser L, Davison BH, Beatty JT, Harwood CS, Tabita FR, Hettich RL, Larimer FW. 2006. Determination and comparison of the baseline proteomes of the versatile microbe *Rhodopseudomonas palustris* under its major metabolic states. J. Proteome Res. 5: 287-298.

Volkov II, Rozanov AG. 2006. Fundamentals of biohydrochemistry of anoxic basins. Oceanology 46: 803-816.

Waring WS. Werkman CH. 1944. Iron deficiency in bacterial metabolism. Arch. Biochem. 4: 75-87.

Welsh DT, Wellsbury P, Bourgues S, Wit R, Herbert RA. 1996. Relationship between porewater organic carbon content, sulphate reduction and nitrogen fixation (acetylene reduction) in the rhizosphere of *Zostera noltii*. Hydrobiologia 329: 175-183.

Widdel F, Kohring GW, Mayer F. 1983. Studies on dissimilatory sulfate-reducing bacteria that decomposed fatty acids. III. Characterization of the filamentous gliding *Desulfonema limocola* gen. nov. sp. nov., and *Desulfonema magnum* sp. nov. Arch. Microbiol. 134: 286-294.

Wijsman JWM, Middelburg JJ, Herman PMJ, Böttcher ME, Heip CHR. 2001. Sulfur and iron speciation in surface sediments along the northwestern margin of the Black Sea. Mar. Chem. 74: 261-278.

Winters GV, Buckley DE. 1986. The influence of dissolved $Fe_2Si(OH)_8^0$ on chemical equilibria in pore waters from deep sea sediments. Geochim. Cosmochim. Acta 50: 277-288.

5. Fractionation of sulfur isotopes by *Desulfovibrio vulgaris* mutants lacking periplasmic hydrogenases and cytochrome c_3

5.1. Abstract

Sulfate reduction is the principal microbial process responsible for the anaerobic mineralization of organic compounds, and the associated isotope fractionation has been widely used to trace the biogeochemical cycling of sulfur and carbon. However, intracellular mechanisms behind the wide range of fractionations observed in nature and cultures are not fully understood. In this study, we investigate the influence of electron transport chains on the fractionation of sulfur isotopes by using *Desulfovibrio vulgaris* Hildenborough mutants lacking periplasmic hydrogenases and cytochrome c_3.

Mutants lacking Type I tetraheme cytochrome c_3 (*ΔcycA*) fractionated the $^{34}S/^{32}S$ ratio approximately 50% more than the wild type, evolving H_2 in the headspace and exhibiting a lower cell specific respiration rate. These observations imply that the reduced flow of electrons from organic acids to terminal reductases increases the magnitude of S-isotope fractionation during microbial sulfate reduction. In addition, the growth of *ΔcycA* on pyruvate relied largely on fermentation rather than sulfate reduction, suggesting that simultaneous sulfate reduction and fermentation may be responsible for some of the large naturally-occurring S isotope effects. The deletion of periplasmic [FeNiSe] hydrogenase increased S-isotope fractionation by 2‰, while other periplasmic hydrogenase mutants fractionated $^{34}S/^{32}S$ ratio to the extent similar to their parent strains. This small, but distinct, effect may be due to the repression of non-Se hydrogenases by Se present in the medium. Overall, our results demonstrate the link between electron transfer chains and S-isotope effects, identifying a complex biochemical base for the interpretation of S-isotope signatures.

5.2. Introduction

Microbial sulfate reduction (MSR) is the principal anaerobic metabolism that remineralizes organic compounds. This process uses sulfate as an electron donor, produces sulfide and results in significant isotope effects, where the product sulfide is depleted in heavy isotopes, ^{33}S, ^{34}S, and ^{36}S with respect to the starting sulfate. Consequently, the isotopic composition of various sulfur species can be used to probe the coupled cycling of S and C in nature (Canfield and Teske, 1996; Lyons, 1997; Wortmann *et al.*, 2001; Zerkle *et al.*, 2010). While sulfate reducing microbes prefer lighter S isotopes, the magnitude of fractionation varies spatially and temporally from 0 to 77‰ in nature (Fry *et al.*, 1995; Canfield and Teske, 1996; Rudnicki *et al.*, 2001). To probe the origin these large variations and identify their potential

environmental implications, a number of studies have investigated factors controlling S-isotope fractionation in pure and mixed cultures of sulfate reducing microbes (Kaplan and Rittenberg, 1964; Chambers *et al.*, 1975; Detmers *et al.*, 2001; Kleikemper *et al.*, 2004; Johnston *et al.*, 2005; Hoek *et al.*, 2006; Sim *et al.*, 2011a).

To date, culture studies investigating the fractionation of S isotopes during MSR focused on the influence of organic substrates (Chambers *et al.*, 1975; Kleikemper *et al.*, 2004; Sim *et al.*, 2011a), sulfate (Habicht *et al.*, 2002, 2005), sulfide (Eckert *et al.*, 2011), iron (Sim *et al.*, *submitted*), nitrogen (Sim *et al.*, *submitted*), and temperatures (Canfield *et al.*, 2006; Mitchell *et al.*, 2009). On one hand, these studies revealed an apparent link between the physiology of sulfate reducing microbes and the magnitude of S-isotope fractionation. On the other hand, only few of these studies attempted to directly address intracellular mechanisms and enzymatic activities dictating the measured fractionation of S isotopes (Mangalo *et al.*, 2008). Fortunately, recent advances in molecular biology have enabled investigation of the biochemical basis of MSR by mutant analyses of *D. vulgaris* lacking cytoplasmic hydrogenases (Stolyar et al., 2008; Walker et al., 2009), periplasmic hydrogenases (Poherlic *et al.*, 2002; Goenka *et al.*, 2005; Caffrey *et al.*, 2007), cytochromes (Semkiw et al., 2010), and transmembrane complexes (Dolla et al., 2000; Zane et al., 2010). These analyses can probe the contribution of individual enzymes to MSR, providing the complementary information to classical culture studies that often treat the cell as a black box.

MSR is a respiration process that is intrinsically linked to the oxidation of electron donors such as organic substrates or H_2. Thus, the flow of electrons to terminal reductases is suspected to regulate S-isotope fractionation, in particular when MSR is limited by electron donors (Hoek *et al.*, 2006; Sim *et al.*, 2011a) and iron (Sim et al., *submitted*). Currently, two electron transport pathways for the conservation of energy are thought to operate in *Desulfovibrio vulgaris* (Noguera *et al.*, 1998; Keller and Wall, 2011): a hydrogen cycling pathway using hydrogen as an intermediate electron carrier (Fig. 5.1), and a pathway bypassing hydrogen cycling and transferring electrons directly to the membrane-bound menaquinone pool. Although the relative contribution of these pathways may vary in the wild type depending on the environmental conditions (Noguera et al., 1998), mutations of specific components in each pathway can modulate the flow of electrons at the enzymatic level. A hydrogen cycling pathway requires both cytoplasmic and periplasmic hydrogenases for the formation of H_2 in cytoplasm and the subsequent oxidation in periplasm. Cytochromes are also essential to that pathway, because they deliver electrons from periplasmic hydrogenases to the transmembrane complexes that ultimately deliver electrons to terminal reductases (Odom and Peck, 1981; Heidelberg *et al.*, 2004). Consequently, the deletion of genes

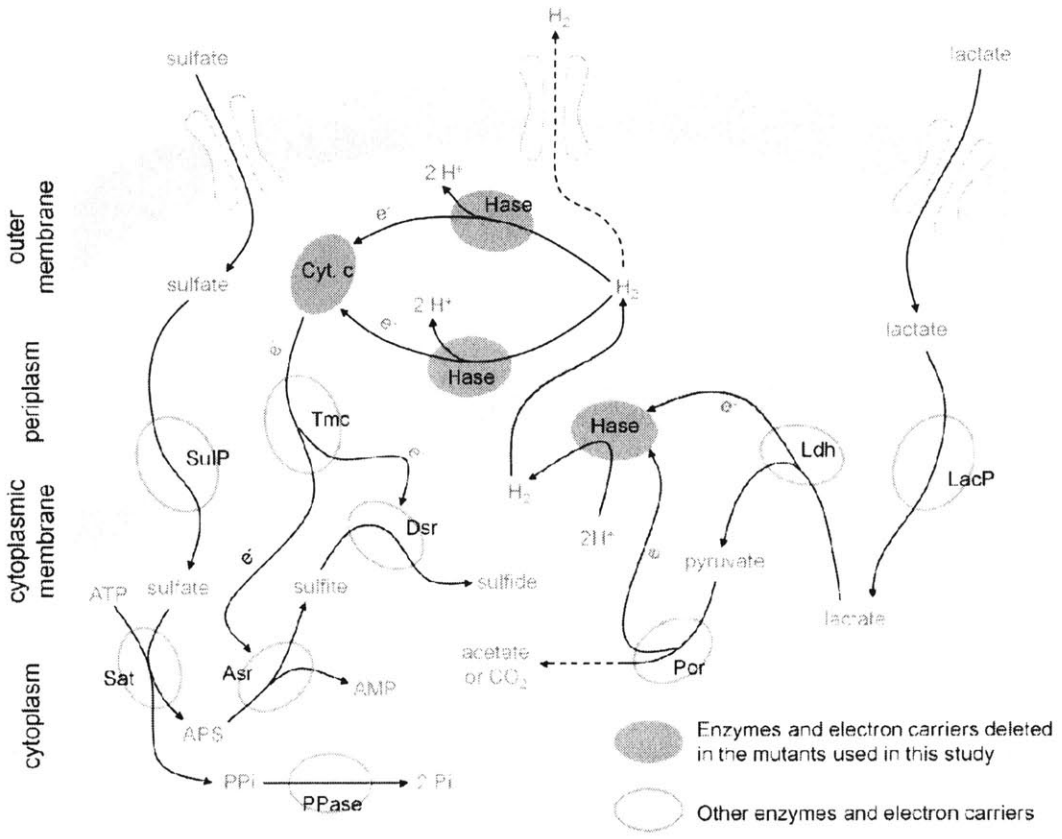

Figure 5.1. Schematic representation of electron flow suggested by the hydrogen cycling model (Odom and Peck, 1981). Reducing equivalents are suggested to flow from the electron donor to sulfur through hydrogen metabolism, which could be mediated by hydrogenases and other electron carriers, including cytochromes (Heidelberg et al., 2004). Recent molecular biological studies suggest that hydrogen cycling may contribute but is not essential to the energy conservation by sulfate reducing microbes (Keller and Wall, 2011; Pereira et al., 2011). Abbreviations: LacP, lactate permease; Ldh, lactate dehydrogenase; Por, pyruvate-ferrodoxin oxidoreductase; Hase, hydrogenase; Cyt. *c*, cytochrome *c*; Tmc, transmembrane redox complex; SulP, sulfate permease; Sat, ATP sulfurylase; Asr, APS reductase; Dsr, dissimilatory sulfite reductase; PPase, pyrophosphate phosphatase.

encoding any of these components can impair the hydrogen cycling pathway, altering the overall flow of electrons (Stolyar *et al.*, 2008; Walker *et al.*, 2009; Semkiw *et al.*, 2010).

Here we ask whether changes in the electron flow can affect S-isotope fractionation, as predicted by previous culture studies (Hoek *et al.*, 2006; Sim *et al.*, 2011a; Sim et al., *submitted*). We use mutant strains of *Desulfovibrio vulgaris* Hildenborough lacking cytochrome c_3 and hydrogenases, characterize their growth and sulfate reduction rates, and measure the resulting S-isotope fractionation. To the best of our knowledge, none of thes previous studies attempted to link mutant analyses of a sulfate reducing microbe to the resulting S isotope effects.

5.3. Methods

5.3.1. Bacterial Strains and Growth Medium

Various mutant and corresponding parent strains of *Desulfovibrio vulgaris* Hildenborough (DvH) were kindly provided by Dr. Judy Wall (University of Missouri, MO, USA) and Dr. Gerrit Voordouw (University of Calgary, Alberta, Canada). The strains include: four periplasmic hydrogenase mutants (Δ*hydAB*, Δ*hynBA-1*, Δ*hynBA-2*, and Δ*hysBA*), two cytoplasmic hydrogenase mutants (Δ*echA*, Δ*cooL*), and one Type I tetraheme cytochrome c_3 (Tp1-c_3) mutant (Δ*cycA*) (Table 5.1). All strains were cultured in a chemically defined, phosphate-buffered medium containing (per 1 L): 3g Na_2SO_4, 7g NaCl, 0.3g Na_3-citrate·$2H_2O$, 0.32g KH_2PO_4, 0.25g K_2HPO_4, 1g $MgCl_2·6H_2O$, 0.1g KCl, 0.1g $CaCl_2·2H_2O$, 1mg resazurin, 1 ml of trace metal solution and 10 ml of vitamin solution. The trace metal solution contained (per liter): 1g $FeCl_2·4H_2O$, 0.5g $MnCl_2·4H_2O$, 0.3g $CoCl_2·4H_2O$, 0.2g $ZnCl_2$, 0.05g $Na_2MoO_4·4H_2O$, 0.02g H_3BO_3, 0.1g $NiSO_4·6H_2O$, 2mg $CuCl_2·2H_2O$, 6mg $Na_2SeO_3·5H_2O$, and 8mg $Na_2WO_4·2H_2O$). The vitamin solution contained (per liter): 2mg biotin, 2mg folic acid, 10mg pyridoxine-HCl, 5mg thiamin-HCl, 5mg riboflavin, 5mg nicotinic acid, 5mg pantothenic acid, 5mg *p*-aminobenzoic acid, and 1 mg vitamin B_{12}). Titanium (III) citrate (0.1 mM) was added as a reducing agent (Zehnder and Wuhrmann, 1976; Louie and Mohn, 1999). Cultures contained either lactate (20 mM) or pyruvate (40 mM) as electron donors and carbon sources. The pH of the medium was adjusted to 7.5 using NaOH, flushed with N_2 gas, and sterilized by autoclaving. Filter-sterilized anaerobic solutions of titanium citrate, vitamins, and Ca/Mg were added to the medium after autoclaving. The final pH of the medium was between 7 and 7.5.

5.3.2. Culture Experiments

All strains were incubated in batch cultures at 37°C. Culture bottles containing sterile media (20 ml) were inoculated with washed cells. The cells were washed three times by anaerobic centrifugation and

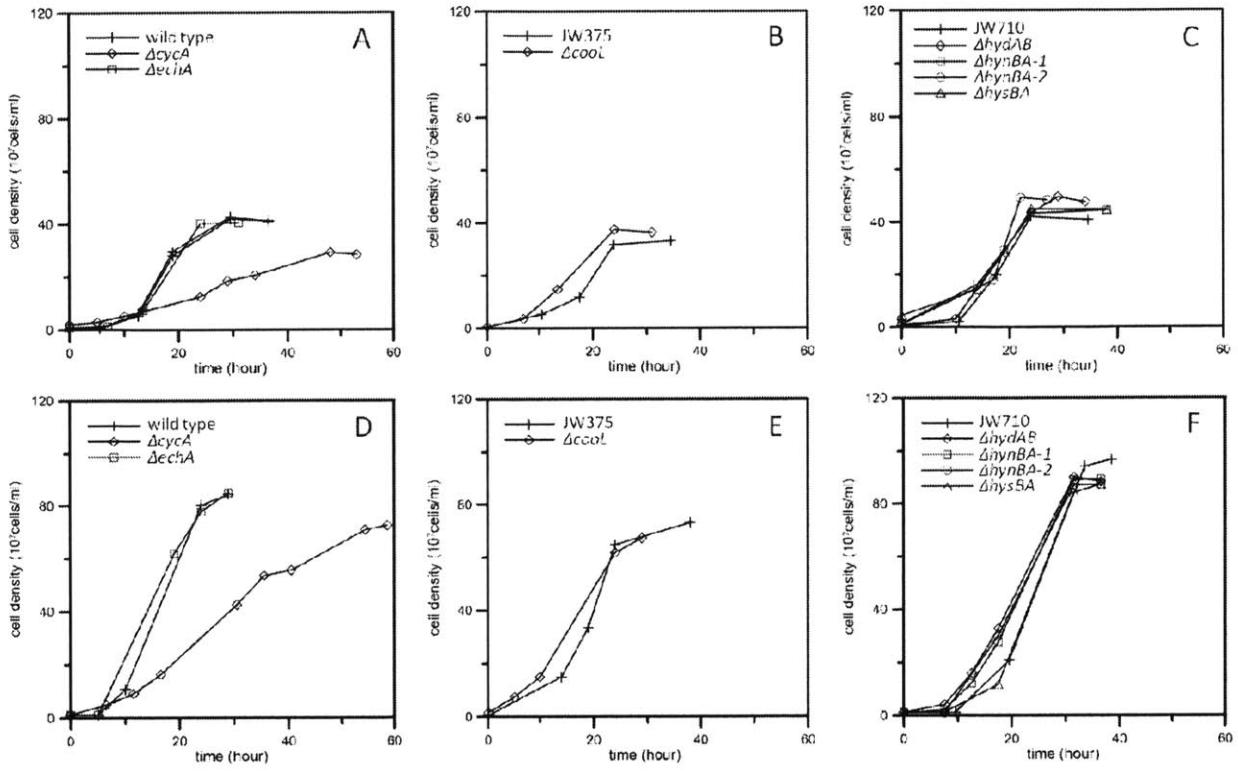

Figure 5.2. Growth of wild type and mutant *Desulfovibrio vulgaris* cultures on lactate (A, B, C) and pyruvate (D, E, F). Growth curves for mutants are displayed in parallel with their parent strains: wild-type (A, D); JW375 (B, E); JW710 (C, F). Cell densities are subject to a ±15% error.

resuspension in sterile, fresh medium to reduce the carryover of sulfide. Cell growth and sulfide concentration were monitored at least three times a day. Sulfide concentration was measured by a modified methylene blue assay (Cline, 1969) in 200 µL culture samples that were mixed by 1 ml of 0.05 M Zn–acetate solution. Growth was monitored by measuring the optical density at 630 nm using the Synergy2 Biotek microplate reader, (BioTek, VT, USA) and by microscopic counts of cells stained by SYTOX-Green nucleic acid stain (Invitrogen S7020, Paisley, UK) using a Zeiss Axio Imager M1 epifluorescence microscope (Carl Zeiss, Thornwood, NY, USA). Gases in the headspace of early stationary phase cultures were examined for hydrogen or carbon monoxide by withdrawing 300 µl of headspace gas using a gas-tight syringe and analyzing the samples by a GC-TCD-methanizer-FID (Shimadzu GC-2014) with a Carboxen-1000 packed column (60/80 mesh, 1/8" OD, length, Supelco).. Procedural and analytical reproducibility was 8%. At the end of the incubation, 3 ml of 1 M Zn-acetate were added to terminate microbial activity and to precipitate dissolved sulfide as zinc sulfide.

Cell-specific sulfate reduction rates (csSRRs) were compared to the magnitude of S-isotope fractionation. The csSRR was calculated for exponentially growing cells using the change in concentration of sulfide and cell density as previously described (Sim *et al.*, 2011a):

$$csSRR = \frac{\ln(c_x) - \ln(c_1)}{t_x - t_1} \cdot \frac{[H_2S]_x - [H_2S]_1}{c_x - c_1} \quad (1)$$

where t_1 and t_x are the onset of growth and the time of sampling, respectively, and C and $[H_2S]$ are cell densities (number of cells/ml) and sulfide concentrations at the time of sampling, respectively.

5.3.3. Isotopic Measurements

S-isotope fractionation factors during MSR were calculated using the measured isotopic compositions of the initial sulfate and the produced sulfide that is precipitated as zinc sulfide at the end of experiments. Depending on the concentration of sulfide at the end of incubation, the proper volume of sample was centrifuged so as to collect approximately 10 µmole of ZnS. The collected ZnS was resuspended in 400 µl of distilled water, mixed with 500 µl of $AgNO_3$ stock solution (1.7g of $AgNO_3$ in 100 ml of 0.1 M HNO_3), and incubated at 65°C overnight. The resulting Ag_2S was washed three times with distilled water to eliminate the residual silver nitrate, and dried at 80°C for one day. Sulfate in the fresh medium (3 ml) was reduced to sulfide by the reaction with 30 ml of the reducing agent (mixture of HI, H_3PO_2 and HCl, Thode *et al.*, 1961). Samples were boiled and purged by N_2 gas for two hours. Volatile products were

passed through a condenser and a trap containing distilled water, and the sulfide was collected in a Zn-acetate trap. ZnS was converted to Ag_2S as described above. The Ag_2S samples were allowed to react with an excess of fluorine gas for more than 5 hours at 300°C, and the produced SF_6 was purified by gas chromatography. Purified SF_6 was transferred into an isotope-ratio mass spectrometer for multiple sulfur isotope measurements in the dual inlet mode (Ono *et al.*, 2006).

Sulfur isotopic compositions are reported using the conventional delta notation.

$$\delta^{34}S = 1000 \cdot \left(\frac{R_{sample}}{R_{reference}} - 1\right) \quad (2)$$

where R are the isotopic ratios ($^{34}S/^{32}S$) of sample and reference materials. Our study reports all isotopic ratios with respect to the starting sulfate. The analytical uncertainty of sulfur isotope measurements is 0.2‰. The isotope fractionation factor (α) in this study was calculated using the Rayleigh distillation equation (Mariotti *et al.*, 1981):

$$^{34}\alpha = \frac{1}{\ln f_r} \ln\left(1 + (1 - f_r)\frac{\delta_{\Delta p} + 1000}{\delta_o + 1000}\right) \quad (3)$$

where f_r is the fraction of the remaining sulfate, δ_o and $\delta_{\Delta p}$ are sulfur isotope compositions of the initial sulfate and sulfide produced during the incubation, respectively. The isotope enrichment factor is defined as:

$$^{34}\varepsilon = 1000 \cdot (1 - ^{34}\alpha) \quad (4)$$

According to this definition, positive values represent the depletion of heavy isotopes in the product.

5.4. Results

All tested mutants were capable of growth on lactate or pyruvate, respectively, as the sole carbon and energy sources (Fig. 5.2). When grown on lactate, all tested strains reduced sulfate to sulfide (Table 5.2), and most mutants grew at rates similar to their parent strains (Figs. 5.2A, 5.2B, 5.2C). An exception to this was *cycA* mutant, which grew more slowly and to a lower cell density relative to the wild type (Fig. 5.2A), and exhibited slower csSRR than other strains (Fig. 5.3). Respiration in pyruvate-grown cultures was slower, but all strains reached a higher cell density when growing on pyruvate than when growing on lactate (Figs. 5.2, 5.3). With the exception of Δ*cycA*, parent and mutant strains grew at comparable rates

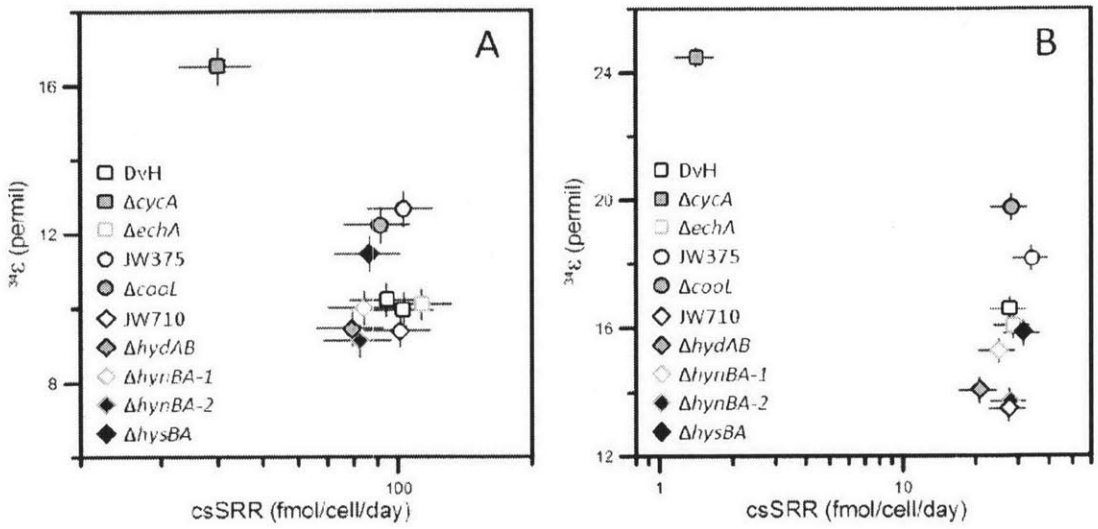

Figure 5.3. Relationship between S-isotope fractionation and csSRR produced by *Desulfovibrio vulgaris* wild-type and mutant strains grown on lactate (A) and pyruvate (B).

electron donor	strain	csSRR (fmol/cell/day)	produced H_2S (mM)	produced H_2 (μmole)	$\delta^{34}S_{sulfide}$ (‰)	$^{34}\varepsilon$(‰)
lactate	DvH	94.1 ± 15.5	9.2	< 0.1	-7.6	10.2 ± 0.4
		102.9 ± 17.0	9.9		-7.1	10.0 ± 0.5
	ΔcycA	40.1 ± 7.1	8.9	77.6	-12.5	16.5 ± 0.5
	ΔechA	112.9 ± 18.8	8.4		-7.8	10.1 ± 0.4
	JW375	91.3 ± 15.2	9.6		-8.9	12.2 ± 0.5
	ΔcooL	102.7 ± 17.0	9.2		-9.4	12.7 ± 0.5
	JW710	101.2 ± 16.7	8.9		-7.1	9.4 ± 0.4
	ΔhydAB	79.4 ± 13.3	10.1		-6.7	9.5 ± 0.5
	ΔhynBA-1	84.5 ± 14.3	9.5		-7.3	10.0 ± 0.4
	ΔhynBA-2	82.7 ± 13.9	9.7		-6.6	9.1 ± 0.4
	ΔhysBA	86.7 ± 14.5	9.6		-8.3	11.5 ± 0.5
pyruvate	DvH	27.6 ± 4.6	6.3	0.2	-13.8	16.6 ± 0.4
	ΔcycA	1.4 ± 0.2	0.9	100.7	-23.9	24.5 ± 0.3
	ΔechA	28.6 ± 4.7	6.7		-13.2	16.1 ± 0.4
	JW375	33.9 ± 5.5	6.0		-15.4	18.2 ± 0.4
	ΔcooL	28.0 ± 4.7	6.3		-16.5	19.8 ± 0.4
	JW710	27.3 ± 4.5	6.9		-11.0	13.5 ± 0.4
	ΔhydAB	20.8 ± 3.6	6.9		-11.5	14.1 ± 0.4
	ΔhynBA-1	24.9 ± 4.2	6.1		-12.8	15.3 ± 0.4
	ΔhynBA-2	27.6 ± 4.6	7.1		-11.1	13.7 ± 0.4
	ΔhysBA	31.5 ± 5.2	6.7		-13.0	15.8 ± 0.4

Table 5.2. Growth parameters and sulfur isotope effects estimated from the wild type and the mutant strains of *Desulfovibrio vulgaris*.

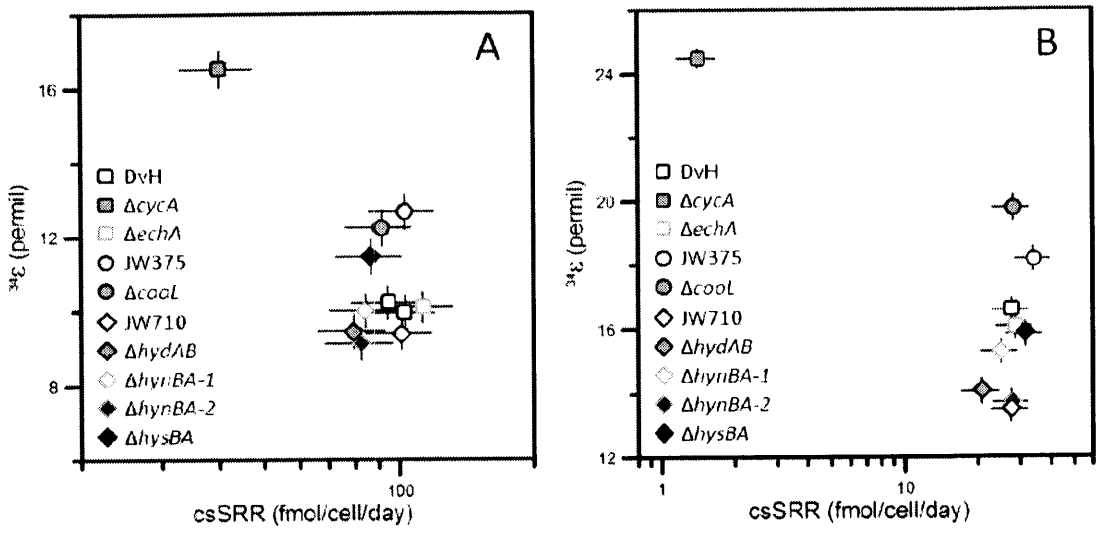

Figure 5.3. Relationship between S-isotope fractionation and csSRR produced by *Desulfovibrio vulgaris* wild-type and mutant strains grown on lactate (A) and pyruvate (B).

and attained the similar cell densities in stationary cultures (Figs. 5.2D, 5.2E, 5.2F). Δ*cycA* cells had a lower growth rate, but attained the final cell density (7.2×10^8 cells/ml) comparable to that of the wild type (8.4×10^8 cells/ml) (Fig. 5.2D). Sulfide concentration in the cultures of Δ*cycA* was as low as 0.9 mM when the growth ceased (Table 5.2), resulting in much lower csSRR relative to other strains grown under identical conditions (Fig. 5.3).

Because the deletion of *cycA* impaired the growth, we hypothesized that some of the reducing equivalents may be released from the cell in the form of H_2 or CO, instead of being used to reduce sulfate (Voordouw, 2002). We thus examined their concentrations in the headspace of cultures in early stationary phase (Table 5.2). The wild type grown on lactate or pyruvate produced negligible amounts of hydrogen (< 1 μmole). In contrast, Δ*cycA* produced 78 and 101 μmoles of hydrogen when grown on lactate and pyruvate, respectively, i.e., more than 100-fold more H_2 than the wild type. Under our experimental conditions, CO in the headspace of all early-stationary-phase cultures was not detected.

In keeping with the reduced growth and sulfate reduction rates by Δ*cycA*, sulfide in the same cultures was most depleted with respect to the heavy isotope (^{34}S) (Table 5.2 and Fig. 5.3). Δ*cycA* grown on lactate and pyruvate fractionated $^{34}S/^{32}S$ at 16.5‰ and 24.5‰, respectively, while the corresponding values for the wild type were 10.1 and 16.6‰, respectively. Calculated enrichment factors ($^{34}\varepsilon$) in cultures of mutants other than Δ*cycA* ranged from 9.1 to 12.7‰ in lactate-grown cultures and from 13.5 to 20.0‰ in pyruvate-grown cultures (Fig. 5.3). Variations within these ranges were largely driven by the use of different parent strains in the construction of mutants (Table 5.1). In addition, mutant lacking *hysBA* fractionated $^{34}S/^{32}S$ ratio 2‰ greater than its parent strain. This increase was smaller than that associated with the deletion of *cycA* but larger than the analytical uncertainties (Table 5.2). All strains in pyruvate-grown cultures fractionated $^{34}S/^{32}S$ by 4‰ more than when oxidizing lactate (Fig. 5.3). A similar effect of pyruvate and lactate was previously reported in cultures of a different *Desulfovibrio* species (Sim *et al.*, 2011a).

5.5. Discussion

Our experiments demonstrated the effect of disruptions in electron transfer chains on S-isotope fractionation during MSR. This disruption was the largest in cells of DvH lacking a Type I tetraheme cytochrome c_3 (Tp1-c_3) (Δ*cycA*). Tp1-c_3 is proposed to shuttle electrons from periplasmic hydrogenases to transmembrane complexes, which then transport electrons to cytoplasmic terminal reductases (Heidelberg *et al.*, 2004; Semkiw *et al.*, 2010) (Fig. 5.1). Consequently, Tp1-c_3 is essential for the hydrogen cycling pathway, but not required for the transfer of electrons to the membrane-bound menaquinone pool

(Noguera *et al.*, 1998; Keller and Wall, 2011). DvH mutants lacking Δ*cycA* exhibited lower csSRR, suggesting an impaired flow of electrons from organic acids to sulfur. Two factors may contribute to this "sluggish" electron transfer to the sulfate reducing pathway in Δ*cycA* mutant. First, the accumulation of H_2 in the headspace of Δ*cycA* cultures indicates that some reducing equivalents escape from the electron transfer chain. Second, the midpoint potential of menaquinone (-73mV) is relatively high compared to SO_3^{2-}/HS^- (-116 mV) (Thauer *et al.*, 1977), while that of the cytochrome c_3 ranges from -125 to -325 mV (Rabus *et al.*, 2006), suggesting that cytochrome c_3 may be more favored as an electron donor. Our data do not allow us to distinguish between these hypotheses, but identify some intracellular processes and biochemical components that can influence the magnitude of S-isotope fractionation.

The MSR pathway consists of several enzymatic steps and operates in a reversible manner, and the overall isotope effect during sulfate reduction depends on the ratio between forward and backward fluxes at each enzymatic step (reversibility; Rees, 1973; Brunner and Bernasconi, 2005). According to this model, a reduced flow of electrons should slow down the reductive reactions, increase the reversibility, and in turn, increase the overall S-isotope fractionation during MSR. Such reduced flow is consistent with both the slower growth rates of Δ*cycA* and an increased S-isotope effect produced by this mutant. Larger S-isotope fractionation in the absence of Tp1-c_3 may also inform interpretations of sulfur isotope data in modern and past environments. First, although the multiheme cytochromes *c* are widespread among sulfate reducing microbes (Postgate, 1956; Pereira *et al.*, 2011), several species, including *Desulfotomaculum acetoxidans*, *Caldivirge maquilingensis*, and *Desulfotomaculum reducens*, contain no cytochromes *c* (Pereira *et al.*, 2011). These organisms are unlikely to rely on hydrogen cycling for the delivery of electrons during sulfate reduction. A sharp contrast in S-isotope fractionation between the Δ*cycA* mutant and the wild type suggests that species lacking cytochromes *c* and other components of the classical hydrogen cycling pathway (Pereira *et al.*, 2011) may produce larger fractionations than organisms that cycle hydrogen. Moreover, intracellular levels of Tp1-c_3 can be altered by environmental factors. For example, iron deficiency impairs the synthesis of cytochrome *c* in sulfate reducing bacteria (Postgate, 1956; Sim *et al.* submitted), and increases S-isotope fractionation (Sim *et al.*, submitted). Here, we confirm this link more directly, by using cells that cannot synthesize Tp1-c_3.

The largest S-isotope effect observed in this study was associated with the lowest concentrations of sulfide produced at the end of exponential growth (Table 5.2). Δ*cycA* produced only 0.9 mM sulfide when grown on pyruvate, but attained cell densities comparable to the wild type, pointing to comparable energy yields relative to sulfate reduction. This apparent decoupling between growth and sulfate reduction is consistent with the growth of Δ*cycA* supported by pyruvate fermentation as well as by pyruvate oxidation

and transfer of electrons to sulfate. Simultaneous sulfate reduction and fermentation have been reported in other sulfate reducing bacteria (Sass *et al.*, 2002; Sim *et al.*, 2011b). As previously discussed, if electrons are diverted away from the respiratory chain, the reversibility of the MSR pathway should increase, resulting in larger S-isotope fractionation. According to the steady state model (Rees, 1973; Brunner and Bernasconi, 2005), the maximum fractionation during MSR is expected when the backward fluxes equal the forward fluxes. However, when the generation of ATP depends exclusively on sulfate respiration, a minimum respiration rate is required to fulfill the maintenance energy requirement (Pirt, 1965), thereby resulting in the S-isotope fractionation much smaller than the theoretical maximum. In contrast, when sulfate reduction occurs simultaneously with fermentation, fermentation can provide some of the maintenance energy, allowing slower csSRR that leads to larger $^{34}\varepsilon$ values. This hypothesis may explain why Δ*cycA* grown on pyruvate yielded the largest enrichment factor obtained in this study. A similar decoupling of carbon and sulfur metabolisms is reported during MSR associated with the production of large S-isotope fractionation (Sim *et al.*, 2011b). Given that many sulfate reducing microbes are also facultative fermenters (Rabus *et al.*, 2006), fermentation by SRMs in natural habitats and S isotope signatures produced in such communities deserves further exploration.

DvH mutant lacking the [FeNiSe] hydrogenase (Δ*hysBA*) produced sulfide that was depleted by 2‰ relative to sulfide produced in the cultures of parent strain of Δ*hysBA*. Due to the apparent redundancy of four periplasmic hydrogenases (Caffrey *et al.*, 2007), Δ*hysBA* mutant was not expected to produce a larger fractionation than mutants lacking other periplasmic hydrogenases. This small, but distinct, effect may be due to the presence of selenium in the medium (see Methods). If Se is present, [FeNiSe] hydrogenase becomes the major periplasmic hydrogenase in DvH, and the synthesis of other hydrogenases is repressed at a transcriptional level (Valente *et al.*, 2006). Under these growth conditions, the deletion of other minor hydrogenases might not significantly alter total hydrogenase activity in periplasm. On the other hand, mutants lacking *hys* genes should oxidize less cytoplasmically-produced hydrogen, reduce the flow of electrons to MSR pathway, and consequently, increase the S-isotope effect.

To the best of our knowledge, this is the first study relating the fractionation of S-isotopes to the absence of specific genes in sulfate reducing microbes. Our results reveal links between electron transfer chains and S-isotope effect, and point to various biochemical components that can contribute to the production of the observed S-isotope signatures in nature. Future studies can investigate S-isotope fractionation by mutant strains of DvH lacking other key components of the electron transfer chain, such as the Hmc and Qmo complexes (Dolla *et al.*, 2000; Zane *et al.*, 2010) to provide better constraints on the relationship between the flow of electrons and the fractionation of sulfur isotopes. This approach also

should be expanded to different species of sulfate reducing bacteria (Rapp-Giles, 2000; Casalot et al., 2002) and to other reactions contributing to MSR. For example, mutants lacking sulfate permeases and enzymes containing various metal cofactors may help better constrain effects of sulfate concentrations and trace metals on S-isotope fractionation.

References

Caffrey SM, Park H-S, Voordouw JK, He Z, Zhou J, Voordouw G. 2007. Function of periplasmic hydrogenases in the sulfate-reducing bacterium *Desulfovibrio vulgaris* Hildenborough. J. Bacteriol. 189: 6159-6167.

Canfield DE, Olesen CA, Cox RP. 2006. Temperature and its control of isotope fractionation by a sulfate-reducing bacterium. Geochim. Cosmochim. Acta 70: 548-561.

Canfield DE, Teske A. 1996. Late Proterozoic rise in atmospheric oxygen concentration inferred from phylogenetic and sulphur-isotope studies. Nature 382: 127-132.

Casalot L, Valette O, De Luca G, Dermoun Z, Rousset M, de Philip P. 2002. Construction and physiological studies of hydrogenase depleted mutants of Desulfovibrio fructosovorans. FEMS Microbiol. Lett. 214: 107-112.

Chambers LA, Trudinger PA, Smith JW, Burns MS. 1975. Fractionation of sulfur isotopes by continuous cultures of *Desulfovibrio desulfuricans*. Can. J. Microbiol. 21: 1602-1607.

Cline JD. 1969. Spectrophotometric determination of hydrogen sulfide in natural water. Limnol. Oceanogr. 14: 454-458.

Detmers J, Bruchert V, Habicht K, Kuever J. 2001. Diversity of sulfur isotope fractionations by sulfate reducing prokaryotes. Appl. Environ. Microbiol. 67: 888-894.

Dolla A, Pohorelic KJ, Voordouw KJ, Voordouw G. 2000. Deletion of the hmc-operon of *Desulfovibrio vulgaris* subsp. *vulgaris* Hildenborough hampers hydrogen metabolism and low-redox potential niche establishment. Arch. Microbiol. 174: 143-151.

Eckert T, Brunner B, Edwards EA, Wortmann UG. 2011. Microbially mediated re-oxidation of sulfide during dissimilatory sulfate reduction by *Desulfobacter latus*. Geochim. Cosmochim. Acta 12: 3469-3485.

Fry B, Giblin A, Dornblaser M, Peterson B. 1995. Stable sulfur isotopic compositions of chromium-reducible sulfur in lake sediments. In Geochemical Transformation of Sedimentary Sulfur (eds. Vairavamurthy MA, Schoonen MAA), ACS Symposium Series 612. American Chemical Society, Washington, DC, pp. 397-410.

Goenka A, Voordouw JK, Lubitz W, Gärtner W, Voordouw G. 2005. Construction of a [NiFe]-hydrogenase deletion mutant of *Desulfovibrio vulgaris* Hildenborough. Biochem. Soc. Trans. 33: 59-60.

Habicht KS, Gabe M, Thamdrup B, Berg P, Canfield DE. 2002. Calibration of sulfate levels in the Archean ocean. Science 298: 2372-2374.

Habicht KS, Salling L, Thamdrup B, Canfield DE. 2005. Effect of low sulfate concentrations on lactate oxidation and isotope fractionation during sulfate reduction by *Archaeoglobus fulgidus* Strain Z. Appl. Environ. Microbiol. 71: 3770-3777.

Heidelberg JF,Seshadri R,Haveman SA, Hemme CL, Paulsen IT, Kolonay JF, Eisen JA, Ward N, Methe B, Brinkac LM, Daugherty SC, Deboy RT, Dodson RJ, Durkin AS, Madupu R, Nelson WC, Sullivan SA, Fouts D, Haft DH, Delengut J, Peterson JD, Davidsen TM, Zafar N, Zhou L, Radune D, Dimitrov G, Hance M, Tran K, Khouri H, Gill J, Utterback TR, Feldblyum TV, Wall JD, Voordouw G, Fraser CM. 2004.The genome sequence of the anaerobic sulfate-reducing bacterium *Desulfovibrio vulgaris* Hildenborough. Nat.Biotechnol. 22: 554–559.

Hoek J, Reysenbach A, Habicht KS, Canfield DE. 2006. Effect of hydrogen limitation and temperature on the fractionation of sulfur isotopes by a deep-sea hydrothermal vent sulfate-reducing bacterium. Geochim. Cosmochim. Acta 70: 5831-5841.

Johnston DT, Farquhar J, Wing BA, Kaufman AJ, Canfield DE, Habicht KS. 2005. Multiple sulfur isotope fractionations in biological systems: A case study with sulfate reducers and sulfur disproportionators. Am. J. Sci. 305: 645-660.

Kaplan IR, Rittenberg SC. 1964. Microbiological fractionation of sulphur isotopes. J. Gen Microbiol. 34: 195-212.

Keller KL, Bender KS, Wall JD. 2009. Development of a markerless genetic exchange system for *Desulfovibrio vulgaris* Hildenborough and its use in generating a strain with increased transformation efficiency. Appl. Environ. Microbiol. 75: 7682-7691.

Keller KL, Wall JD. 2011. Genetics and molecular biology of the electron flow for sulfate respiration in Desulfovibrio. Front. Microbio. 2:135.

Kleikemper J, Schroth MH, Bernasconi SM, Brunner B, Zeyer J. 2004. Sulfur isotope fractionation during growth of sulfate reducing bacteria on various carbon sources. Geochim. Cosmochim. Acta 68: 4891-4904.

Louie TM, Mohn WW. 1999. Evidence for a chemiosotic model of dehalorespiration in *Desulfomonile tiedjei* DCB-1. J. Bacteriol. 181: 40-46.

Lyons TW. 1997. Sulfur isotopic trends and pathways of iron sulfide formation in upper Holocene sediments of the anoxic Black Sea. Geochim. Cosmochim. Acta 61: 3367-3382.

Mangalo M, Einsiedl F, Meckenstock RU, Stichler W. 2008. Influence of the enzyme dissimilatory sulfite reductase on stable isotope fractionation during sulfate reduction. Geochim. Cosmochim. Acta 71: 4161-4171.

Mariotti A, Germon JC, Hubert P, Kaiser P, Letolle R, Tardieux A, Tardieux P. 1981. Experimental determination of nitrogen kinetic isotope fractionation: some principles; illustration for the denitrification and nitrification processes. Plant Soil 62: 413-430.

Mitchell K, Heyer A, Canfield DE, Hoek J, Habicht KS. 2009. Temperature effect on the sulfur isotope fractionation during sulfate reduction by two strains of the hyperthermophilic *Archaeoglobus fulgidus*. Environ. Microbiol. 11: 2998-3006.

Noguera DR, Brusseau GA, Rittmann BE, Stahl DA. 1998. A unified model describing the role of hydrogen in the growth of *Desulfovibrio vulagris* under different environmental conditions. Biotechnol. Bioeng. 59: 732-746.

Odom JM, Peck HD Jr. 1981. Hydrogen cycling as a general mechanism for energy coupling in the sulfate reducing bacteria, *Desulfovibrio* sp. FEMS Microbiol. Lett. 12: 47-50.

Ono S, Wing B., Rumble D, Farquhar J. 2006. High precision analysis of all four stable isotope of sulfur (^{32}S, ^{33}S, ^{34}S and ^{36}S) at nanomole levels using a laser fluorination isotope-ratio-monitoring gas chromatography-mass spectrometry. Chem. Geol. 225: 30-39.

Pereira IAC, Ramos AR, Grein F, Marques MC, Marques da Silva S, Venceslau SS. 2011. A comparative genomic analysis of energy metabolism in sulfate reducing bacteria and archaea. Front. Microbio. 2: 69.

Pirt SJ. 1965. The maintenance energy of bacteria in growing cultures. Proc. Soc. London 63: 224-231.

Pohorelic BK, Voordouw JK, Lojou E, Dolla A, Harder J, Voordouw G. 2002. Effect of deletion of genes encoding Fe-only hydrogenase of *Desulfovibrio vulgaris* Hildenborough on hydrogen and lactate metabolism. J. Bacteriol. 184: 679-686.

Postgate JR. 1956. Iron and synthesis of cytochrome c_3. J. gen. Microbiol. 15: 186-193.

Rabus R, Hansen TA, Widdel F. 2006. Dissimilatory sulfate- and sulfur- reducing prokaryotes. In The Prokaryotes (eds M Dworkin, S Falkow, E Rosenberg, KH Schleifer, E Stackbrandt). Springer-Verlag, New York.

Rapp-Giles B, Casalot L, English RS, Ringbauer Jr JA, Dolla A, Wall JD. 2000. Cytochrome c3 mutants of Desulfovibrio desulfuricans. Appl. Environ. Microbiol. 66: 617-677.

Rudnicki MD, Elderfield H, Spiro B. 2001. Fractionation of sulfur isotopes during bacterial sulfate reduction in deep ocean sediments at elevated temperatures. Geochim. Cosmochim. Acta 65: 777-789.

Sass A, Rütters H, Cypionka H. 2002. *Desulfobulbus mediterraneus* sp. nov., a sulfate-reducing bacterium growing on mono- and disaccharides. Arch. Microbiol. 177: 468-474.

Semkiw ES, Zane GM, Wall JD. 2010. The role of the type-1 tetraheme cytochrome c3 in Desulfovibrio vulgaris Hildenborough metabolism (Abstract). 110th General Meeting of American Society for Microbiology, San Diego, CA, K-773.

Sim MS, Ono S, Donovan K, Templer SP, Bosak T. 2011a. Effect of electron donors on the fractionation of sulfur isotopes by a marine Desulfovibrio sp. Geochim. Cosmochim. Acta 75: 4244-4259.

Sim MS, Bosak T, Ono S. 2011b. Large sulfur isotope fractionation does not require disproportionation. Science 333: 74-77.

Sim MS, Bosak T, Ono S. *submitted.* Effect of iron and nitrogen limitation on S-isotope fractionation during microbial sulfate reduction.

Stolyar S, Pinel N, Walker CB, Wall JD, Stahl DA. 2008. The physiology of the cytoplasmic hydrogenases in Desulfovibrio vulgaris (Abstract). 108th General Meeting of American Society for Microbiology, Boston, MA, K-074.

Thauer RK, Jungermann K, Decker K. 1977. Energy concervation in chemotrophic anaerobic bacteria. Bacteriol. Rev. 41: 100-180.

Thode HG, Monster J, Dunford HB. 1961. Sulphur isotope geochemistry. Geochim. Cosmochim. Acta 25: 158-174.

Valente FM, Almeida CC, Pacheco I, Carita J, Saraiva LM, Pereira IAC. 2006. Selenium is involved in regulation of periplasmic hydrogenase gene expression in *Desulfovibrio vulgaris* Hildenborough. J. Bacteriol. 188: 3228-3235.

Voordouw G. 2002. Carbon monoxide cycling by *Desulfovibrio vulgaris* Hildenborough. J. Bacteriol. 184, 5903-5911.

Walker CB, He Z, Yang ZK, Ringbauer JA, He Q, Zhou J, Voordouw G, Wall JD, Arkin AP, Hazen TC, Stolyar S, Stahl DA. 2009. The electron transfer system of syntrophically grown *Desulfovibrio vulgaris*. J. Bacterol. 191: 5793-5801.

Wortmann UG, Chernyavsky B, Bernasconi SM, Brunner B, Bottcher ME, Swart PK. 2007. Oxygen isotope biogeochemistry of pore water sulfate in the deep biosphere: Dominance of isotope exchange reactions with ambient water during microbial sulfate reduction (ODP Site 1130). Geochim. Cosmochim. Acta 71: 4221-4232.

Zane GM, Bill Yen H, Wall JD. 2010. Effect of the deletion of qmoABC and the promoter-distal gene encoding a hypothetical protein on sulfate reduction in Desulfovibrio vulgaris Hildenborough. Appl. Environ. Microbiol. 76: 5500-5509.

Zehnder AJB, Wuhrmann K. 1976. Titanium (III) citrate as a nontoxic oxidation-reduction buffering system for culture of obligate anaerobes. Science 194: 1165-1166.

Zerkle AL, Kamyshny A, Kump LR, Farquhar J, Oduro H, Arthur MA. 2010. Sulfur cycling in a stratified euxinic lake with moderately high sulfate: Constraints from quadruple S isotopes. Geochim. Cosmochim. Acta 74: 4953-4970.

6. Conclusions and Future Work

6.1. Conclusions

6.1.1 Effect of Organic Electron Donor

The relationship between the growth of a newly isolated marine sulfate reducing bacterium, DMSS-1 and the fractionation of sulfur isotopes are examined as a function of seven different organic electron donors in batch cultures, and as a function of the dilution rate in lactate-limited continuous cultures. An actively growing culture of DMSS-1 produces sulfide depleted in ^{34}S by 6 to 66‰, depending on the availability and chemistry of organic electron donors. The magnitude of the isotope effect correlates well with the cell specific sulfate reduction rate (csSRR). The use of multiple sulfur isotopes in the model of metabolic S fluxes shows that the availability and the nature of the organic electron donor alter the fluxes along each step of sulfate reduction. The largest isotope effects occur when cultures grow slowly on glucose, a recalcitrant organic substrate. These findings bridge the long-standing discrepancy between the upper limit for sulfur isotope effect ($^{34}\varepsilon$) in laboratory cultures and the corresponding observations in nature and provide an alternative model for the large isotope fractionation, which has been thought to be indicative of oxidative sulfur-recycling. Instead, the strong dependence of $^{34}\varepsilon$ on the availability and quality of natural organic matter suggests that temporal or spatial changes in sulfur isotope effects may reflect the changing nature of organic material that fueled sulfate reduction. The relative contributions of sulfate reduction alone and of the environmental-scale oxidative recycling toward large present and past natural fractionations of S isotope ratios now remain to be evaluated.

6.1.2 Limitation of Nitrogen and Iron

The influence of ammonium and iron limitation on multiple-S isotope fractionation by DMSS-1 is examined by reducing the concentrations of nitrogen and iron in a defined medium down to < 100 μM and < 1 μM, respectively. The availability of iron controls S-isotope fractionation in a manner similar to that of the organic electron donor. Nitrogen limitation produces smaller, but distinct isotopic signatures. During iron limitation, the increase in S-isotope fractionation is accompanied by a decrease in the cytochrome c content as well as csSRR. Given that iron is present in many enzymes and electron carriers linking the oxidation of organic electron donor to the reduction of sulfate, iron appears to affect the S-isotope fractionation by influencing carbon and sulfur catabolism. Some areas where nitrogen and iron limitation may lead to large observed S-isotope effects include highly productive benthic microbial mats or euxinic solutions.

6.1.3 Mutants Lacking the Enzymes Involved in Sulfate Respiration

A comparison between a wild-type organism and mutants lacking a specific enzyme allows one to attribute the difference in S-isotope fractionation to one enzymatic step. The mutant strains of *Desulfovibrio vulgaris* Hildenborough lacking cytochromes and hydrogenasese are cultured with lactate or pyruvate as an electron donor, and the resulting S-isotope fractionations are examined. The mutant lacking Type I tetraheme cytochrome c_3 fractionates $^{34}S/^{32}S$ ratio approximately 50% greater relative to the wild type. The deletion of periplasmic [FeNiSe] hydrogenase also increases S-isotope fractionation by 2‰, while other periplasmic hydrogenase mutants fractionate $^{34}S/^{32}S$ ratio to the extent similar to their parent strains. Overall, the inefficient delivery of electrons from organic acids to terminal reductases increases S-isotope fractionation during MSR. These results confirm the link between the flow of electrons and the fractionation of S-isotopes, which was suggested by the culture experiments using DMSS-1.

6.2. Future Work

In this thesis, I have shown the relationships between the physiology of SRM grown in pure cultures and the resulting S-isotope fractionations. The relative significance of these factors in an environmental context remains to be determined. Further geochemical and microbiological studies of microbial S-isotope fractionation in modern and ancient sediments should test feedbacks that link S-isotope signatures and geochemical cycles of other essential elements. This research should have two major components: the first would include field studies of different environments with distinct S-C-N-Fe cycles, whereas the second would focus on the fate of intermediate sulfur species and the associated isotope effects that can contribute to the sulfur isotope signatures in nature along with MSR.

6.2.1. Do Limitations by Organic Substrate and Other Nutrients Affect the S-isotope Effect in Nature?

My recent findings suggest that substrates used by sulfate-reducing microbes can influence the magnitude of S-isotope fractionation in nature. Although volatile fatty acids are commonly used as growth substrates for SRMs, the contribution of these compounds to sulfate reduction can be as low as 20% in some environments (Finke *et al.*, 2007). Instead, MSR appears to be fueled by other electron donors, including sugars, aromatic compounds, and longer alcohols and fatty acids. The oxidation of organic compounds coupled with MSR can be studied by radiotracer or molybdate inhibition experiments. A good model system in which to examine the influence of organic matter on MSR is Lake

McCarrons (MN). This low sulfate, permanently anoxic lake is characterized by large S-isotope fractionations up to 50‰ (Gomes and Hurtgen, in prep), although MSR is thought to produce little S-isotope fractionation when sulfate is limiting (Habicht *et al.*, 2002). Lake McCarrons is thus of great interest, since other environmental factors, such as the composition of organic substrates, may outweigh the effect of low sulfate levels.

More broadly, S-isotopic and chemical (sulfur, nitrogen, iron, and other trace metals) analyses should be integrated with the characterization of organic matter in different environments, including estuarine terrestrial sediments, grass-covered carbonate sediments, and hypersaline microbial mats. Each of these environments is distinct in terms of electron donors and other nutrients. Given the difference in primary production, not only the amount, but also the reactivity or C/N ratio of the organic compounds can vary among ecosystems. For example, organic compounds in grass-covered carbonate sediments and terrigenous sediments include organic matter released by higher plants, while those from microbial sources are dominant in hypersaline ponds. Depending on the presence or absence of detrital input, levels of iron can also contrast sharply. Therefore, integrated studies can evaluate the importance of the parameters tested in the laboratory on isotopic fractionation in diverse natural environments. Ultimately, these may be extrapolated to ancient S-isotope records. For example, Florida Bay consists almost entirely of calcium carbonate derived from the skeletal debris of marine organisms that contain much less iron than terrigenous materials (Berner, 1984). This shallow and oligotrophic lagoon is colonized by seagrass beds dominated by *Thalassia testudinum* (Ruiz-Halpern *et al.*, 2008). In addition, the carbonate sediment system is of particular interest because the S-isotope signature of carbonate-associated sulfate (CAS), along with pyrite, is a key proxy for the ancient sulfur cycle (Hurtgen *et al.*, 2002, 2005).

6.2.2. Multiple S-isotope Fractionation during Oxidative S Cycling

Prior to this study, none of pure culture studies have reported the sulfur isotope effects larger than 47‰ that have been commonly observed in nature. Large S-isotope fractionation in nature were thus attributed to a combination of MSR, extracellular oxidative recycling of sulfur by abiotic or microbial processes, and microbial sulfur disproportionation (MSD) (Canfield and Thamdrup, 1994). Although our study shows that MSD is not the only explanation for large S-isotope fractionations, a significant portion of biogenic sulfide is recycled by microbial or chemical oxidation (Thamdrup *et al.*, 1994). Recent studies have utilized the multiple S-isotope model to track the biogeochemical cycling of sulfur (Li *et al.*, 2010; Wu *et al.*, 2010; Zerkle *et al.*, 2010). Although these model estimates draw heavily on S-isotope fractionation attributed to each process, the input parameters to these models are constrained by a relatively small number of studies. In particular, there is only one study reporting the multiple S-isotope

fractionations during MSD (Johnston *et al.*, 2005). Johnston *et al.* (2005) reported the fractionation between two products, sulfate and sulfide, but the S-isotope fractionations between reactant (intermediate S species) and products (sulfate and sulfide) are as important as those between two products. Factors controlling fractionation during MSD are not well understood.

For better constraints on the global S cycle, therefore, it is necessary to culture sulfur disproportionating bacteria under different growth conditions and to measure multiple S-isotope fractionation among the reactant, an intermediate sulfur species, and the products of disproportionation, sulfide and sulfate. More than ten strains are known to couple the disproportionation of intermediate S species to growth (Finster, 2008), but *Desulfovibrio oxyclinae* is of interest because of its versatility in using sulfite, one of the important intermediate sulfur species as a substrate. *Desulfovibrio oxyclinae* can reduce sulfite to sulfide, disproportionate sulfite to sulfate and sulfide, and even oxidize sulfite to sulfate, depending on growth conditions (Krekeler *et al.*, 1997). Experiments can be conducted to test the magnitude of S-isotope fractionation during MSD by varying the level of substrate or other essential nutrients such as nitrogen or trace metals. This versatile microbe may also provide an opportunity to examine the S-isotope fractionation during both oxidative and reductive transformation of sulfite, which probably uses the same machinery as MSD (Kramer and Cypionka, 1989). These experiments will provide a physiological perspective to the fractionation of sulfur isotopes during oxidative S cycling. Additional measurements of multiple S-isotope data produced by MSD under various growth conditions also may clarify whether minor isotope fractionation factors can be used to distinguish between the isotopic signatures of MSR and MSD (Johnston *et al.*, 2005; Sim *et al.*, 2011).

References

Berner RA. 1984. Sedimentary pyrite formation: an update. Geochim. Cosmochim. Acta 48: 605-615.

Canfield DE, Thamdrup B. 1994. The production of ^{34}S-depleted sulfide during bacterial disproportionation of elemental sulfur. Science 266: 1973-1975.

Finke N, Vandieken V, Jørgensen BB. 2007. Acetate, lactate, propionate, and isobutyrate as electron donors for iron and sulfate reduction in arctic marine sediments, Svalbard. FEMS Microbiol. Ecol. 59: 10-22.

Finster K. 2008. Microbiological disproportionation of inorganic sulfur compounds. J. Sulfur Chem. 29: 281-292.

Gomes ML, Hurtgen MT. in preparation. Sulfur isotope systematics of a euxinic, low-sulfate lake: A modern analogue to ancient ocean.

Habicht KS, Gabe M, Thamdrup B, Berg P, Canfield DE. 2002. Calibration of sulfate levels in the Archean Ocean. Science 298: 2372-2374.

Hurtgen MT, Arthur MA, Halverson GP. 2005. Neoproterozoic sulfur isotopes, the evolution of microbial sulfur species, and the burial efficiency of sulfide as sedimentary pyrite. Geology 33: 41-44.

Hurtgen MT, Arthur MA, Suits NS, Kaufman AJ. 2002. The sulfur isotopic composition of Neoproterozoic seawater sulfate: implications for a snowball Earth? Earth Planet. Sc. Lett. 203: 413-429.

Johnston DT, Farquhar J, Wing BA, Kaufman AJ, Canfield DE, Habicht KS. 2005. Multiple sulfur isotope fractionations in biological systems: A case study with sulfate reducers and sulfur disproportionators. Am. J. Sci. 305: 645-660.

Kramer M, Cypionka H. 1989. Sulfate formation via ATP sulfurylase in thiosulfate- and sulfite-disproportionating bacteria. Arch. Microbiol. 151: 232-237.

Krekeler D, Sigalevich P, Teske A, Cypionka H, Cohen Y. 1997. A sulfate-reducing bacterium from the oxic layer of a microbial mat from Solar Lake (Sinai), Desulfovibrio oxyglinae sp. nov. Arch. Microbiol. 167: 369-375.

Li X, Gilhooly WP, Zerkel AL, Lyons TW, Farquhar J, Werne JP, Varela R, Scranton MI. 2010. Stable sulfur isotopes in the water column of the Cariaco Basin. Geochim. Cosmochim. Acta 74: 6764-6778.

Ruiz-Halpern S, Macko SA, Fourqurean JW. 2008. The effect of manipulation of sedimentary iron and organic matter on sediment biogeochemistry and seagrasses in a subtropical carbonate environment. Biogeochem. 87: 113-126.

Sim MS, Bosak T, Ono S. 2011. Large sulfur isotope fractionation does not require disproportionation. Science 333: 74-77.

Thamdrup B, Fossing H, Jørgensen BB. 1994. Manganese, iron, and sulfur cycling in a coastal marine sediment, Aarhus Bay, Denmark. Geochim. Cosmochim. Acta 58: 5115–5129.

Wu N, Farquhar J, Strauss H, Kim ST, Canfield DE. 2010. Evaluating the S-isotope fractionation associated with Phanerozoic pyrite burial. Geochim. Cosmochim. Acta 74: 2053-2071.

Zerkle AL, Kamyshny A, Kump LR, Farquhar J, Oduro H, Arthur MA. 2010. Sulfur cycling in a stratified euxinic lake with moderately high sulfate: Constraints from quadruple S isotopes. Geochim. Cosmochim. Acta 74: 4953-4970.